European Commission

Research Programme of the Research Fund for Coal and Steel

Technical Group: TGS8/TGA4

TRAFIR: Characterization of TRAvelling FIRes in large compartments

Final Report

Marion Charlier, Olivier Vassart, Antoine Glorieux
ArcelorMittal Belval & Differdange (Luxembourg)

Jean-Marc Franssen, Antonio Gamba, Fabien Dumont
Liège University (Belgium)

Alastair Temple, Johan Sjöström, Johan Anderson
RISE Research Institutes of Sweden (Sweden)

Stephen Welch, Xu Dai, David Rush
The University of Edinburgh (The United Kingdom)

Ali Nadjai, Naveed Alam
Ulster University (The United Kingdom)

Grant Agreement 754198

1st July 2017 – 31st December 2020

1. Project brief

1.1. Abstract

Inspection of recent fire events in large compartments reveals them to have a great deal of non-uniformity, they generally burn locally and move across floor plates over a period of time. This phenomenon which generates transient heating of the structure is idealized as “travelling fire”.

A first series of tests was launched to define a fire load representative of an office building according to Eurocodes. Additional tests where the fire dynamics were controlled were launched to develop an understanding of the fire exposure to steel structures.

Then, a second series of large scale tests were performed in real building dimensions. These tests had no artificial control over the dynamics, which allowed a realistic characterization of the fire. The fire load was identical for all tests, only the openings were modified.

CFD numerical models were developed to reproduce the experimental campaign and to launch parametrical analyses. This allowed to provide information concerning the conditions which may lead (or not) to a travelling fire scenario.

An analytical model for the characterization of a travelling fire was developed and implemented in a simple calculation tool. It allows to evaluate the fire location, the gas temperatures in the flames, the heat fluxes in the different parts of the compartment and the temperature in a steel member. In addition, the methodology is introduced in the FEM software SAFIR and OpenSees.

Ultimately, a design guide was prepared including worked examples which are detailed step-by-step and for which the influence of the inputs on the results is analysed.

1.2. Overview

Grant Agreement No.:	754198
Title:	Characterization of TRAvelling FIRes in large compartments
Acronym:	TRAFIR
Consortium:	ArcelorMittal Belval & Differdange, Liège University, RISE Research Institutes of Sweden, The University of Edinburgh, Ulster University
Period covered by this project:	1st July 2017 - 31st December 2020
Work Undertaken:	The project TRAFIR allowed to perform small and large scale fire tests, with and without control over the fire dynamics, and to launch extensive CFD numerical simulations. This enabled to develop an analytical procedure which allows to characterize the thermal impact generated by a travelling fire, and to provide guidance regarding the parameters influencing the occurrence of this fire scenario. Updated versions of FEM software and a design guidance were prepared to improve structural safety as well as to further optimize the design of structures.
Main Results:	• Experimental data allowing to define a uniformly distributed fire load arrangement representative of an office building (according to the Eurocodes) • Experimental data (controlled tests) allowing to assess the optical thickness related to multiple fires as well as experimental data of the near and far field fire exposure to steel structures • Experimental data from a series of tests in two purposely constructed experimental buildings with steel frames and with different ventilation conditions – for which no artificial control over the fire dynamics was applied • Numerical models (CFD) representing travelling fires: well-resolved ones (providing precise assessments of the burning behaviours), and simplified ones (allowing to launch analyses in real building geometries) • Guidance regarding the parameters which influence the occurrence – or not – of a travelling fire • An analytical procedure which allows to characterize the thermal impact from a travelling fire (and the resulting steel temperature of a structural member); implemented in a simple tool (Excel sheet with user-friendly interface)

	• Updated versions of FEM software SAFIR and OpenSees (as well as examples), to numerically apply the developed procedure • A design guide including worked examples, to support practitioners
Future work to be undertaken:	Further research is needed to improve the following points: • to assess the glazing breakage evolution; influencing the fire dynamics (both for numerical and analytical models); • to better understand what influences the fire front speed – and therefore to be able to provide guidance regarding this parameter; • exploration of the impact of alternative fuels on dynamics of compartment fires, i.e. plastics and mixed fuels, as there are known limitations in extrapolating from observations derived from timber cribs to "real" fuels (cf. Gupta et al., 2021); • to assess the impact of fuel islands on the fire spread over a large space; • to develop an improved CFD representation of the cooling phase of the fire to include the role of the char and glowing embers.

1.3. Objectives of the project

Inspection of recent fires in large compartments reveals them to have a great deal of non-uniformity, they generally burn locally and move across floor plates over a period of time. This phenomenon which generates transient heating of the structure is idealized as a "travelling fire".

The TRAFIR project aims at characterizing travelling fires: which parameters influence their occurrence and development, as well as the thermal impact they generate on the surrounding structure. Indeed, it is found that the main obstacle of developing the travelling fire knowledge is the lack of understanding of the physical mechanisms behind this kind of fire scenario, which requires more reasonable large scale travelling fire experiments to be set up and carried out. Furthermore, existing travelling fire models generally don't consider the conditions in which a travelling fire may develop, i.e. there is no guidance concerning the conditions leading to such fire scenario (Dai et al., 2017).

In the frame of this project, small scale tests for which the fire dynamics are well-controlled are first planned. They will allow for the evaluation of the influence of the flame depth and the fire load arrangement that comes as close as possible to values representative of an office building according to the Eurocodes.

Then, large scale tests will be performed in real building dimensions: they will be performed with no control over the dynamics, using the fire load arrangement previously defined which allows a realistic characterization of the fire source, as well as the calibration of numerical and analytical models. Only the openings are to be modified to assess the influence of the ventilation conditions.

Indeed, following the tests, numerical models using CFD will be developed, reproducing the experimental campaign. The model will be used to perform a parametric study covering a broader range of practical scenarios. This will allow to provide information concerning the conditions which may lead (or not) to a travelling fire scenario.

An analytical model for the characterization of a travelling fire will be proposed and implemented in a simple calculation tool. Then, the methodology will be introduced in the FEM software SAFIR and OpenSees in order to have a large utilisation of the proposed model in the construction market.

Finally, design guidance will be provided: it will provide a simplified version of the project, describe the analytical model which allows to characterise the thermal attack caused by travelling fire (as well as the resulting temperature of a steel structural member), and realistic worked examples.

To conclude, the TRAFIR project will characterize travelling fires to improve structural safety as well as to further optimize the design of structures through a comprehensive approach: several series of experimental campaigns, numerical modelling, analytical modelling (in both a simple calculation tool and in FEM software) and design guidance.

1.4. Summary

1.4.1. Preliminary analyses of the parameters influencing travelling fires (WP1)

The two tasks of this Work Package (WP1) had as objective to provide scientific information related to the conditions leading to the development of a travelling fire. The first task consisted in carrying out analytical procedure while the second task consisted in undertaking numerical procedure (CFD).

Analytical investigation

The work has been performed by analysing from the literature experimental results on compartment fires leading either to non-uniform temperature development or to travelling fire development. Existing analytical models published so far have also been considered. Also, the main parameters for which some values are recommended in EN 1991-1-2 (CEN, 2002) as a function of the type of occupancy have been organised in such a way that the likelihood of developing a travelling fire can be estimated for each type of occupancy.

From these observations, it appears that the most important parameters are the geometry and the ventilation conditions. If the fuel in the tests is made of wood, spontaneous travelling fires occurred for moisture content from 10% to 14%. There is no test that shows travelling fire with a non-uniformly distributed fire load. Travelling fires have been observed for uniformly distributed fuel load density in a range from 173 [MJ/m^2] to 700 [MJ/m^2]. Solely considering the values from EN 1991-1-2 for different types of occupancy, a travelling fire is not likely to develop in a dwelling, a hotel room, a hospital room or an office of small size. It would require significant dimensions in an office building, a library or a shopping centre but is very likely to develop in a theatre or a public space (assuming the fire load is uniformly distributed).

Numerical investigation

To facilitate study of the conditions leading to establishment and progression of travelling fires in large compartments an extensive series of CFD simulations was undertaken with the Fire Dynamics Simulator (FDS) (McGrattan et al., 2021). The fire load was represented by discrete timber crib fuel sources on a regular spacing. Both long and square compartments were studied, with different opening geometries, ceiling heights, crib spacings and ignition locations. Fire spread progression was analysed, giving valuable insights into the interrelation of the various design parameters, and it proved possible to interpret all of the observed trends in terms of fundamental principles of fire dynamics. For example, in a long compartment with openings on side walls the main fire zone moves quickly to the edge of the opening and stabilises there before continuing to move further along the length, with generally more rapid spread in more confined cases with smaller openings and away from openings, and with reduced crib spacings and reduced ceiling height (Charlier et al., 2018).

Considering generalisation of the findings, it is recognised that timber cribs are rather idealised structures for which burning rates may be fairly weakly coupled to compartment conditions due to their porosity (Drysdale, 2011; Gupta et al., 2020b). Fire front progression is expected to

vary in cases involving exposed combustible surfaces and obviously with different fuels, e.g. plastics (Gupta et al., 2021); though spread rates may be more rapid, if burning rates are also higher, then the critical length of any travelling may be mitigated, though some cases will go to flashover before reaching burn-out at the rear edge (Gupta et al., 2020b). Due to these important uncertainties, it is not possible to definitely establish the potential for travelling fires in scenarios of arbitrary complexity, but it has been shown that CFD tools have potential to provide insights into relevant fire dynamic phenomena and can be used to compare and rank the influence of different design parameters, which is a pioneering development in the field (Charlier et al., 2018). These capabilities are further extended in the later work of the project, encompassing much more detailed representations of the fuel load, and careful validation against well instrumented experiments (reported under Work Package 4).

1.4.2. Experimental investigation of travelling fire (WP2 & WP3)

Characterization of fuel loads (WP2)

This part of the project consists of small scale experiments designed to reduce the controlling parameters and allow for individual relationships, such as relationship of fire growth rate to fuel density, to be better examined. These tests provide input to the design of the subsequent large-scale tests and experimental data for subsequent work packages and future studies.

Experimental tests have been made with linear timber elements of standardised sections, with fuel bed surfaces of two different sizes, namely 5 tests with a dimension in plane of 2 m x 2 m (labelled as “LA” tests) and 6 tests with a nearly circular fuel bed and a diameter of around 4 meters (labelled as “LB” tests). A first preliminary task was to develop an ignition system that would be defined by engineering parameters and quantities, that would be safe for the staff, that would not involve a too great a quantity of accelerant (to avoid influencing the fire), that could be activated from a distance and that would ensure that the fire load ignites without any further intervention.

A first series of 5 tests has been performed in the fire laboratory of Liège University with fire source of the maximum size that could be accommodated in this laboratory. The fuel load consisted of several layers of timber sticks at a constant distance from each other and turned by 60 degrees from layer to layer. These tests allowed measuring the pyrolysis rate, the propagation of the fire, the temperature evolution of thermocouples located on the sticks of the upper layers, the heat fluxes just above the fire source as well as at a distance from it, and the influence of a horizontal barrier at a distance above the fire load.

A second series of 6 tests was then performed in a larger facility with a ceiling above the fire source for all tests, with down stands of 0.35 m on the four sides of the ceiling. The parameter that was mostly investigated here was the percentage in volume of wood in the gross fire load.

This task lead to a proposal of a uniformly distributed fire load arrangement based on 30 mm x 35 mm timber sticks that can lead in experimental tests to a slow, a medium of a fast fire propagation rate (following EN 1991-1-2) with a fire load density that corresponds to the one recommended for office buildings in EN 1991-1-2 (CEN, 2002).

Influence of near field & far field and lame thickness dependence (WP2)

The task had the objectives on analysing the thermal impact of travelling flames on steel members, investigating differences between near- and far-field, the flame thickness behaviour in both near and far field and gathering data for model calibration.

Two experimental test series were carried out. The first, and primary series, was implemented within a well-ventilated steel structure of 18 m long, 6 m wide and 3 m high, constructed in identical bays. One of the short ends was closed off, while the opposite end was left open, and down-stands were constructed on the long sides to control the total ventilation for the space. Two non-structural columns were also placed along the centreline of the compartment, one at mid-length and one at the open end. The series contained 5 fire tests designed to study the effect of travelling fires on the exposure of steel structures in the near and far field, including the exposure from both the fire itself and the effect of any pre-heating via the smoke layer away from the burning area. These tests utilised two different fuel, the first 4 tests had diesel pool fires (within the first half of the compartment) to provide a controlled HRR (heat release rate) and steady spread rate, and a final test with wood cribs over the full length.

The tests were well instrumented thereby providing significant volumes of data on gas and steel temperatures as well as the radiation exposure across the compartment. The data is especially important considering the low number of travelling fire test conducted prior to TRAFIR, and in addition to assisting the later work packages within this project, provides a vital resource for future experimental and computational studies. The diesel pool tests provided a clear picture of the near and far field effects on the steelwork. There were strong temperature gradients, both vertically and horizontally. In the far field, the heating was dominated by the convection from the smoke layer causing a hot zone, almost homogeneous along the horizontal dimension (at the top of the column which is within the smoke). This relationship changes as the fire gets close to the structural element and the near field takes over, with radiation and direct convection from the flames becoming dominant and causing the lower portion of the column to rapidly heat up. There is also a strong horizontal gradient visible in the temperatures, with the flange of the column furthest from the fire being much cooler than the closer one. The timber test also provided important data, as well as demonstrating, for the first time experimentally, that it is possible to have a fire with a continuous spread rate despite a very high opening factor.

A secondary set of small scale experiments were performed with diesel pool fires to establish the flame thickness dependence on the radiation exposure to the near and far field. From these experiments it was concluded that the classic theory flame thickness dependence, as developed for circular pool fires, on the flame properties are valid also for the elongated pans. Using values of absorptivity derived from circular pools it was found that the mean free path of an elongated pool is described by $L = 1.25D$, where D is the width of the burning area. However, it should be remembered that the energy from the most distant flame will contribute to the smoke layer, which, even though mostly affecting members through convection, also contributes through radiation from the host gas layer.

Large-scale natural fire tests (WP3)

Three large natural fire tests involving a continuous wood crib fuel bed in a steel structure were conducted, aiming at performing large-scale tests in real building dimensions with no artificial control over the fire dynamics, to be able to understand in which conditions a travelling fire develops, as well as how it behaves and impacts the surrounding structure. Three tests were planned: a fuel controlled travelling fire with large opening factor, referred as Test 1, a ventilation controlled fire intended to lead to a flashover, referred as Test 3, and another travelling fire, with less ventilation than in Test 1, referred as Test 2.

The test compartment is a representative of a modern office building and represents a part of the entire office layout. The test compartment consisted of steel beams and columns as the main structural frame while hollow-core precast slabs were used for construction of the ceiling. The steel columns were separated into two categories, the structural columns and the dummy columns. The structural columns were part of the steel frame transmitting the loads to the foundation while the dummy columns were not part of the structural steel frame and were left unprotected (see Table I) to allow for steel temperature measurements. The floor plan between the outer gridlines of the test structure was 15 m x 9 while the level of the ceiling from the floor finish surface was 2.90 m (see Figure 1). The fuel bed was 14 m long stretching from wall to wall along the longer dimension of the test compartment. For convenience, a gap of 500 mm was maintained between the walls and the edge of the fuel bed at both ends. The width of the fuel bed was 4.2 m and was aligned with the centre line of the compartment. The fire load is identical for the three tests (resulting from WP2 Task 1) and representative of an office building following EN1991-1-2 (only the opening layouts were modified, see Figure 2).

The large scale tests data represents valuable information since very few uncontrolled large scale travelling fire tests were realized up to now. They allow the characterization of the fire source and the calibration of numerical and analytical models developed in the frame of TRAFIR. The results of the tests also allow examination of the veracity of the different assumptions from some conceptual models presented in the literature.

Table I: Description of the steel structure

Description	Sections	Section Factor (m^{-1})	Length Height (m)	Protection Applied
Structural columns	HEA 200	209.5	3.5	Yes: R60 (protection applied before each test)
Dummy columns	HEA 200	209.5	2.7	No
Long beams	HEA 200	172.3	4.8	No
Short beams	HEA 160	138.0	3.0	No

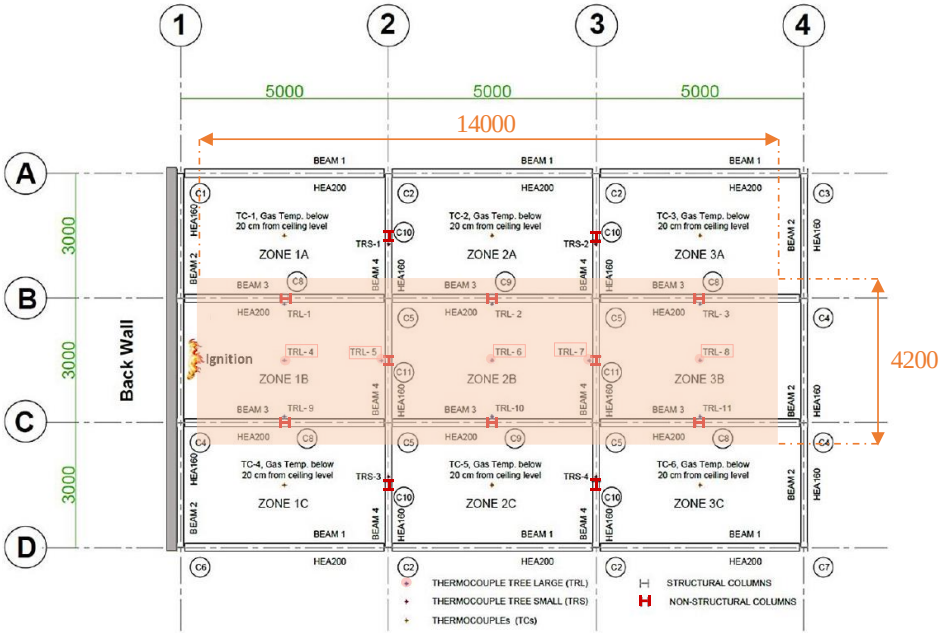

Figure 1: Fuel load arrangement and steel columns (with and without fire protection)

(a) Test 1: Fuel controlled fire, opening area 87 m^2, no flashover, duration fire 82 min,	(b) Test 2: Between fuel/ventilated fire, opening area 30 m^2, no flashover, duration fire 82 min	(c) Test 3: Ventilated controlled fire, opening area 9.6 m^2, with flashover, duration time 111 min

Figure 2: Different opening layouts were used for the three tests

1.4.3. Numerical modelling and parametric studies (WP4)

This work concerns the calibration and parametrical analysis of the numerical models, with the purpose of establishing a simulation based complement to experimental tests and using it to perform numerical experiments to investigate travelling fire behaviour. Calibration relates to the matching to the test series in WP2 ("Characterization of fuel loads" and "Influence of near field & far field") and WP3 ("Large-scale natural fire tests") while the parametrical variations seek to effectively extend the experimental dataset, thereby revealing the sensitivities of fire exposures to parameters of potential interest to designers.

Modelling the fire tests

The first part of this task is the development and calibration of an advanced CFD numerical model with FDS. The initial work of the project exploring the conditions for travelling fires adopted simplified representations of the crib fuel sources; this concept was subsequently developed to provide a model for continuous fuel beds, which have been studied experimentally and may be closer to many real world scenarios. A more detailed representation of the fuel is provided via a series of small wood blocks, which still limit computational demands, and also via more ambitious approaches based on a full "stick-by-stick" representation. While the latter may be extremely computationally demanding, especially at compartment scale, it is used here to explore burning behaviours and model sensitivities which inform the application of more simplified models.

The Liège LB7 test case was first modelled for calibration with the experimental data (Dai et al., 2021). The wood sticks were represented with real cross-section dimensions (30 mm × 35 mm) in the detailed model. Cell size within the crib volume was half that of the physical dimensions of the sticks, while in the gas phase in the horizontal surrounds of the crib the cell side was doubled, and doubled again above the top surface of the crib. A total computational domain size was symmetrical with side 5.04 m and height 2.73 m, thus the total number of cells was approximately 1.3 million, which were divided into 16 numerical meshes. The simulations were performed using the computational clusters ARCHER (UK National Supercomputing Service, per UKCTRF) and Eddie (Edinburgh Compute and Data Facility), each run taking around 170 hours for a 1200 s simulation. Illustrative results are presented in Figure 3 showing an excellent agreement in terms of the key parameters of fire spread rate and heat release rate via this calibrated model. A grid sensitivity study confirmed that the suggested relaxation of the grid resolution outside the crib volume is appropriate, which we believe is a novel demonstration. Encouraging results were also achieved in application to the WP3 full scale test.

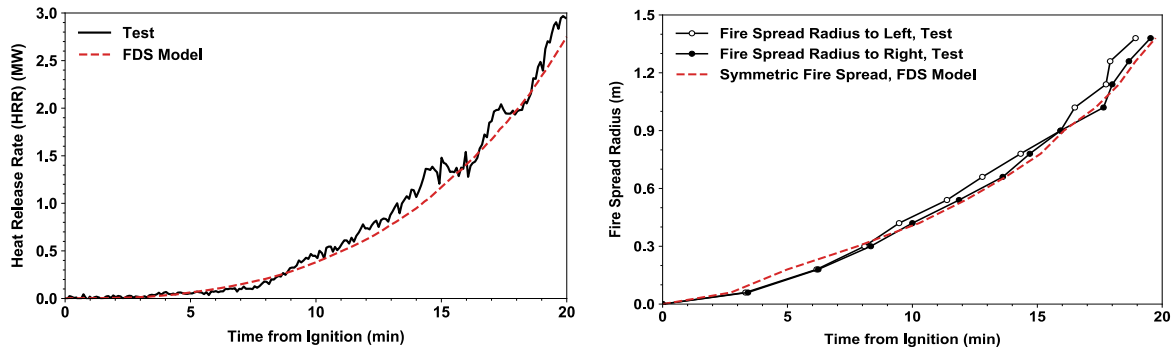

Figure 3: (a) HRR comparison for LB7 test ; (b) : Fire spread radius comparison for LB7 test

A wood block model was developed as the main basis for exploring predictive capabilities for the large-scale natural fire tests (WP3). The global fire spread is generally well captured, as well as the main tendency in terms of temperatures.

Parametric studies

For the subsequent generalised parametric studies the same "wood block" model was used as had been calibrated for the large-scale natural fire tests (WP3). Scenarios encompassed different fires loads (511 MJ/m^2 (office); 250 MJ/m^2 (sparsely loaded office); 730 MJ/m^2 (commercial)) and compartment geometries (opening heights of 25%/50%/75% of compartment height, representing different glazed areas); floor plans c. 30x15 and 70x25 (m); ceiling heights of 3 m (baseline) and 8 m.

The sensitivities of the evolution of fire exposures are assessed by a detailed analysis, spanning fire spread behaviours (fire mode and flame thickness) and associated temperatures and heat release rates. The observations reinforced the findings of Work Package 1 (significant influence of compartment dimensions, total opening area and fire load) but extended the scope to bigger floor areas where limited access to air deeper into compartments had potentially large impacts on the fire. Travelling fire behaviour was analysed in relation to a generic opening factor, $O = \left(A_v\sqrt{h_{eq}}\right)/A_t$ (m$^{1/2}$), which references both the compartment dimensions via the total area A_t (m^2) and the opening area and height, via A_v (m^2) and h_{eq} (m). A "binary classification" sets a value of "1" for travelling fires and a value of "0" when no travelling fire occurred (i.e. instead a compartment fire with flashover took place). Figure 4 suggests that for a given opening factor a low fire load and a low distance between openings increase the potential for travelling fire scenario, while for a given fire load (and therefore a given occupancy type) this tends to occur at higher opening factors.

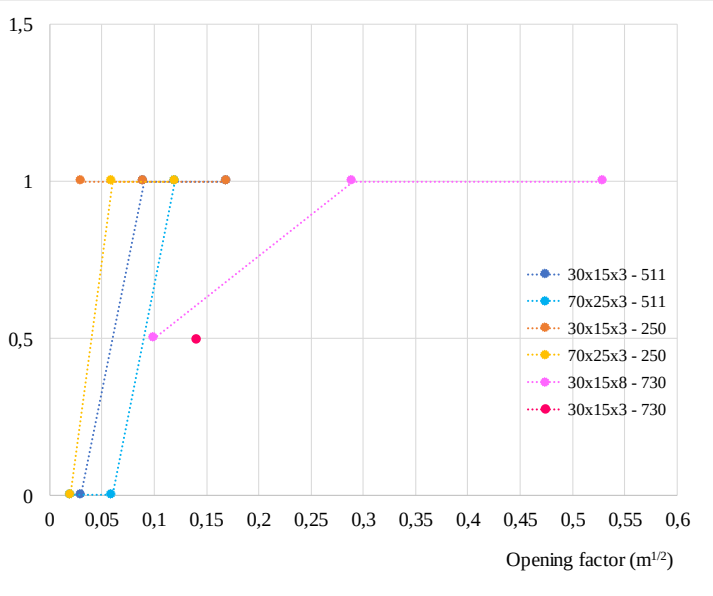

Figure 4: Binary values (0 for no travelling fire; 1 for travelling fire) for different opening factors. The legend provides first the compartment dimensions (length x width x height, in m) and then the fire load (in MJ/m²).

The current results are naturally not definitive in terms of the absolute numbers related to the different fire modes but they do provide a useful perspective on the general sensitivities and the kind of trade-offs that may exist in practice between various design parameters, in particular the extent of glazed areas, overall compartment dimensions (in particular the distance between openings across the width, and the ceiling height) and fire loads.

1.4.4. Analytical procedure (WP5)

This Work Package is concerned with the evaluation and development of improved analytical models for the characterisation of travelling fire, and its thermal effects. As a first step in this process, the first task seeks to evaluate the capabilities of existing models used for this purpose, exploring the impact of some of their foundational assumptions. Then, in the frame of subsequent tasks: a new analytical procedure which allows to characterize the thermal impact of a travelling fire and to evaluate the resulting temperature of a steel structural element is developed and implemented in a simple calculation tool.

Inspection of some existing travelling fire models

The general capabilities of existing "analytical procedures" are explored in order to establish any specific limitations and aspects that need further development, thereby informing the subsequent work on a new analytical model. Methodologies considered are:

- The Improved Travelling Fire Methodology (iTFM) (Rackauskaite et al., 2015)
- The Extended Travelling Fire Methodology (ETFM) framework (Dai et al., 2020)

Model capabilities were examined in relation to the full-scale tests conducted within the scope of the TRAFIR project, i.e. wood crib travelling fire test (WP2 "Influence of near field & far field" wood crib test) and the series of full-scale compartment travelling fire tests (WP3 "Large-scale natural fire tests"), with different heat release rates per unit area also (i.e. design and test, 250 and 400 kW/m^2, respectively).

In general, representations of fire temperatures, and related steel member temperatures, are on the conservative side, sometimes markedly so. This is a particular problem for near field fire impacts (depending on flame length with respect to the ceiling, i.e. whether impingement can be expected), but also extends to the far field via both approaches. But the model results clearly show the role of near field and far field thermal impacts on the structural response.

As the opening factor is not considered in the iTFM, conclusions from the comparisons of the large-scale natural fire tests (WP3) n°1-3 are different, with acceptable results in a certain scenario, but too severe in others. Also, the model does not consider any variation of temperature with height. Utilisation of the Hasemi localised fire model in ETFM may significantly over-predict fluxes when the flame does not impinge on the ceiling. Also, uncertainties deriving from the role of the assumed boundary heat losses on the far-field temperatures may be quite significant.

Development of a new analytical model

An improved analytical model for the characterization of a travelling fire and its thermal effect was developed and implemented in a simple calculation tool (Excel spreadsheet). The procedure allows to evaluate (as a function of time): the fire geometry and its location, the rate of heat release, the fire load, the flame length, the gas temperatures in near field (flames), the radiative and convective heat fluxes components and finally the temperature in a steel member placed in the compartment. The large-scale tests performed in WP3 were modelled using this analytical procedure and the latter was verified against steel temperatures in a central column:

the ones directly measured during the tests were compared to the ones obtained analytically (a good correspondence is met, see Figure 5). The following assumptions are considered in the method:

- The compartment is modelled as a parallelepiped rectangle;
- The plan view is divided into bands of equal width;
- The fire load is uniformly distributed and covering the whole floor surface;
- The fire starts in the band close to one of the façade and spreads from band to band;
- The effect of the ventilation is considered through a possible diminution of the of heat release in the burning bands (if and when the fire gets ventilation controlled);
- The spread rate is given as an input and remains constant during the fire;
- The fire load can be defined at another level than the floor level;
- The openings defined in the method are considered as fully open;
- The model computes heat fluxes, depending on where the target lies, based on the equations from EN 1991-1-2. Computed heat fluxes are therefore function of both horizontal and vertical dimensions.

The developed simple tool presents a user-friendly interface, and a document comprehensively describes its assumptions and how to use it, to allow the ease of use for practitioners.

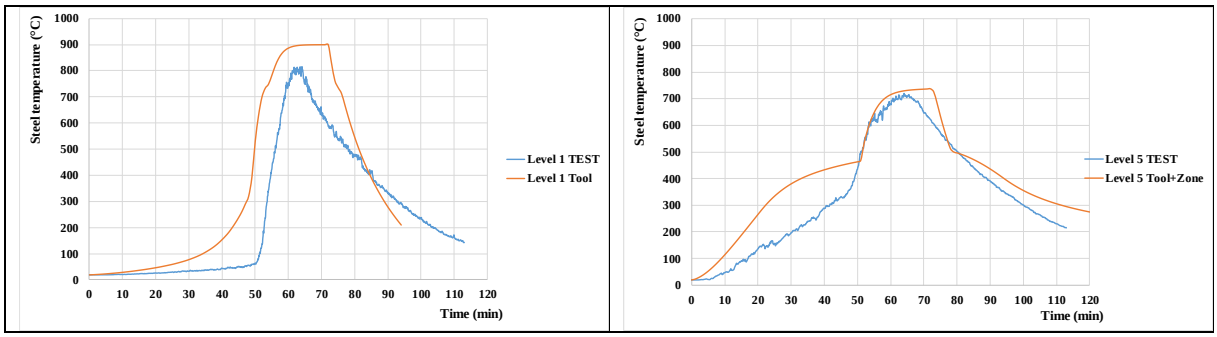

Figure 5: Comparison of the steel temperatures in a central column for WP3 test n°2: experimental results ("TEST") versus TRAFIR analytical results ("Tool"), at Level 1 (0.5 m) and Level 5 (2.5 m)

1.4.5. Application tools (WP6 & WP7)

The analytical model was implemented in two FEM software (SAFIR and OpenSees) in order to make it possible to compute the temperatures and the mechanical behaviour of structural elements that are located in the compartment where the travelling fire has been modelled.

Implementation of the new model in FEM software SAFIR (WP6)

The analytical travelling fire model developed in the project has been implemented in a completely new module called TRAFIR4SAFIR that can be run independently, and which computes the fire propagation and the travelling nature of the fire, then writes in a transfer file the information requested by SAFIR to compute the temperatures in the structure. The format of this file is the same as the one developed in the RFCS project FIRESTRUC and used so far when the thermal environment has been computed by CFD software such as FDS.

Having a new independent software does not lead to an excessively complex and intricate version of SAFIR but to a lighter code with shorter run times. This new software can be made available for free to anyone interested, whereas the SAFIR software is only available after

buying a licence. The transfer file produced by this code can be used for calculating the temperature in a structure, not only with SAFIR but with any other code/software that can read this file. This new freeware will also be easier to maintain, to adapt and perhaps to develop for anyone in the future than a new development in the proprietary SAFIR would have been. These advantages will be favourable to the dissemination and the persistence in time of the results of the TRAFIR project.

Implementation of the new model in FEM software OpenSees (WP6)

The analytical travelling fire model developed in the project was also implemented into the pre-existing SIFBuilder model, which is an OpenSees-based open-source software framework (Dai 2018; Dai et al., 2020). The realisation of the new model follows the same workflow as the current available localized fire model in OpenSees, thereby integrating the travelling fire representation and associated heat transfer analysis, which in turn is coupled to the thermo-mechanical analysis for modelling 3D structural response.

After inputting basic information for generating the structural model, including the geometrical details of the compartment, the user defines the structural loading and thereafter the fire loading information (i.e. fuel load characteristics). When running the analysis, the travelling fire and heat transfer modules interact via their interfaces at each time step in order to specify the transient fire-imposed boundary conditions at the structural surfaces. The spatial and temporal non-uniform heat fluxes from the analytical model are iteratively updated on each structural element according to the travelling fire location. Then the heat transfer analysis module is launched and the nodal temperature histories are automatically mapped to the fibres of the structural mesh for each structural member. Then the thermo-mechanical analysis is performed on the whole structure, while considering the impact of the travelling fire.

This new version of OpenSees provides an alternative access to the newly developed analytical model, integrating it with an advanced and efficient structural analysis; the resulting software framework is a flexible approach for examining the impact of fire on structural behaviour under realistic design fire scenarios, at reduced cost in time and effort.

Design guidance (WP7)

Ultimately, a design guide was prepared. The first part of this guide summarizes the main development of the TRAFIR project. The second part provides some major key learnings from the CFD numerical analyses launched with FDS (WP4) as well as a clear description of the new analytical model and of how to use the simple tool to ease the use of the method.

The last part of this design guide provides an extensive description of seven realistic worked examples, based on real buildings and on the EN 1991-1-2, following the TRAFIR analytical procedure. The application of the procedure is described step-by-step, to help the user clearly understand how to handle and use the method and the simple tool in which it was implemented. It is important to highlight that the provided information does not represent validated designs; they are presented here as examples to help the user understand how to use the methodology and to assess the differences which may be observed while varying relevant parameters.

2. Preliminary analyses of the parameters influencing travelling fires

2.1. Analytical investigations (WP1)

2.1.1. Introduction

The work has been performed by analysing from the literature experimental results on compartment fires leading either to non-uniform temperature development or to travelling fire development. Existing analytical models published so far have also been considered. Also, the main parameters for which some values are recommended in EN 1991-1-2 (CEN, 2002) as a function of the type of occupancy have been organised in such a way that the likelihood of developing a travelling fire can be estimated for each type of occupancy.

2.1.2. Description of the activities

A critical analysis of the publications from the literature which are relevant to the topic has first been undertaken. It allowed first to underline that several tests which lead to non-uniform temperature development where not recognised and labelled as "travelling fires", although they may give a first insight in the phenomena.

- In the early 90's, nine tests carried out at the BRE Cardington laboratory in the UK were launched by British Steel Technical (BST) and hosted by the Fire Research Station (FRS) in long compartments with openings only in one of the short side. It was clearly observed that the fire that had been ignited at the back of the compartment (away from the opening) was travelling quickly to the opening, seeking for oxygen, where it burnt to travel back when the fire load had been consumed where oxygen was available. Such behaviour was confirmed in tests performed in 2005 by Thomas (Thomas and Bennetts, 2005) on similar conditions.
- The "office demonstration test" performed by BRE in Cardington around 1995 also led to the observation that that the ventilation conditions and the ignition method used generated non-uniform (migrating) fire scenario during the test made in a compartment with openings on the long side.
- A non-uniform temperature distribution was also noticed in terms of temperature and heat flux in the tests made by BRE in Cardington at the turn of the millennium in compartments with a square plan view and openings in either one or in two opposite sides (Welch et al., 2008).
- Different tests have been performed more recently with the aim to analyse specifically the phenomena of travelling fires (Veselí 2001, University of Edinburgh and BRE 2013, Tisova 2015). A complete review of experimental campaigns is described in Dai et al. (2017).

From these observations, it appears that:

- The most important parameters are the geometry (in a small compartment, travelling fires are not observed) and the ventilation conditions.

- If the fuel in the tests is made of wood, the moisture content is very important. The tests that showed a spontaneous travelling fire are those with moisture content from 10% to 14%. In Tisová 2015, a moisture content of 18-22% was used and the fire propagation had to be manipulated (boosted) with an accelerant.
- Up to now all the tests were performed with a uniformly distributed fuel load; there is no test that shows travelling fire with a non-uniformly distributed fire load.
- Travelling fire has been observed for uniformly distributed fuel load density in a range from 173 [MJ/m^2] to 700 [MJ/m^2].

Existing analytical models for travelling fire have also been investigated but did not yield any insight into the question investigated as all these models assume *a-priori* the existence of a travelling fire. Finally, the parameters for which values are proposed in EN 1991-1-2 (CEN, 2002) as a function of the type of occupancy have been used to determine in which types of occupancy a travelling fire is likely to develop or not if the fire is fuel controlled. A travelling fire in the fuel controlled regime can only develop if the flame thickness is smaller than the length of the compartment. Considering the parameters provided in EN 1991-1-2, it appears that a travelling fire is not likely to develop in a dwelling, a hotel room, a hospital room or an office of small size. It would require significant dimensions in an office building, a library or a shopping centre and is likely to develop in a theatre or a public space (assuming a uniformly distributed fire load).

2.1.1. Conclusions

From the analyses of experimental data, the main results can be summarised in Figure 6 that presents each test with a dot, with the travelling fires coloured in blue or in grey (some interpretation needed) and those with no travelling fire in orange.

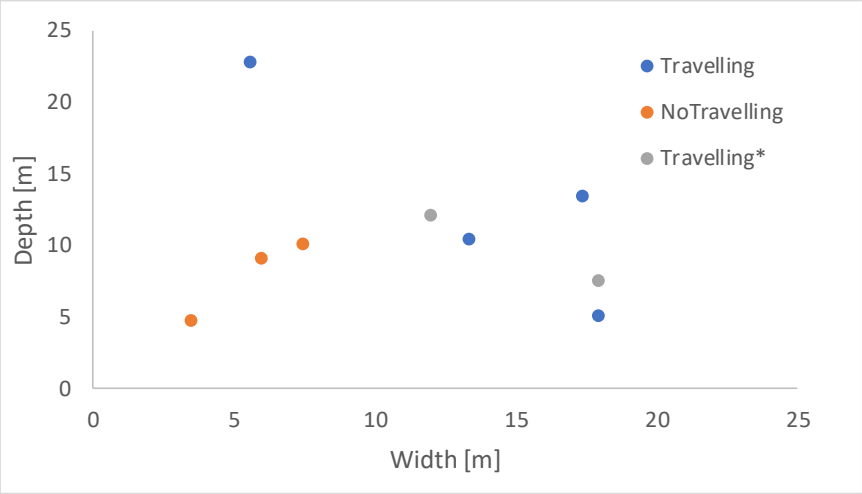

Figure 6: Occurrence of travelling fire for different compartment geometries (width = dimension parallel to the side with openings)

A travelling fire in fuel controlled regime can only develop if the flame thickness is smaller than the length of the compartment. Following a preliminary analysis (solely) based on the parameters from EN 1991-1-2 (2002), considering the different types of occupancy, a travelling fire is not likely to develop in a dwelling, a hotel room, a hospital

room or an office of small size. It would require significant dimensions in an office building, a library or a shopping centre but is very likely to develop in a theatre or a public space (assuming a uniformly distributed fire load).

2.2. Numerical investigations (WP1)

2.2.1. Introduction

A large number of CFD simulations were undertaken in order to explore the conditions supporting travelling fire development, spanning variations of compartment geometry including the essential floorplan (long/square), overall length and size of openings, and the ceiling height, as well as crib spacings with detailed results reported, and a conference (Charlier et al., 2018) and journal papers (Charlier et al., 2020) presented the main outcomes.

2.2.1. Description of the activities

In the absence of any general analytical methods, and with the advent of advanced fire modelling tools based on CFD, enabled by parallel processing on modern compute clusters, parametric studies undertaken via simulations present a potentially useful avenue for exploring travelling fire behaviours. There are many possible avenues for representing the crib combustion, and the challenges of using even a prescribed mass loss approach (following Degler et al., 2016) have been demonstrated for the underventilated fire (Dai et al., 2019). The work reported here focussed on exploration of the conditions under which travelling fires might develop, and the influences on their behaviours, as covered below; there is an important link to later work which considered the ability of the models to replicate conditions in the three series of experiments performed in the TRAFIR project, and looked at the generalisation of those conditions to establish broad parametric studies spanning fire compartment conditions (geometries, fire load densities, HRRPUA, etc.) as well as fire model parameters (ignition temperature, heat of combustion, soot yield, etc.) (Dai et al., 2021).

An extensive series of CFD simulations was undertaken with the Fire Dynamics Simulator, and using localised wood crib fuel loads represented as discrete burning items, arranged on regular grids within the compartment. Different geometrical arrangements are examined, in terms of compartment length, opening size and ceiling height, and the conditions supporting flashover explored (Charlier et al., 2018). It was shown that it is possible to obtain useful results at the compartment scale by means of a simplified whole crib ignition mechanism, bypassing the significant computational limitations of exact geometry representations (Dai et al., 2021) and it proved possible to interpret all of the main trends in terms of fundamental principles of fire dynamics. In terms of overall spread rates, specific findings include:

<u>Long plan compartments (sc1 series)</u>

- fire spread is enhanced with smaller openings and reduced crib spacing;

- fire spread is more rapid in parts of the enclosure which are more confined, but delayed at openings where there is greater heat loss
- different behaviour results from ignition in the centre or end of compartment

Square plan compartments (sc4 series)

- fire spread is enhanced with smaller openings and reduced crib spacing;
- fire spread is enhanced with lower ceilings;

The following results highlight the different fire behaviour in a two long rectangular compartments with the same overall geometry (50 x 10 x 4 m) and fire load, but different inverse opening factors, i.e. 2.5 $m^{-1/2}$ in configuration 1.a and 6.25 $m^{-1/2}$ for 1.b (Figure 7).

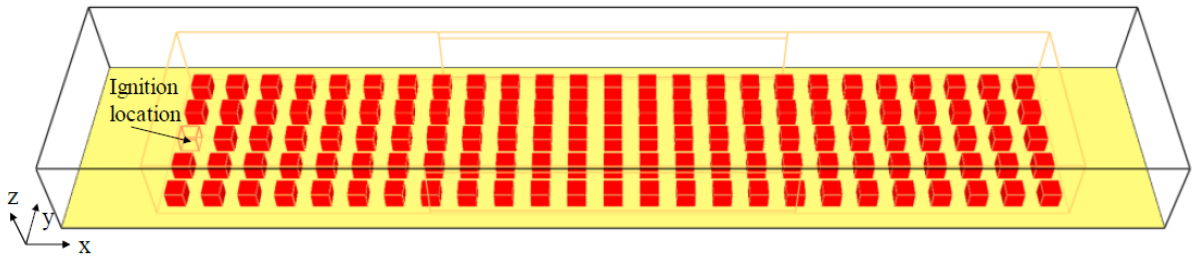

Figure 7: Model of configuration 1.b (which has a lower opening factor than configuration 1.a)

According to Figure 8, in configuration 1.a the fire spreads slowly at the beginning (0m – 15m), then faster (15m – 50m) when the effects of pre-heating by radiation from the hot layer become more significant. Specifically, at beginning of the fire (0 – 20 minutes), the pattern of the burning area indicates a t^2 development, but the acceleration is soon damped with the remaining spread being closer to a steady rate of increase along the length of the compartment. Steady spread can be expected when the process is being driven primarily by local crib-to-crib spread and where the effects of preheating from the hot layer to cribs ahead of the front is relatively minor, and does not significantly increase with time. The lag in the fire spread front edge in the area near the openings, when pyrolysis is moderated by heat loss to the environment and the main combustion zone at the diffusion interface in the gas phase is not moving ahead of the pyrolysis zone, is shown on Figure 9. Comparing Figure 8 and Figure 9, the fire spreads much faster overall under configuration 1.b (52 minutes to traverse the whole compartment) compared with configuration 1.a (90 minutes). This can be explained by more energy leaving the compartment through the larger openings of configuration 1.a and also due to the fact that the burning zone in the gas phase is driven to seek oxygen at the more distant opening in configuration 1.b.

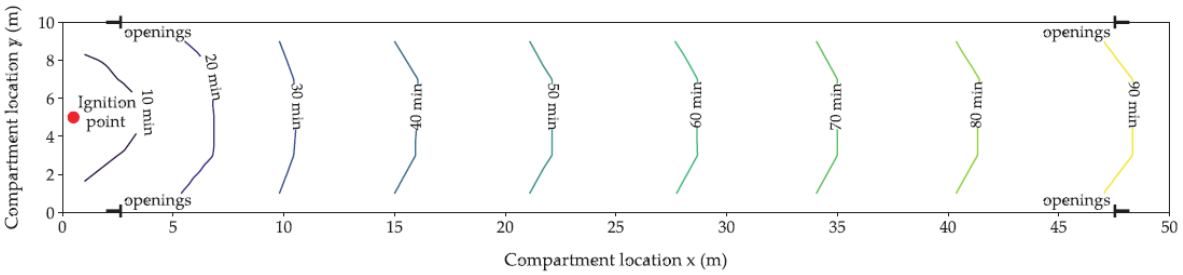

Figure 8: Fire spread time vs. compartment location, under configuration 1.a

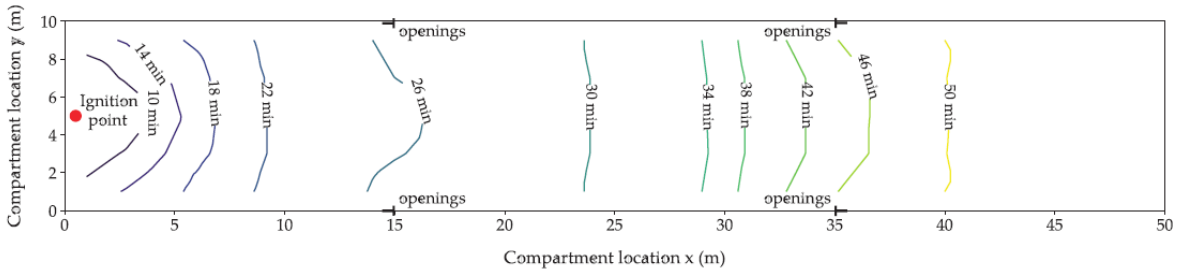

Figure 9: Fire spread time vs. compartment location, under configuration 1.b

In configurations 2.a and 2.b, the compartment dimensions are respectively 20m x 20m x 8m and 20m x 20m x 3.5m and the model domains respectively 24m x 24m x 9m and 24m x 24m x 4m. The openings are placed 0.25m above floor level. The fire starts by the ignition of the wood crib placed at the centre of the compartment and the fire load consists of $1m^3$ wood cribs spaced 2m away from each other. This fuel density was chosen to represent the rate of heat release density of an office building prescribed by EN1991-1-2 Annex E, which is 250 kW/m^2. When compared with configurations 1, the results indicate generally slower spread rates, which is consistent with the greater crib spacing. Also, a 2D spread is observed in both cases, but with a slightly slower spread at the openings side for configuration 2.a where less heat is retained, as depicted in Figure 10a. In configuration 2.b the fire spread accelerates more rapidly, taking 28 minutes to spread over the entire floor versus 45 minutes in configuration 2.a. This difference is suggested to result mainly from lowering the ceiling height, due to the stronger coupling between the hot gases and the pyrolyzing cubes. The change of opening factor also impacts on the ventilation airflows at the openings, and the more regular spread depicted on Figure 10b is a net result of the enhanced heat transfer with the lower ceiling together with changes in burning behaviour related to ventilation differences and the reduced overall duration of spread.

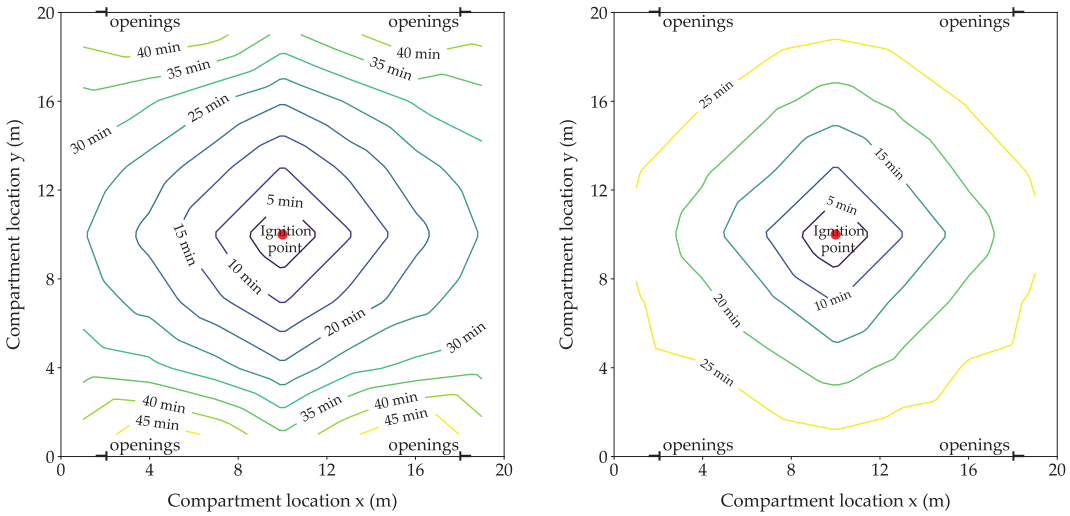

Figure 10: Fire spread time vs. compartment location under (a) configuration 2.a ; (b) configuration 2.b

Many more detailed interpretations and insights were possible via examination of fine details in the predictions. This type of information may be combined with theoretical knowledge derived from more recent studies of ventilation effects on travelling fires (Gupta et al., 2020a; Gupta et al., 2020b); in crib experiments, burning rates are known to be weakly coupled to compartment conditions (Kawagoe, 1958), which implies that the main drivers of travelling fire development are the various influences on fire front speed, including those identified above. An important proviso is that the results may be very different in cases involving more diversity of fuel type, e.g. plastics, and where fuel surfaces are more exposed, i.e. not concealed in a porous crib; under both of these conditions the expectation is for a trend towards enhanced fire spread acceleration but enhanced burning rates may mitigate any extension in the length of the travelling fire due to more rapid burn out (Gupta et al., 2020b). The work is a novel application of CFD to representation of travelling fires and a subsequent journal publication (Charlier et al., 2020).

2.2.2. Conclusions

CFD models based on discrete fuel items, with ignition triggered from any surface, have a value in illustrating the fire dynamic behaviours of travelling fires, despite being simplified. Travelling fires tend to be supported in larger spaces with modest fuel loads. Fire spread rates are strongly influenced by confinement, opening locations and ceiling height and in the limit may accelerate and produce a flashover transition.

3. Experimental investigation of travelling fire

3.1. Characterization of fuel loads (WP2)

3.1.1. Introduction

Experimental tests have been made with linear timber elements of standardised sections, with fuel bed surfaces of two different sizes, namely 5 tests with a dimension in plane of 2 x 2 m² of and 6 tests with a nearly circular fuel bed and a diameter of around 4 meters. A conference and journal papers presented the main outcomes (Franssen et al., 2019) (Gamba et al., 2020).

3.1.2. Description of the activities

A first preliminary task that was necessary to ensure a good completion of the planned fire tests was to develop an ignition system that would be defined by engineering parameters and quantities (in order to be reproducible), that would be safe for the staff, that would not involve a too great quantity of accelerant (because we don't want this to constitute a significant fire load compared the fire load that is of interest in the test), that could be activated from a distance (because it will be located amid the carefully arranged intricate piles of timber wood sticks) and that would ensure that the fire load ignites without any further intervention.

This proved to be more difficult than anticipated, and the proposed method is based on only 40 ml of methylated ethanol at 96% located in a steel cup and ignited from a distance by an electric lighter connected by electrical wires to an AC/DC transformer of the kind used in P.C.'s. Two electric lighter were put in place in each test to offer a second chance in case the first one fails, thus improving the reliability of the system. The first layers of thin wood sticks directly in place above the steel cup was also defined in order to ensure a transition between combustion of the ethanol and that of wood sticks of larger sections that made the fuel load of interest, see Figure 11.

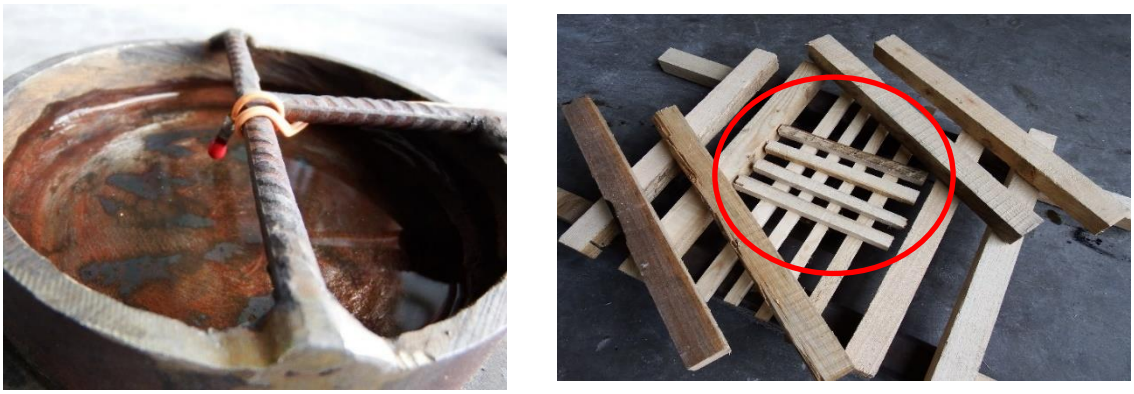

Figure 11: Steel cup with electric lighter (left) - thin timber sticks above the steel cup (right)

A first series of 5 tests has been performed in the fire laboratory of Liège University with fire source of the maximum size that could be accommodated in this laboratory. This first

series, compared to the second series of tests with larger fire sources in a facility that had to be rented, offered the advantages of much greater flexibility, in terms of logistics, and also by the fact that it allowed more time to be spent between each test for a preliminary analysis of the results used to define the next test.

The fuel load consisted of several layers of timber sticks at a constant distance from each other and turned by 60 degrees from layer to layer. The fire load was located on a weighting platform which allowed computing the pyrolysis rate (in kg/s). The propagation of the fire was measured by visual inspection of flaming on, the sticks of the uppermost layer, as well as by temperature evolution of thermocouples located on these sticks. Heat fluxes produced by the fire were also measured just above the fire source as well as at a distance from it.

The tests were performed in the parallelepipedic 3 x 4 m² horizontal of the lab. No obstruction was present above the fire source for the first 3 tests, whereas the upper side of the furnace was partially obstructed for the last 2 tests in order to mimic the presence of an eventual ceiling with the hot smoke layer and the radiation to the fire source that it can generate. In addition to the presence or not of a ceiling, the parameters that were varied were the dimensions of the wood sticks and the horizontal distance between them.

A second series of 6 tests was then performed in a larger facility rented in Marchienne-au-Pont. A ceiling was located at a distance of around 2.2 m above the fire source for all tests (see Figure 12, left), with down stands of 0.35 m on the four sides of the ceiling. The parameter that was mostly investigated here was the percentage in volume of wood in the gross fire load: volume of timber / apparent volume of the fire load. In addition to the parameters measured in the first test series, temperatures were also recorded in a thermocouple tree located on the centreline above the fire source (see the steel mesh that supported the thermocouples, Figure 12, right).

The innovative aspects of these tests is that, to our knowledge, they constitute the first documented series of tests indicating the influence of the main parameters in a uniformly distributed fire load on the fire propagation.

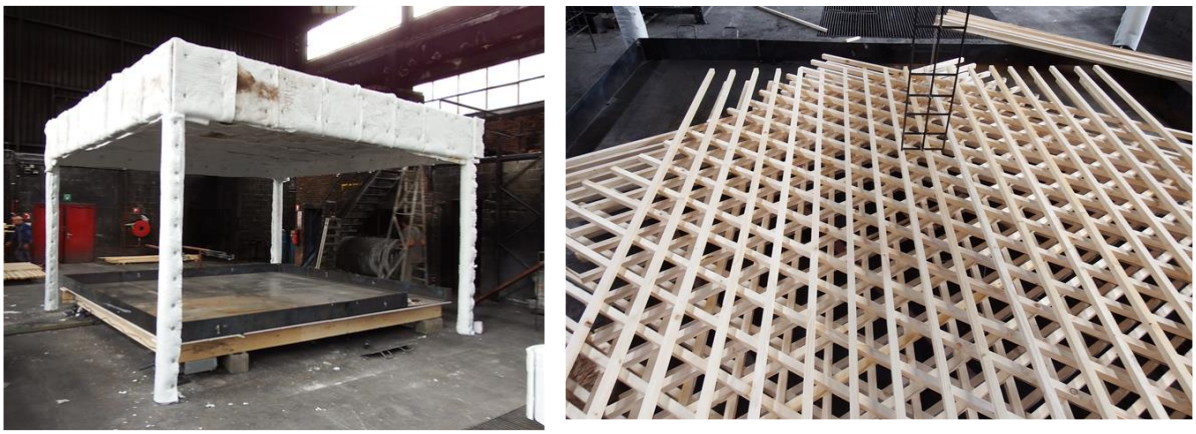

Figure 12: Test setup (left) and fire load arrangement (right)

3.1.3. Conclusions

From the analyses of experimental data performed in Liège and in Marchienne, the main results are the definition of a reproducible experimental protocol that ensures ignition of the uniformly distributed fire load, as well as the definition of a load arrangement that ensures a quasi-isotropic fire propagation without any manipulation of the fire load (no use of accelerant), see Figure 13.

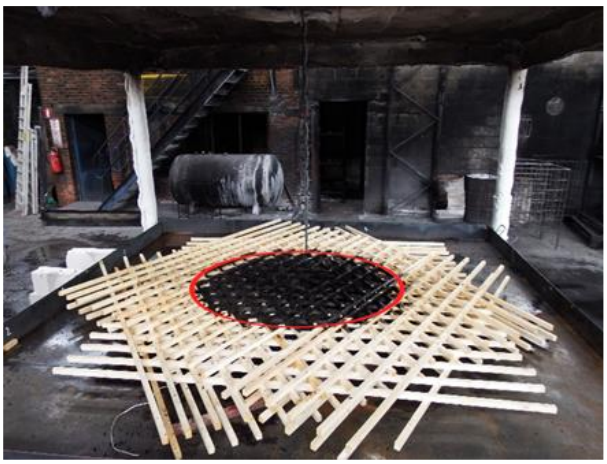

Figure 13: Isotropic fire propagation after the upper layers of sticks have been removed

The following conclusions can also be brought:

- The highlight of the influence of the ceiling in the propagation rate, even in a completely fuel controlled situation.
- The fact that propagation in the fire source without manipulation can be obtained for timber in which the moisture content corresponds to the values that can be observed in a service class 1 or service class 2 environment according to Section 2.3.1.3 of EN 1995-1-1 (ranging here from 13% to 17%, with the exception of one test that incorporated also a small quantity of PMMA).
- The fact that the volumetric ratio of timber in the apparent fire source seems to be the dominant factor that is driving the propagation rate, rather than the size of the sticks themselves.
- The proposal of a uniformly distributed fire load arrangement (see Table II) based on 30x35 mm² timber sticks that can lead in experimental tests to a slow, a medium of a fast fire propagation rate (according to EN 1991-1-2) with a fire load density that, based on a specific mass of 468 kg/m³ and a calorific (nominal) value of 14 MJ/kg (=0.8 * 17.5), corresponds to the one recommended for office buildings in EN 1991-1-2, i.e. 511 MJ/m^2.

	Pitch between the sticks [mm]	**Horizontal shift from layer I to layer i+3**	**Number of layers**	**Fire load [MJ/m²]**
Slow fire	90	No	7	535
Medium fire	135	Yes	10	510
Fast fire	175	Yes	13	511

Table II: Recommendations for arrangement of the sticks

3.2. Influence of near field & far field and lame thickness dependence (WP2)

3.2.1. Introduction

Several tests studying the flame thickness dependence on radiative properties, the radiative and convective behaviour in far- and near-field as well as the effect of spread rate were launched, as well as a number of free burning tests on radiative properties of the flames.

3.2.1. Description of the activities

The first six tests utilised a steel structure, 18 m long, 6 meters wide and 3 m tall (see Figure 14). The structure was comprised of two identical 9m by 6m bays. One short end was open while the other was closed and downstands were situated along the long sides. The opening factor for the structure was comprised between 0.21 and 0.28 $m^{1/2}$ (see Table III**)**. In comparison to historical travelling fire experiments (Dai et al., 2017) the structure utilised for this task has a large amount of openings, however the compartment remains within the bounds of what is expected from an open plan office building in a high rise building (Brandon et al., 2020). In addition to the structural steelwork, two "dummy" columns (which provided no structural support) were used for the heating of structural columns by the fire. These were placed along the centreline of the compartment, one at the open end, and one at the centre of the compartment.

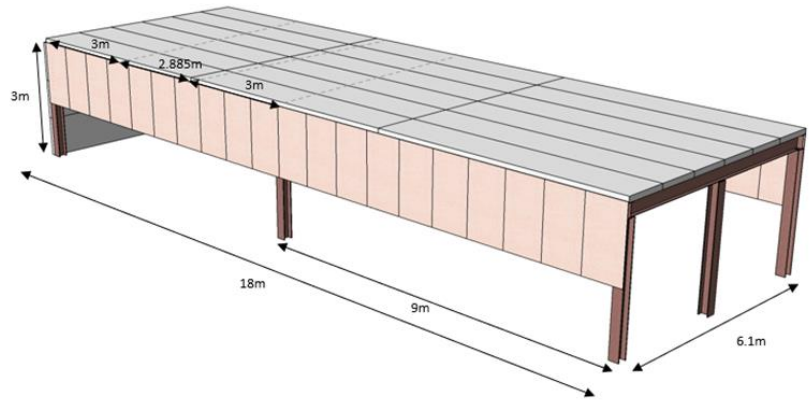

Steel Member Dimensions		
	Column	Beam
Height (mm)	230	300
Width (mm)	220	150
Flange (mm)	16	10.7
Web (mm)	9.5	5.9

Figure 14: Illustration, with dimensions, of the structure used for the small scale travelling fire experiments conducted in WP2 Task 2

The tests were completed with two different fuel types, 5 tests using diesel pans (each 4m x 0.5m in area) covering the rear half of the compartment, and a final test with wood cribs covering 2.5m of width over the full length of the compartment, as described in Table III. In the diesel pan test the flame propagation was manually controlled; the pans were covered with gypsum plaster boards to prevent ignition faster than the prescribed flame propagation speed.

TEST	VENT.	FUEL TYPE	FUEL LOAD [litres]	FUEL LOAD [KG][2]	AVERAGE IGNITION SPREAD (m/min)	DOWNSTAND HEIGHT[3]	OPENING FACTOR [M½]
1	High	Diesel	112[1]	91	0.50	1.4 m	0.28
2	High	Diesel	122	99	0.21	1.4 m	0.28
3	High	Diesel	211	171	0.13	1.4 m	0.28
4	Low	Diesel	166	134	0.16	1.4 m	0.28
5	Low	Diesel	168	136	0.16	1.8 m	0.21
6	Varying with length	Wood cribs	-	1588	0.06[4]	1.4 m (L<6m; L>12 m) 2.4 m (6<L<12 m)	0.22

[1] Test 1 was aborted after the ignition of the first two burners.
[2] ASSUMING A DIESEL DENSITY OF 810 KG/M[3].
[3] DISTANCE FROM CEILING lower surface
[4] CALCULATED FROM TEST RESULTS BY AVERAGING LENGTH OVER TOTAL FIRE TIME.

Table III: Overview of test series

In these tests a clearly defined smoke layer was formed in the structure and a relatively one-dimensional flow from the fires was established (see Figure 15). Considering the central dummy column, it was clear how the steel members in the far-field were heated up convectively by the hot gas layer. Within the hot gas layer there was a very low horizontal temperature gradient, implying that the shading effect of the flange closest to the fire had little effect and that the temperatures were close to homogeneous in the upper hot zone. Lower down the column, where it was within the cold gas layer, the horizontal gradient within the section was significantly larger (see Figure 16). The vertical gradient (i.e. along the height of the column) of temperature increase is about 75 % of the total temperature increase as the flames are still three meters from the member. As the flames move closer to a vertical element the radiant impact from the flames start to dominate, the lower part is now heated up much faster than the part covered in the hot gas layer and gradients increase quickly. When the flame is within one meter from the member the flange facing away from the flames is almost 300 °C along its full length. Meanwhile, the temperature of the flange facing the flames varies from 350 °C in the hot layer to a maximum of 500 °C close to the flame base.

Figure 15: Photo showing the clearly defined smoke layer in the diesel pool fire tests

This heterogeneous heating plays a large role in both the structural response to the fire where loads are being transformed through thermal movement and any possible failure mechanism of members (Sjöström and Lange, 2014). Also, the thick smoke layer is efficient in keeping the upper part of the member relatively uniform in temperature compared to the lower parts, more exposed to radiant heating.

After the controlled diesel oil pan tests, a test on a continuous fuel bed of wood cribs was performed (see Figure 17). This "additional" test was performed at the same time than the WP2 "characterization of fuel loads" tests, and the fire load arrangement established in the frame of this task could therefore not be used. For the first time a monotonic and stable travelling fire was observed under full-scale fire conditions. The flame did not form a thick, opaque gas layer but the ceiling was visible during the full test. The flame and burn out fronts moved about 1 mm/s forming a burning thickness of approximately 1.5 m in depth during the more than 4.5 hour long experiment.

The near-field behaviour of the vertical column is limited to very close proximity of the flame. In the far field prior to the flame front the temperature gradient of the column was monotonically increasing towards the hot gases in the ceiling. After the burn out the central parts of the column was more quickly cooled by the cold air compared to the bottom and the top (which was still under influence of hot gases close to the ceiling).

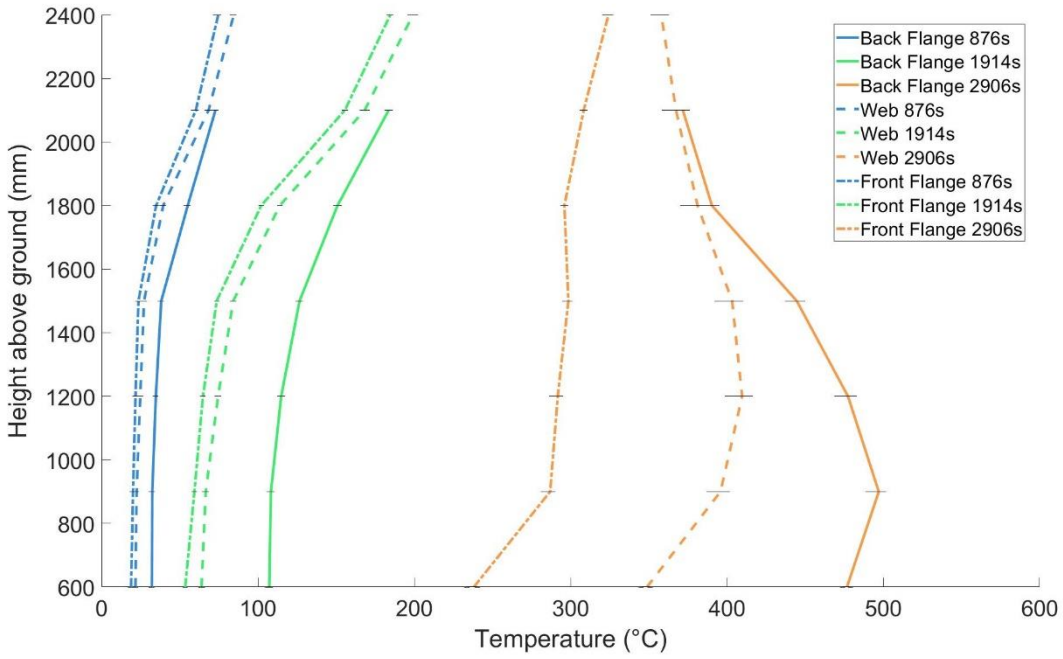

Figure 16: Temperatures with height in central dummy column at 3 different times for single diesel pool fire test (Test 4). Column flanges are perpendicular to the direction of fire travel and the back is flange closest to the fire.

Figure 17: Photo of the wood crib experiment showing the travelling fire

A second series of free burning experiments without a ceiling were conducted to study how much a flame will block radiation from a flame further behind it and how much the flame will radiate depending on its thickness, the experimental setup can be seen in Figure 18. It turns out that classical theory of flame emissivity and absorptivity was valid also for elongated flames (this finding could support the development of the analytical model from subsequent WP5, as described in Chapter 5). However, using the empirical absorptivity coefficient value of diesel oil, derived from circular pool fires, the mean free path of the flame must be set to 1-1.25 times the burning width instead of 0.45**D*, where *D* is the pool diameter for circular pools. This is also in line with the visible flame thickness from an elongated pool compared to the commonly observed narrowing of circular pool flames. Thus, the radiant behaviour in the far field can be well described by classical radiation theory provided the engineer takes the actual thickness of the flames properly into account (i.e. for an elongated flame front, the thickness is larger than that of an equivalent pool).

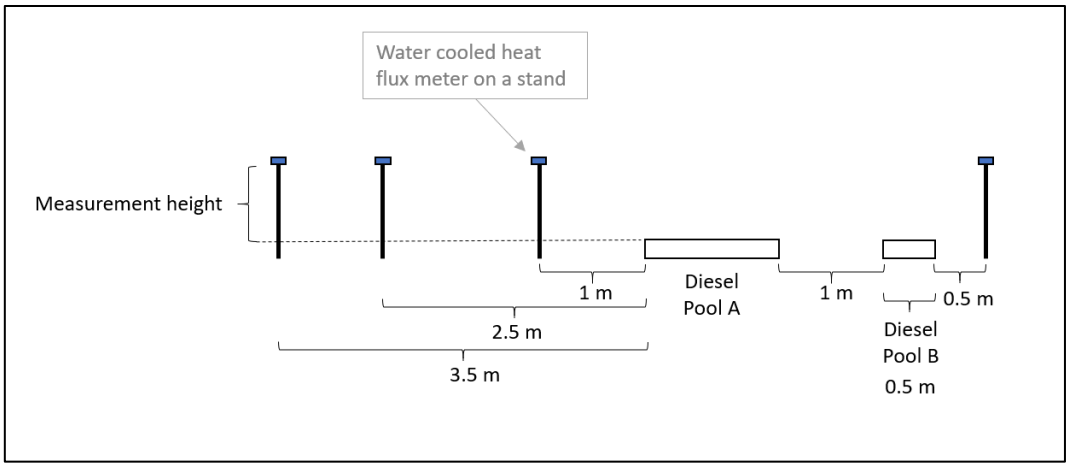

Figure 18: Experimental set-up to study the effect of flame thickness on blocking radiation

3.2.2. Conclusions

The results of this task serve a number of purposes. First, we note how a thick smoke layer, which is typically observed in a structural fire, will divide the heating of steel elements into two zones, a strongly convective driven zone within the smoke layer and strongly radiant driven below the layer. Far field flames will therefore contribute to heating of the upper elements while near field flames more to the lower. These two different mechanisms will in turn induce large thermal gradients in vertical members as flames pass, thereby affecting the structural response. The study also shows that under opening factors statistically relevant for high rise office buildings a continuous travelling fire can be achieved under non-combustible ceilings, something not explicitly shown before.

Finally, the flame thickness dependence on the radiative behaviour of elongated flames follows classical flame absorption theory but the real flame thickness (wider for elongated flames than the D*0.45 assumed for square or circular pools), must be taken into account should the emissivity be calculated as part of any implementation. This is consistent with the assumption considered in the subsequent analytical model (WP5) as the flame emissivity is assumed to be 1 (which is conservative).

3.3. Large-scale natural fire tests (WP3)

3.3.1. Introduction

Three large-scale fire tests were conducted in a compartment representing a steel-framed building with real dimensions and a continuous wood crib fuel bed. The aim was to characterize a realistic travelling fire (i.e. with no manipulation during the course of the fire): its shape and spread as well as how it thermally impacts the surrounding structure. Under WP3, three main objectives were defined and completed:

- Performing large-scale fire tests in real building dimensions and with no control over the dynamics to aim a representation of travelling fires as realistic as possible;
- Conducting three large-scale tests:
  - Test 1 – a travelling fire - fuel controlled situation – 14th June 2019
  - Test 2 – another travelling fire - intermediate between a fuel controlled and a ventilation-controlled situation - 26th July 2019
  - Test 3 – a flashover – ventilation-controlled situation - 30th August 2019;
- Providing recorded observation of the path and geometry of the fire, and measurements of temperatures, heat fluxes and spread rates.

3.3.2. Description of the activities

Building the compartment

Figure 19 shows the erection of the steel structure and the placing of precast concrete slabs. The floor plan between the outer gridlines of the test structure was 15 m x 9 m as shown in Figure 20. The level of the ceiling from the floor finish surface was 2.90 m. The

steel columns were separated into two categories, the structural columns and the dummy columns. The structural columns were part of the steel frame transmitting the loads to the foundation while the dummy columns were not part of the structural steel frame. The structural columns were spaced at 5 m centres along the long compartment dimension and 30 m centres along the short. The structural frame was laterally restrained using four diagonal bracings, two each along the longer and the shorter directions. The dummy columns provided for data acquisition purposes were anchored to the bottom flanges of the steel beams. The structural steel used for the construction of the test compartment was grade S355. Both the structural and dummy columns, as well as the beams provided along the longer direction, consisted for HEA-200 steel sections. On the other hand, the beams in the shorter direction consisted of HEA-160 steel sections.

Figure 19: Compartment preparation build on strong existing reinforced concrete platform

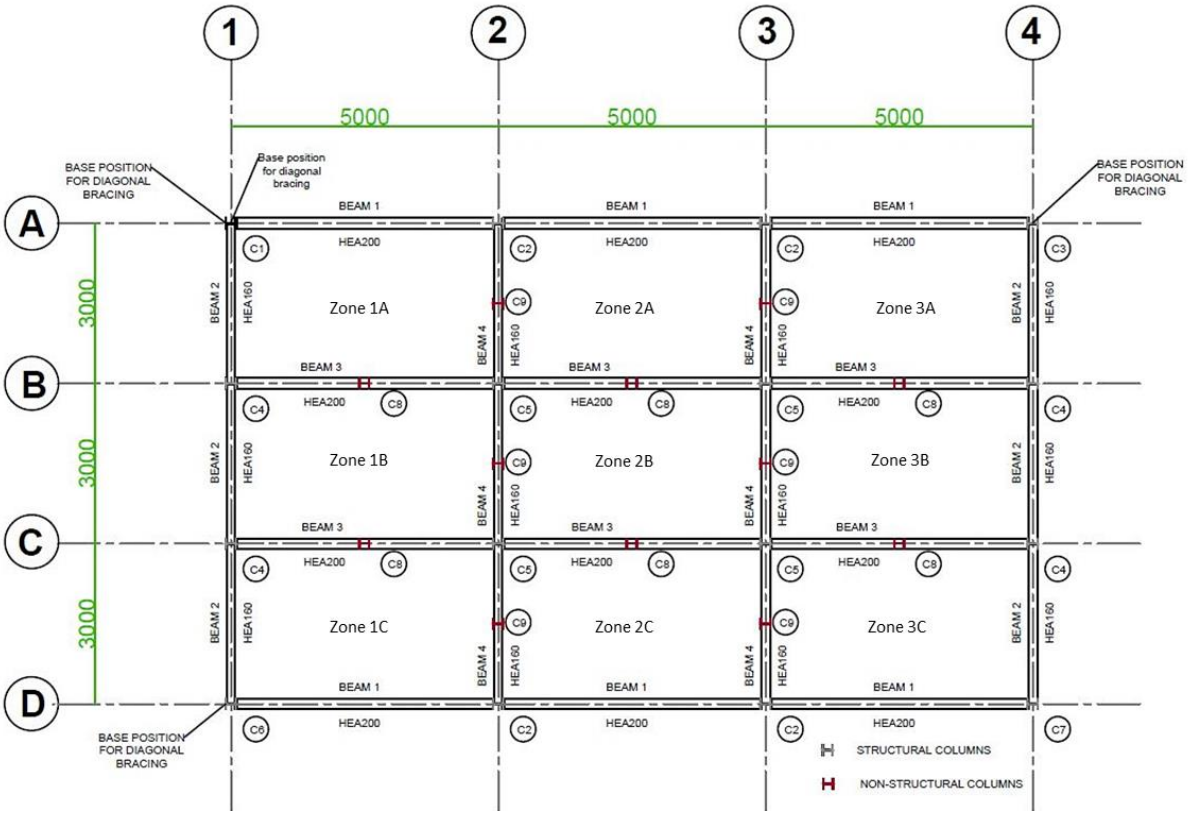

Figure 20: Layout plan of the test compartment

The roof consisted of 120 mm thick hollow-core precast concrete slabs spanning between the beams along the shorter direction of the test compartment. Further protection was added to safeguard the instrumentation cabling from exposure to heat and fire as shown in Figure 21. Keeping in view the usage of the test compartment, the main structural columns of the steel frame were protected using intumescent coating in order to maintain the structural integrity during the fire tests as well as to ensure the use of the test structure multiple times during the project. It can be seen in Figure 21 that only the structural columns are protected while the dummy columns are kept unprotected for data acquisition purposes.

Figure 21: The fire blanket used to protect the cables of instrumentation (left) and the protected columns of the test compartment (right)

The fire load

The fuel bed specifications were defined by the outcome from "Characterization of fuel loads" (WP2). The fuel wood source consisted of the species "*Picea abies*" with an average density 470 kg/m³ having a moisture content of 15.22%. As the test compartment was a representative of a modern office building, Eurocodes propose a medium fire growth rate for such occupancies. To achieve a medium fire growth rate for the office building, the previous TRAFIR findings were used: 9 layers of wooden sticks with an axis distance of 120 mm (90 mm intervals) were provided in three different directions. The wood sticks were 30 mm wide and 35 mm deep. The first layer of the wooden sticks was laid at 60° angle while the second was laid at an angle of 120°. The third layer was at 0° or 180° and the process was repeated in such a way the 6th layer of the sticks laid at 0° or 180° had a lateral offset of 60 mm with respect to the third layer as shown in Figure 22. The final layer, the ninth layer, of the fuel wood was at 0° or 180°, such an arrangement helped to visually observe the travelling behaviour of fire from one stick to another.

The instrumentation and data logging system

The full description of the instrumentation and data logging system is provided in the Appendices: it allows to measure gas temperatures, steel temperatures, heat fluxes and mass loss.

Figure 22: Platform for laying of fuel wood (left) and fuel wood arrangement used during the three large-scale tests (right)

Test 1

The boundary conditions for the fuel-controlled tests were designed by assuming the compartment to be a part of a large open plan office. To replicate such a scenario, a solid concrete wall was constructed along the shorter dimension of the compartment along gridline 1. In addition to the back wall, down-stands were provided along the longer dimension of the test compartment along gridlines A and B as shown in the schematic diagram in Figure 23. Neither the wall nor the down-stands were provided along the shorter dimension of the test compartment along gridline 4.

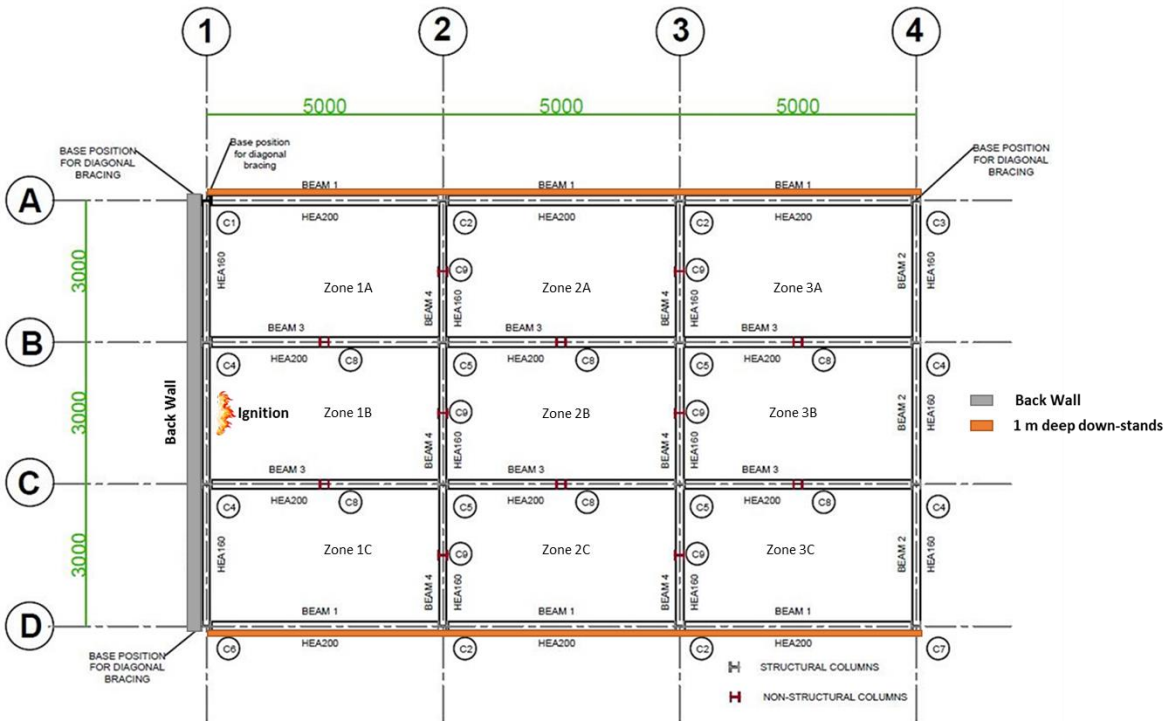

Figure 23: Schematic view of the boundary conditions for Test 1

Figure 24: Boundary conditions for Test 1

The back wall was constructed using precast concrete provided by FP McCann Ltd, while the down-stands consisted of two layers of gypsum fire board panels having a thickness of 2x12.5 mm and a minimum fire rating of 60 minutes. The back wall and the down-stands were provided in such a way that they covered the whole length of the test compartment as shown in Figure 24. The down-stands allowed for smoke accumulation below the ceiling (but still having one escape route as the shorter direction of the test

compartment along gridline 4 was kept open). During Test 1, the area of provided openings was 87 m^2. Figure 25 demonstrates the start and completion of test 1: a clear travelling fire was observed.

Figure 25: Photographs taken during Test 1

The evolution of the maximum flame thickness (i.e. longitudinal distance between the fire front and the burn out) can be evaluated and is represented in Figure 26. The square markers correspond to a translation of the visual observations made during the test, while the triangle markers correspond to inspection made from the video recording of the test. This evolution suggests a fairly constant flame thickness of around 3,5 meters, with the lowest value occurring when the fire reaches the central bay of the compartment. The "travelling" behaviour of the fire starts at 28 minutes from ignition for Test 1.

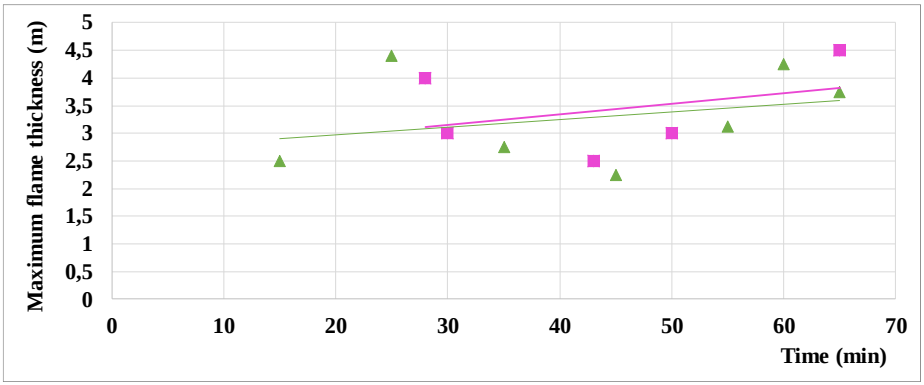

Figure 26: Evolution of the maximum flame thickness for Test 1

Test 2

The boundary conditions for Test 2, the intermediate between the fuel-controlled and the ventilation-controlled fire, were different in comparison to those provided during Test 1 (the change in openings is the only modification by comparison to Test 1). An additional concrete block wall was constructed along the shorter dimension as shown in Figure 27.The wall along shorter dimension was similar to the back wall as it covered the whole depth of the test compartment. In addition to the down-stands, a concrete block wall was constructed along the longer dimensions (see Figure 27). Such a selection of the boundary conditions provided openings with a total area of 30 m^2. Figure 28 demonstrates the completion of the test: a clear travelling fire was observed.

The evolution of the maximum flame thickness (i.e. longitudinal distance between the fire front and the burn out) can be evaluated and is represented in Figure 29. The data of this figure is selected such that only "travelling fire" flame thicknesses are displayed (i.e., no point corresponds to the growing stage of the fire, when the back end hasn't start travelling yet). The "travelling" behaviour of the fire starts at 27 minutes from ignition for Test 2.

Figure 27: Boundary conditions for Test 2

Figure 28: Photographs taken during Test 2

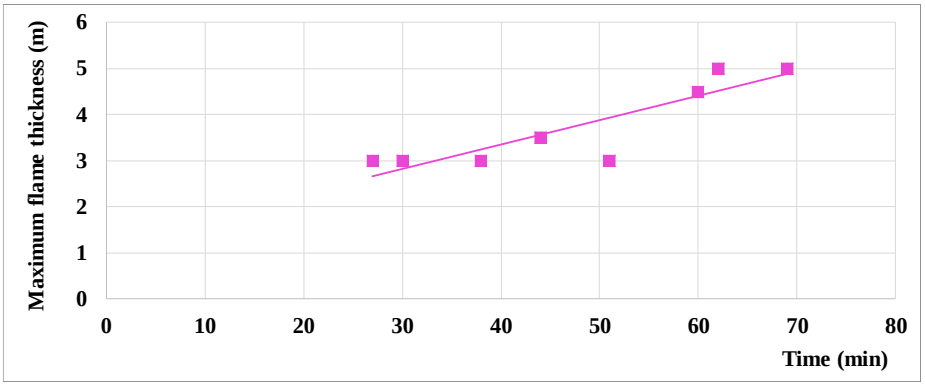

Figure 29: Evolution of the maximum flame thickness for Test 2

Test 3

In order to achieve a ventilation-controlled fire scenario, the area of openings was further reduced during Test 3 (see Figure 30). The walls along the shorter dimension were same as those used during Test 2, while the depth of the walls along the shorter dimension was increased at selected locations. Such provision of the boundary openings provided a total opening area of 9.6 m^2 in the test compartment. Figure 31 demonstrates the completion of Test 3: the fire started to travel, then a flashover occurred.

The evolution of the maximum flame thickness (i.e. longitudinal distance between the fire front and the burn out) can be evaluated and is represented in Figure 32. The data of this figure is selected such that only "travelling fire" flame thicknesses are displayed (i.e., no point corresponds to the growing stage of the fire, when the back end hasn't start travelling yet).

The whole duration of the three fire tests was recorded using video cameras located at different positions. In addition to the video recording, photographic data was also documented.

Figure 30: Boundary conditions for Test 3

Figure 31: Photographs taken during Test 3

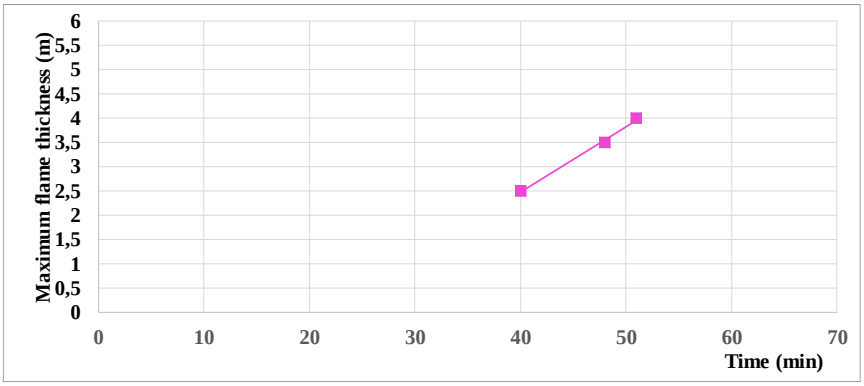

Figure 32: Evolution of the maximum flame thickness for Test 3

3.3.3. Conclusions

Results for Test 1

For Test 1; a clear travelling fire was observed. Referring to the Figure 73 (Appendix) providing the location of thermocouple trees in the test compartment, the Figure 33 (left) provides the gas temperatures recorded using thermocouple tree TRL6 positioned in the middle of the test compartment (and within the fuel bed) while Figure 33 (right) provides the gas temperatures recorded using thermocouple tree TRS3 positioned along gridline 2 and between gridlines C and D of the test compartment (outside the fuel bed).

The Figure 34 provides graphs plotting the evolution of gas temperatures in the compartment along the longer dimension, parallel to the path of the travelling fire, in five thermocouple trees (TRL4 to TRL8) equipped with six sensors each (as described in Figure 72 (left)), Level 1 being close to the floor level and Level 6 being close to the ceiling level. It has to be noted that the Level 1 actually lies within the fuel load. The first thermocouple tree was positioned in the middle of zone 1B at 1.5 m from the source of ignition. The thermocouple trees TRL4 through TRL8, placed along the centreline of the compartment, were equidistant and positioned at 2500 mm centres.

Temperatures were also monitored in the test structure which included the steel columns and beams. In this report, the column and beam along gridline 3 positioned between gridlines B and C have been selected for data presentation purposes. The temperatures recorded in the flanges and the web of the column (close to TRL7) are presented in Figure 35. The label “LHS-F” corresponds to the flange closer to gridline C, “WEB-L” corresponds to the web and “RHS-F” corresponds to the flanges closer to gridline B. It can be observed that the heating profiles vary along the height of the column, but that the steel temperatures within a given section can be considered as uniform. The thermal data recorded in the selected beam during the second test is given in Figure 36 (left). The maximum recorded temperatures reach 706ºC after 63 minutes from ignition. It is was found that the recorded temperatures in the bottom flange, web and the top flange are non-uniform, with temperatures in the top flange being the lowest. The evolution of the mass loss measurement is provided in Figure 36 (right).

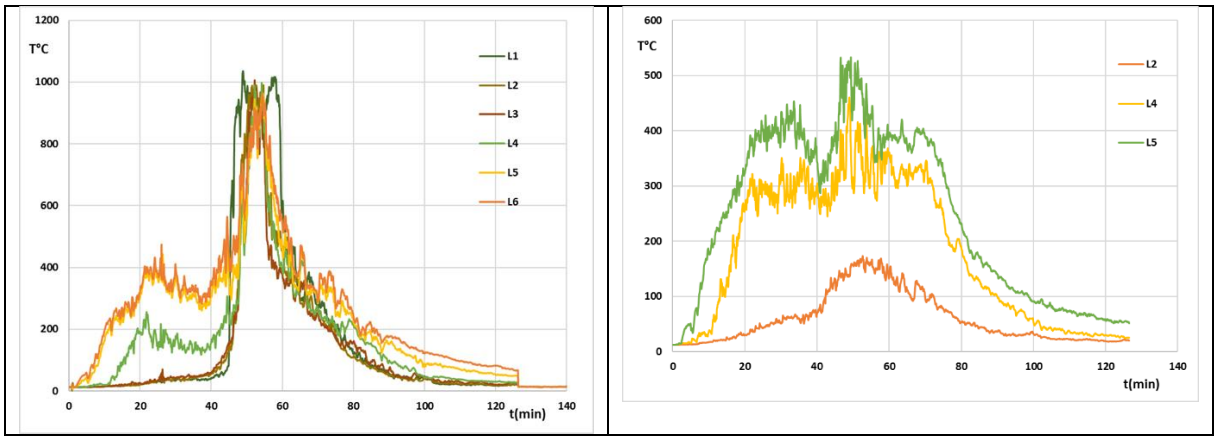

Figure 33: Gas temperatures recorded in TRL6 – Test 1 (left) and recorded in TRS3 – Test 1 (right)

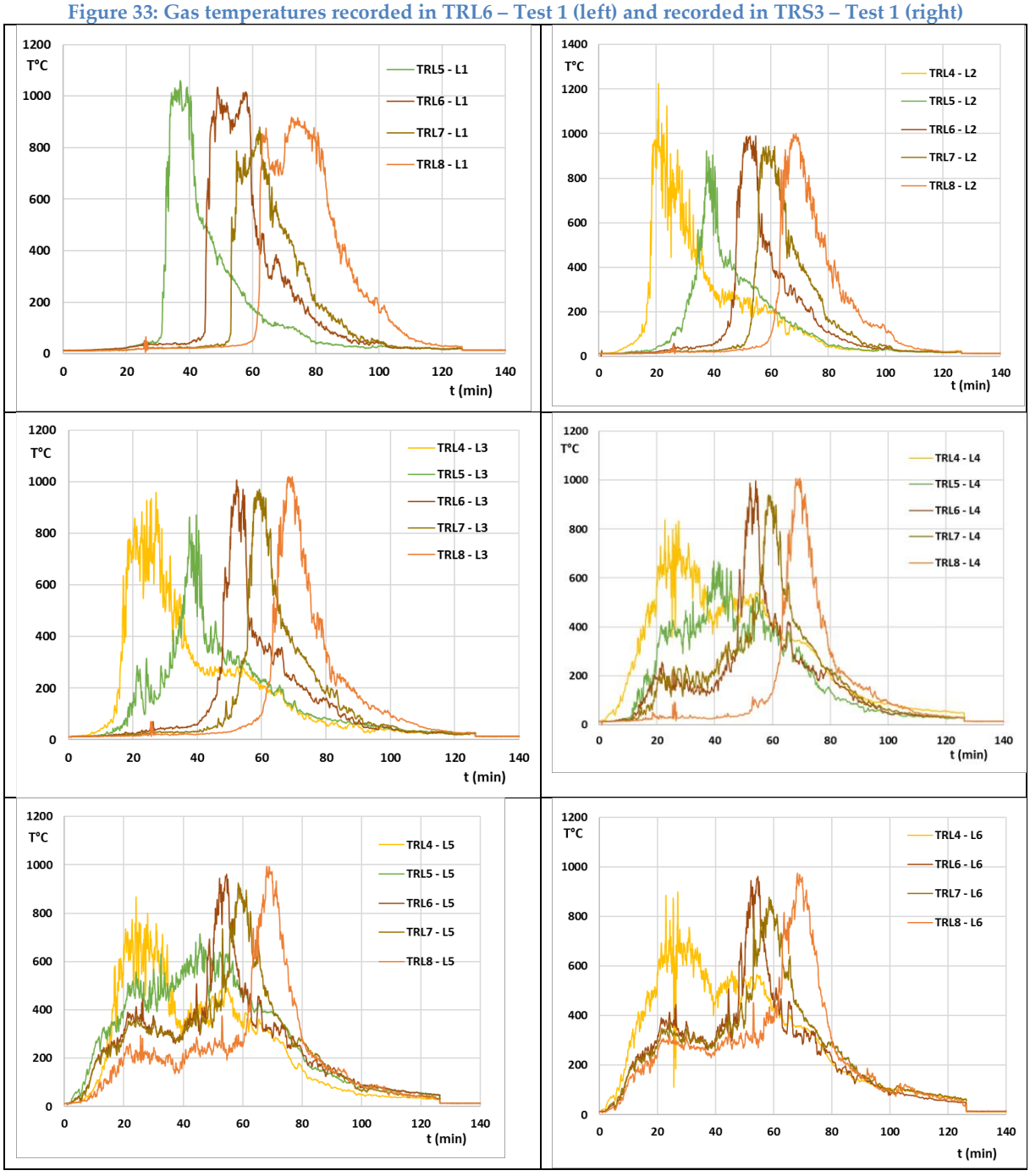

Figure 34: Gas Temperatures recorded in thermocouples trees TRL4 to TRL8 at different levels – Test 1

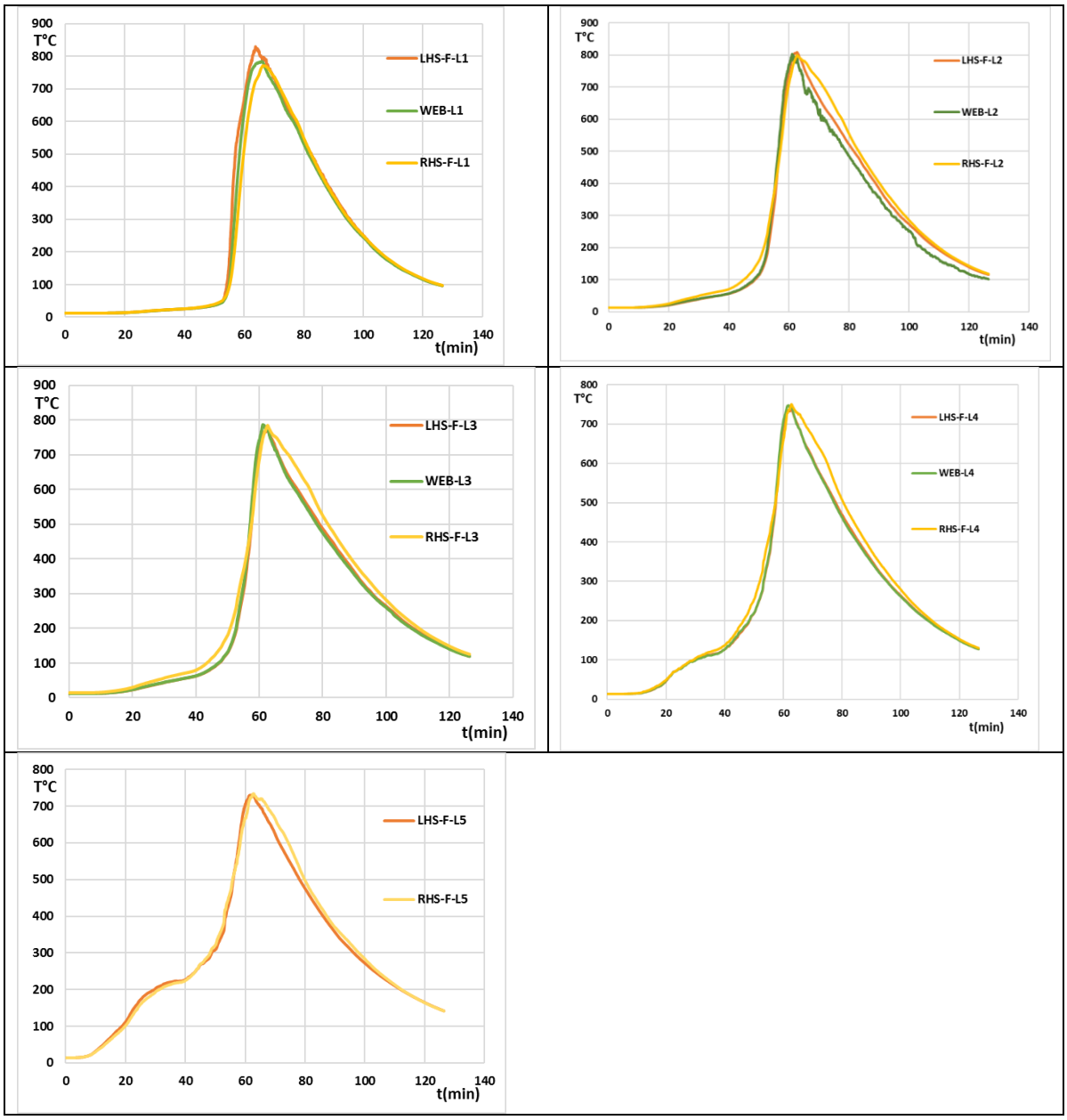

Figure 35: Steel temperatures at different locations along the height of the column close to TRL7– Test 1

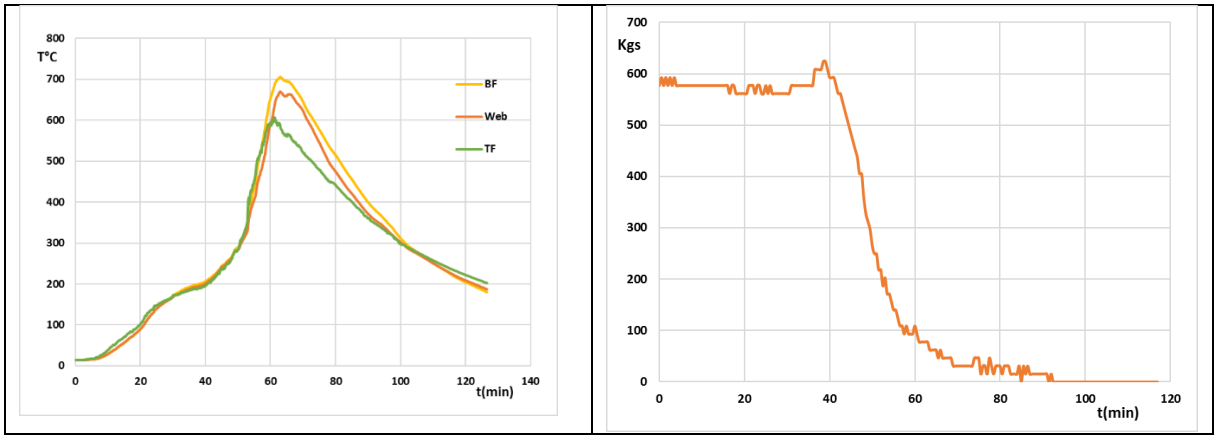

Figure 36: Steel temperatures in the selected beam – Test 1 (left) and evolution of the mass loss measurement – Test 1 (right)

Results for Test 2

Referring to the Figure 73 (Appendix) providing the location of thermocouple trees in the test compartment, the Figure 37 (left) provides the gas temperatures recorded using thermocouple tree TRL6 positioned in the middle of the test compartment (and within the fuel bed) while Figure 37 (right) provides the gas temperatures recorded using thermocouple tree TRS3 positioned along gridline 2 and between gridlines C and D of the test compartment (outside the fuel bed). The Figure 38 provides graphs plotting the evolution of gas temperatures in the compartment along the longer dimension, parallel to the path of the travelling fire in TRL4 to TRL8 equipped with six sensors each (as described in Figure 72 (left)), Level 1 being close to the floor level and Level 6 being close to the ceiling level.

The temperatures recorded in the flanges and the web of the column close to TRL7 are presented in Figure 39. The label "LHS-F" corresponds to the flange closer to gridline C, "WEB-L" corresponds to the web and "RHS-F" corresponds to the flanges closer to gridline B. As for Test 1, it can be observed that the heating profiles vary along the height of the column, but that the steel temperatures within a given section can be considered as uniform. The thermal data recorded in the selected beam during the second test is given in Figure 40 (left). The maximum recorded temperatures are 700ºC after 66 minutes from ignition. It is was found that the recorded temperatures in the bottom flange, web and the top flange are non-uniform, with temperatures in the top flange being the lowest.

The evolution of the mass loss measurement is provided in Figure 40 (right). With the increase in the quantity of the burning fuel, an increase in the mass loss is recoded which is rapid for the next 20 minutes and later decreases as the fuel wood is consumed.

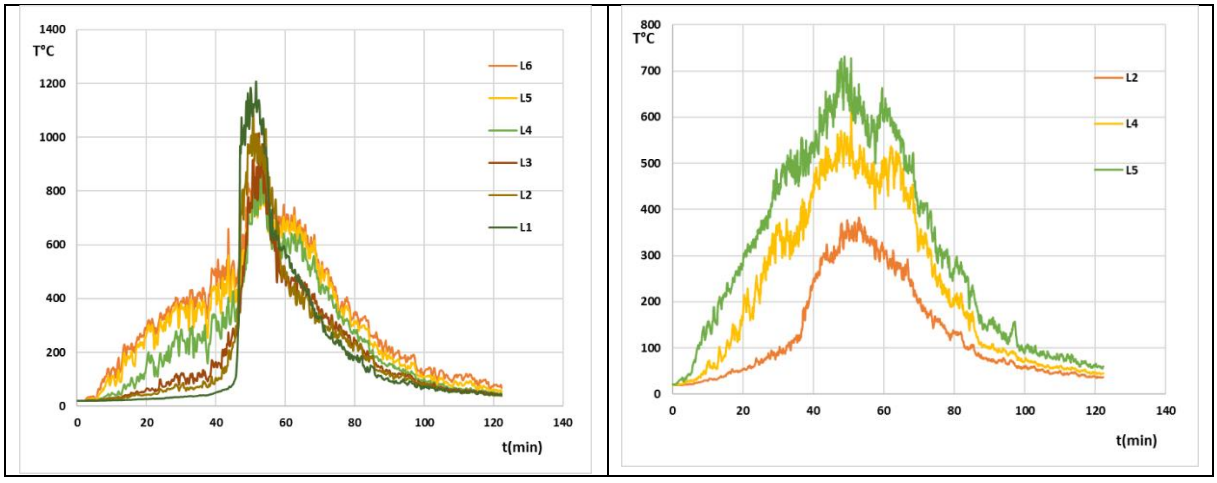

Figure 37: Gas temperatures recorded in TRL6 positioned in the middle of the compartment within the fuel bed – Test 2 (left) and Gas temperatures recorded in TRS3 positioned along gridline 2 and between gridlines C and D of the compartment outside the fuel bed – Test 2 (right)

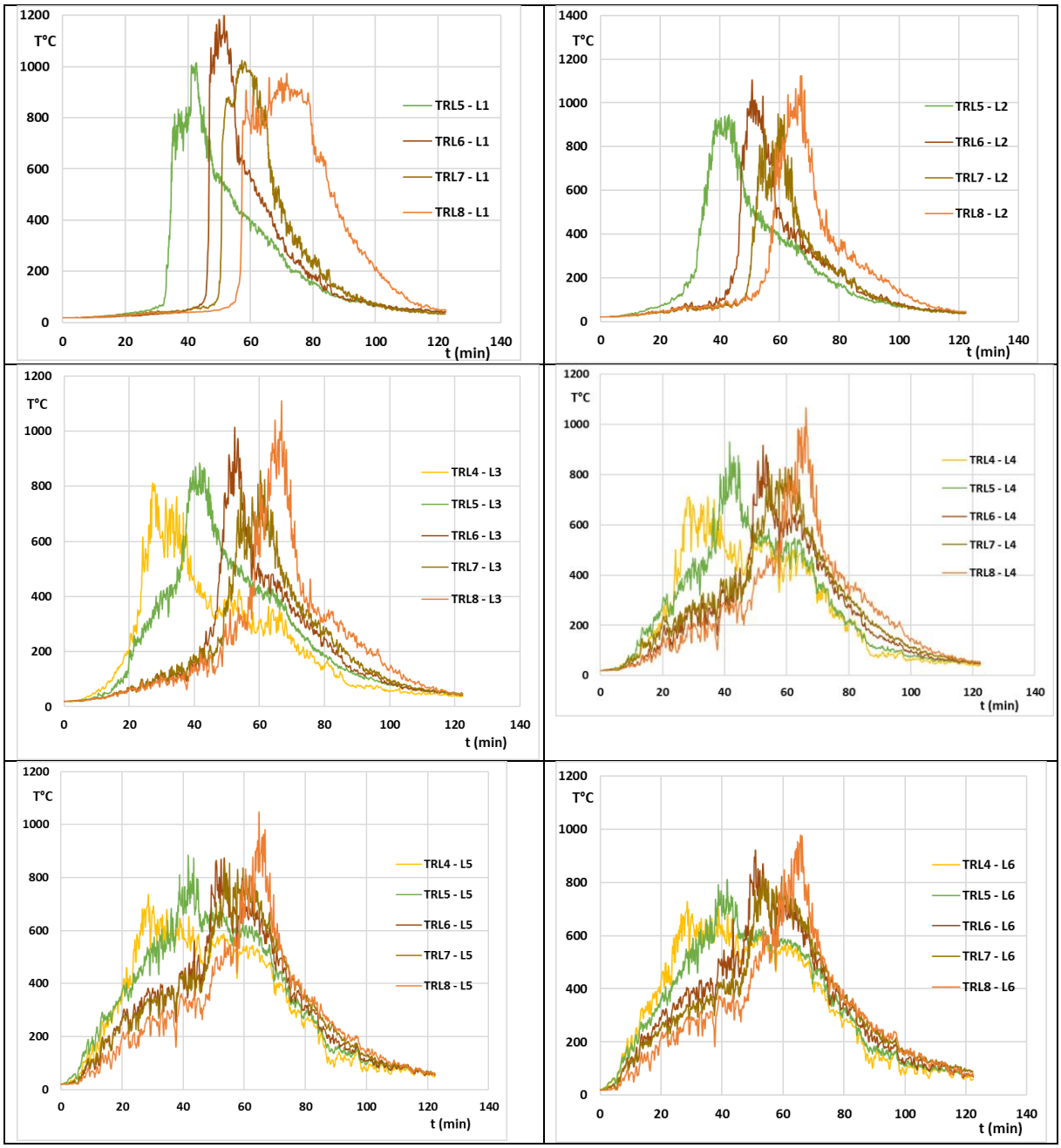

Figure 38: Gas Temperatures recorded along the length of the compartment in thermocouples trees TRL4 to TRL8 at different levels – Test 2

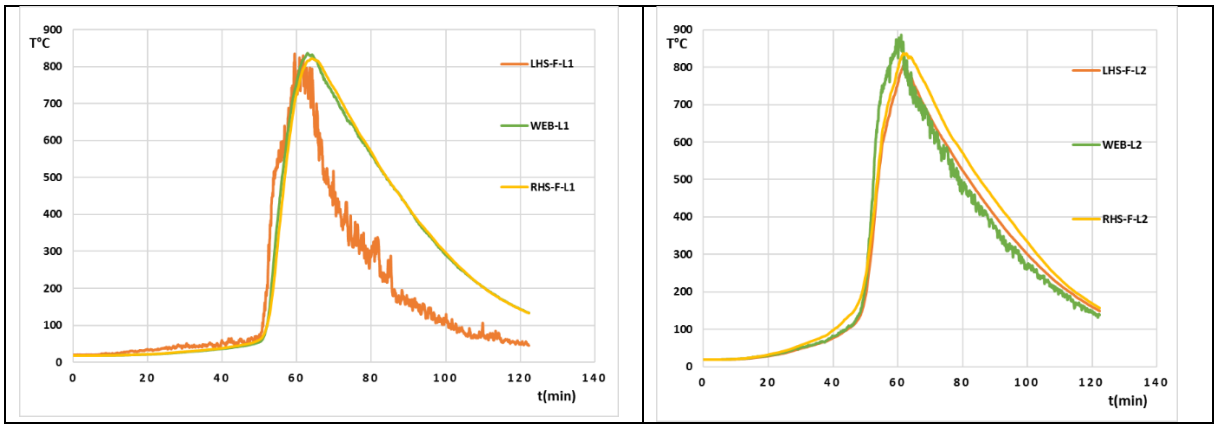

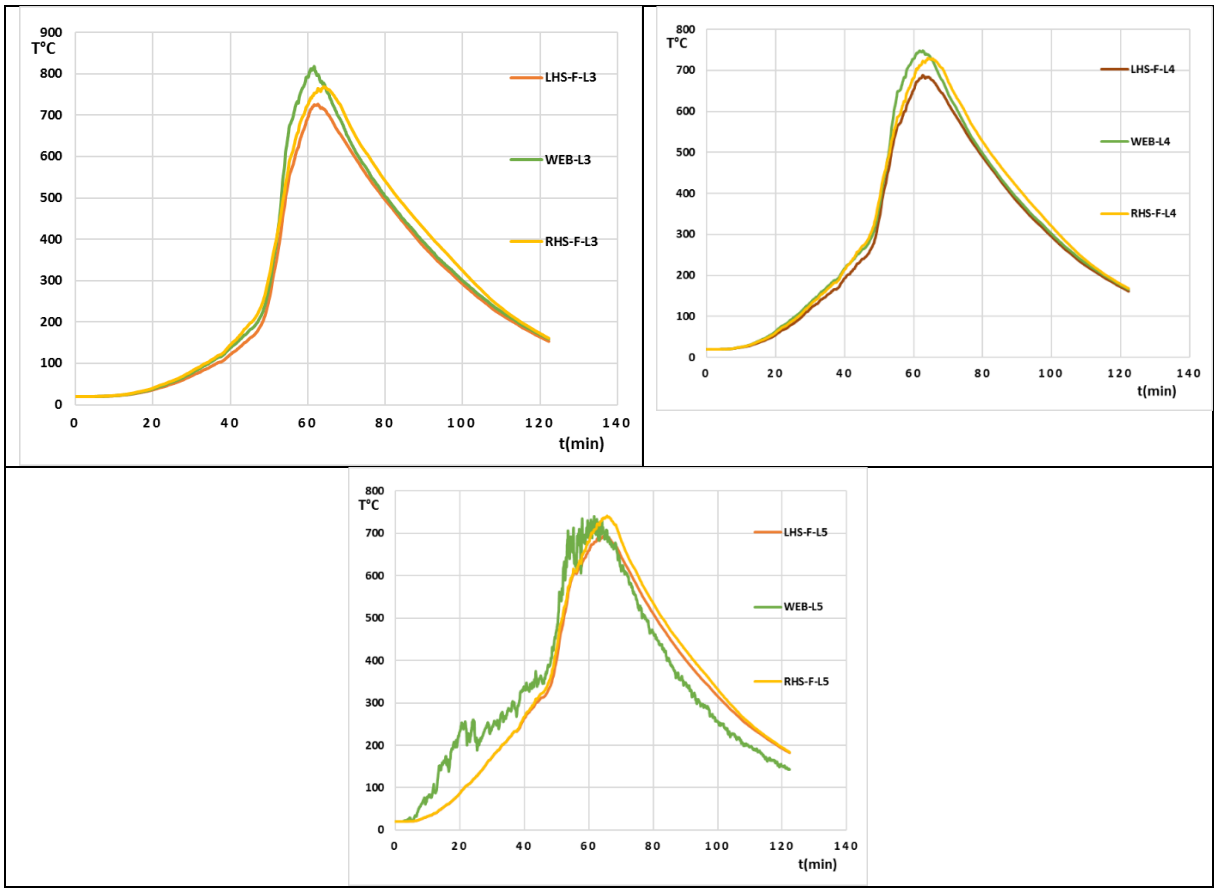

Figure 39: Steel temperatures at different locations along the height of the column close to TRL7– Test 2

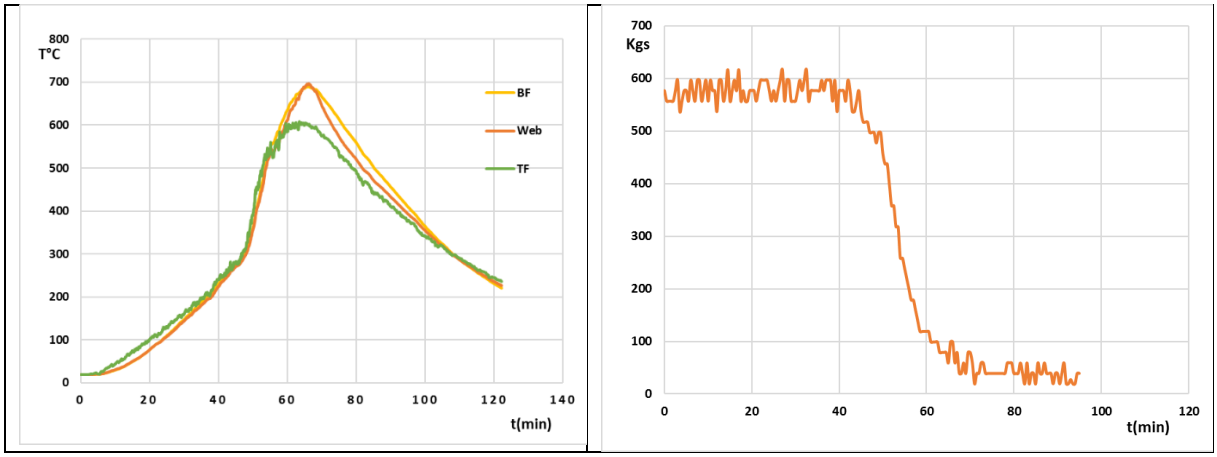

Figure 40: Steel temperatures in the selected beam – Test 2 (left) and evolution of the mass loss measurement – Test 2 (right)

Results for Test 3

Referring to Figure 73 (Appendix) providing the location of thermocouple trees in the test compartment, Figure 41 (left) provides the gas temperatures recorded using thermocouple tree TRL6 while Figure 41 (right) provides the gas temperatures recorded using thermocouple tree TRS3. Figure 42 provides graphs plotting the evolution of gas temperatures in the compartment along the longer dimension, parallel to the path of the travelling fire in TRL4 to TRL8 equipped with six sensors each (as described in Figure

72 (left)), Level 1 being close to the floor level and Level 6 being close to the ceiling level.

The temperatures recorded in the flanges and the web of the column close to TRL7 are presented in Figure 43 (the thermocouple for LHS-F-L1 seems to have been deficient). The label "LHS-F" corresponds to the flange closer to gridline C, "WEB-L" corresponds to the web and "RHS-F" corresponds to the flanges closer to gridline B. The variation in temperatures along the height of the column is smaller than for Test 1 and Test 2. As for Test 1 and Test 2, the steel temperatures within a given section can be considered as uniform. The thermal data recorded in the selected beam during the second test is given in Figure 44. The maximum recorded temperatures reach 792°C after 69 minutes from ignition (versus 706° after 63 minute for Test 1 and 700ºC after 66 minutes for Test 2). It is was found that the recorded temperatures in the bottom flange, web and the top flange are non-uniform, with temperatures in the top flange being the lowest (but this effect is less pronounced than for Test 1 and Test 2).

The evolution of the mass loss could not be measured for Test 3. Unfortunately, there was a malfunctioning of the load cells and attached cables. As a result, data related to MLR could not be recorded despite all efforts to setup the equipment and other relevant accessories.

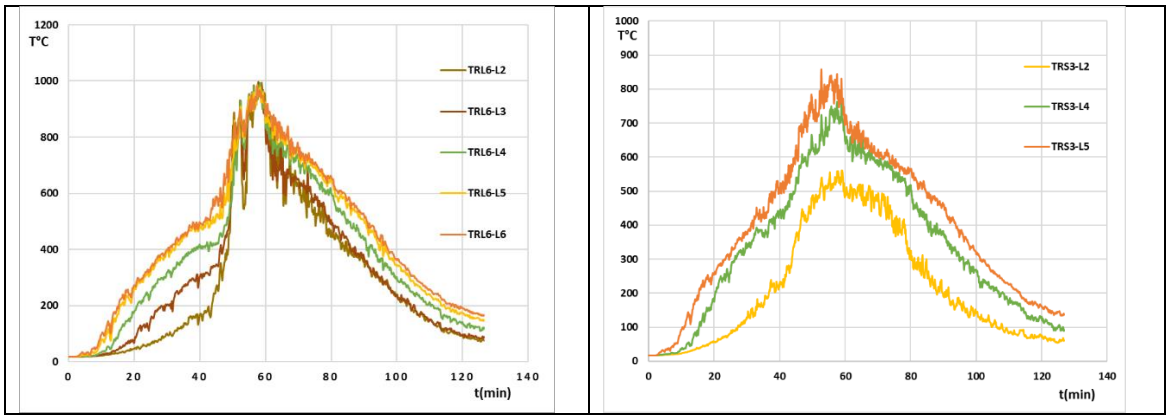

Figure 41: Gas temperatures recorded in TRL6 positioned in the middle of the compartment within the fuel bed – Test 3 (left) and Gas temperatures recorded in TRS3 positioned along gridline 2 and between gridlines C and D of the compartment outside the fuel bed – Test 3 (right)

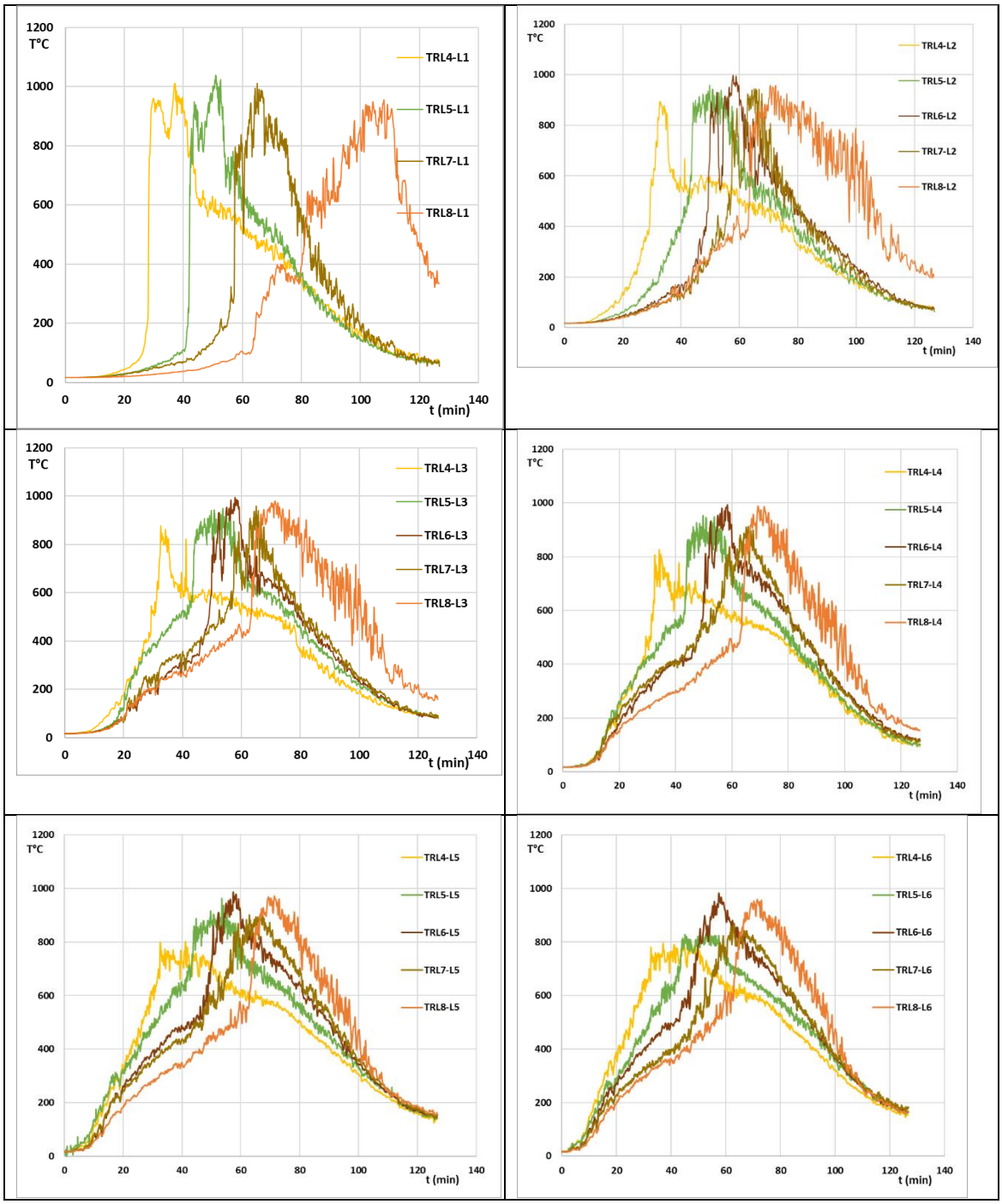

Figure 42: Gas Temperatures recorded along the length of the compartment in thermocouples trees TRL4 to TRL8 at different levels – Test 3

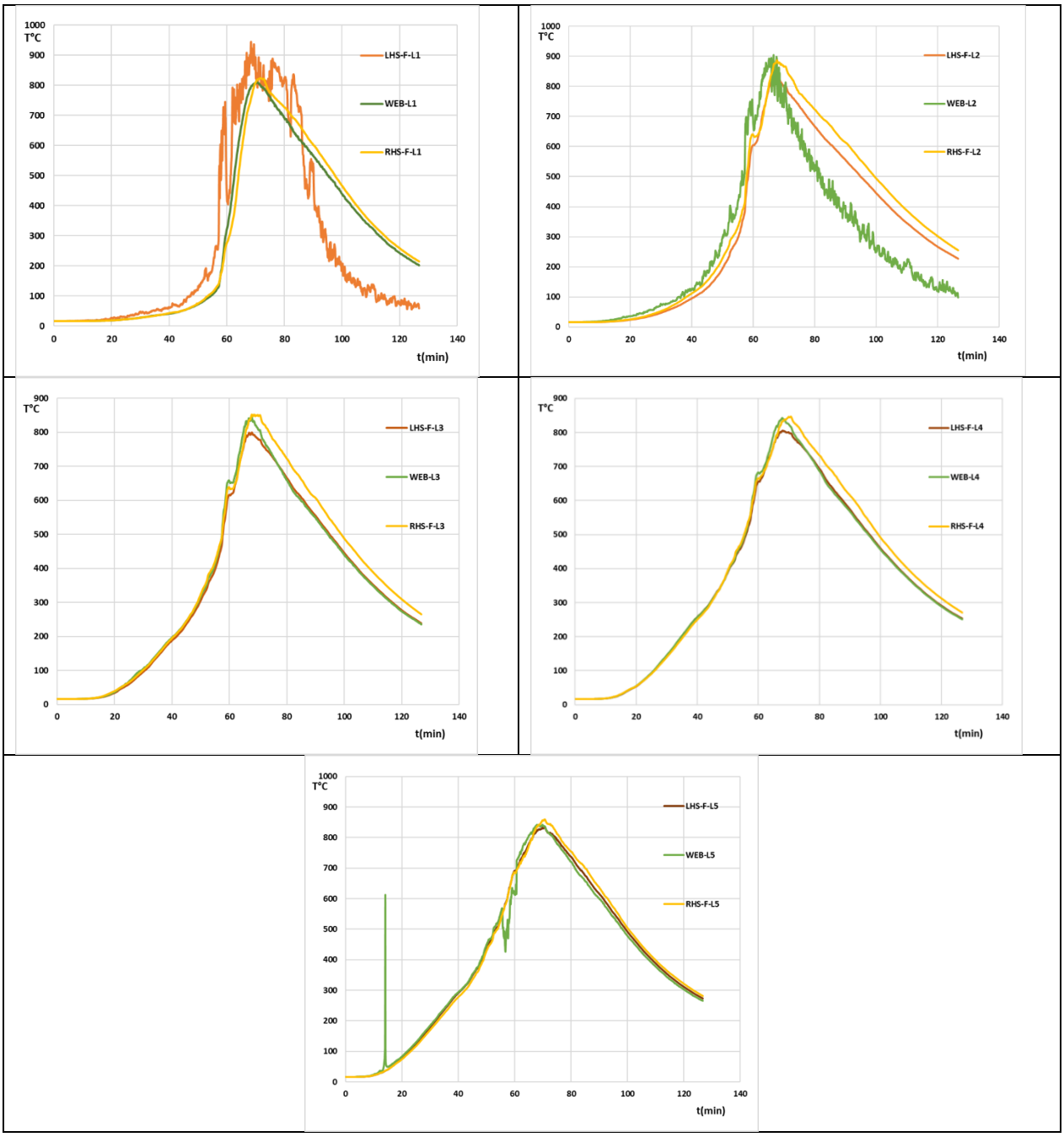

Figure 43: Steel temperatures at different locations along the height of the column close to TRL7– Test 3

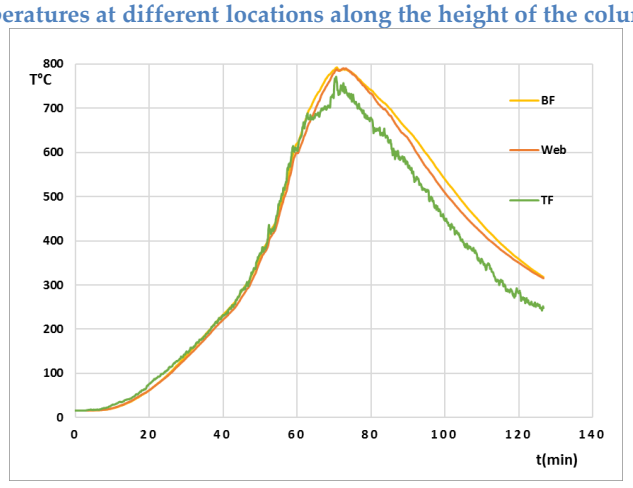

Figure 44: Steel temperatures in the selected beam – Test 2

Main conclusions

These three tests, for which only the total openings surface was varied (openings reduced from Test 1 to Test 2 and from Test 2 to Test 3), highlighted the influence of the ventilation conditions on the type of fire scenario. Indeed, a clear travelling fire was observed for Test 1 and Test 2 while a travelling fire leading to a flashover occurred for Test 3.

For the three tests, it can be observed that the gas temperatures evolutions present different profiles. For a given thermocouple tree, the temperatures measured at higher levels (levels 5 and 6) start to increase at earlier stages of the test as hot gases rise, resulting in a hot layer in the upper part of the compartment. This is followed by the rise in temperatures at the level 4, and then at lower levels (1-2-3) when flames reach the thermocouple tree. For Test 1 and Test 2, the evolution of the gas temperatures along the length of the compartment clearly highlights the travelling nature of the fire. The TRL6 to TRL8 (placed further away than the ignition location) seems to present a shorter temperature peak than TRL4 and TRL5 (placed closer to the ignition location). All of the above mentioned observations become less pronounced when decreasing the total openings surface.

For the steel column temperatures, it can be observed that the heating profiles vary along the height of the column, i.e. there is a vertical gradient of temperatures (effect more pronounced for Tests 1 and 2), but that the steel temperatures within a given section can be considered as uniform. For Test 1, Test 2 and Test 3, the maximum steel temperatures are around 800°C, 850°C and 900°C, respectively.

For the steel beam temperatures, it is was found that the recorded temperatures in the bottom flange, web and the top flange are non-uniform, with temperatures in the top flange being the lowest (but this effect is less pronounced for Test 3 than for Test 1 and Test 2). For Test 1, Test 2 and Test 3, the maximum steel temperatures are around 700°C, 700°C and 800°C, respectively.

4. Numerical modelling and parametric studies

4.1. Modelling the fire tests (WP4)

4.1.1. Introduction

This work concerns the calibration and parametrical analysis of the numerical models, with the purpose of establishing a simulation based complement to experimental tests and using it to perform numerical experiments to investigate travelling fire behaviour. Calibration relates to the matching to the test series in WP2 ("Characterization of fuel loads" and "Influence of near field & far field") and WP3 ("large-scale natural fire tests"). The work done matched the first objective of revisiting the simulations of the experimental configurations of the fire tests performed in WP2 and WP3 in order to explore validation *a-posteriori*, identifying any deficiencies in model representations and possible improvements.

4.1.2. Description of the activities

The initial work of the project exploring the conditions which might support travelling fires adopted a necessarily highly simplified representation of compartment fuel distributions, as described in WP1 "Preliminary analyses of the parameters influencing travelling fires". Specifically, the fuel packages were lumped to cubic objects intended to be representative of timber cribs, but simplified as a set of solid surfaces – with fire spread predicted via an ignition threshold on each surface (with consequent immediate transition to whole crib burning). This methodology, though simplified, is sufficient to allow exploration of some of the important fire behaviours, including both flowfield effects such as the interaction of the fire development with the compartment openings, and heat transfer effects such as the influence of the hot layer via the ceiling/downstands and interactions with the compartment boundaries. Yet it must be recognised that due to the simplification in representing the cribs, it might not be possible to reproduce some of the detailed behaviours known from experimental studies, e.g. the interaction of the crib burning with compartment conditions. Moreover, those initial studies looked at only one idealised representation of fuel loads, i.e. converted entirely to discrete objects which might correspond to cribs, while the expectations from consideration of real world scenarios, and the requirements of matching the simulations to the experiments being performed in TRAFIR, are for a very different situation, i.e. with uniform or continuous fuel beds.

In order to address these challenges, i.e. the requirement to (predictively) model fire spread over continuous fuel beds the modelling approach was further developed, to include a more detailed yet tractable approach with representation of the fuel by a series of small wood blocks, and also via the development and exploration of more ambitious approaches based on a full "stick-by-stick" representation. The latter is extremely computationally demanding at compartment scale but is used here to explore burning

behaviours and give additional insights, which ultimately feed into the more simplified models.

Single crib model

The LB7 test case (from WP2 "Characterization of fuel loads"), which provided the closest match to the desired Eurocode fire parameters for a medium fire) was first modelled for calibration with the experimental data. The wood sticks were represented with real cross-section dimensions, 30 mm (breadth) × 35 mm (height), referred as "stick-by-stick" models. The cell size with the crib volume was half that of the physical dimensions of the sticks, i.e. 15 mm × 15 mm × 17.5 mm, which is a bare minimum for representing the flow and heat transfer processes within the crib structure, as also adopted by Horová (2015). The cell size of the gas phase in the horizontal surrounds of the crib was 30 mm × 30 mm × 35 mm, while above the top surface of the crib was 60 mm × 60 mm × 70 mm, as presented in Figure 47. The total computational domain size was 5.04 m × 5.04 m × 2.73 m, thus the total number of cells was approximately 1.3 million, which were divided into 16 meshes and each mesh was assigned to a single MPI process. The simulations were performed using the computational clusters ARCHER and Eddie, each run taking around 170 hours to complete for a 1200 s simulation for the LB7 test case.

In contrast to the actual LB7 wood sticks arrangement, the representation of the fuel was necessarily simplified to a 2.8 m × 2.8 m square wood crib with nine layers of sticks placed orthogonally, see Figure 45. To approximate the effect of the wood stick lateral shift of 60 mm for every three layers, and being rotated 60° on every layer as per the test, a 60 mm lateral shift was applied to the model for every two layers of the wood sticks. This is an approximation but inevitable due to the impossibility of representing the exact geometrical arrangement within the constraints of a Cartesian/orthogonal CFD grid. The FDS "simple pyrolysis model" was applied to simulate the fire spread, with an ignition temperature and a prescribed burning rate, i.e. heat release rate per unit area (HRRPUA) of wood and its duration ramp, i.e. once the wood stick surface temperature reaches the ignition temperature, the wood ignites and burns with the prescribed HRRPUA ramp. The representation of the wood stick and coordinate system in plan view are shown in Figure 45 and Figure 46, respectively and the meshes are illustrated in Figure 47:

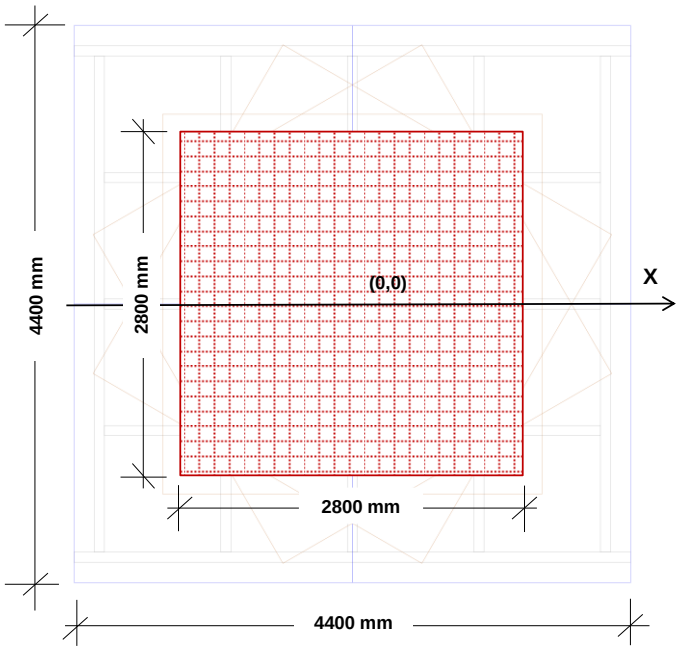

Figure 45: Representation of the wood sticks in the model coordinate in plan view, simplified to a 2.8 m x 2.8 m square wood crib with sticks placed orthogonally

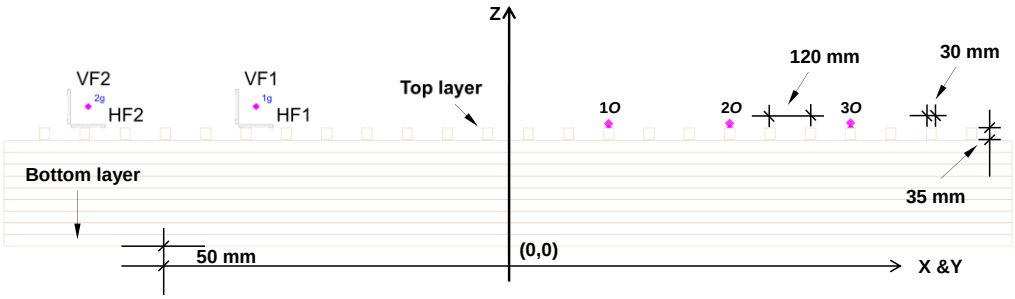

Figure 46: Representation of wood sticks in model coordinates in elevation: stick size 35 mm x 30 mm, stick pitch 120 mm, 24 sticks per layer, 9 layers in total, 50 mm offset between steel panel and bottom wood stick layer for ignition burner and steel tubes

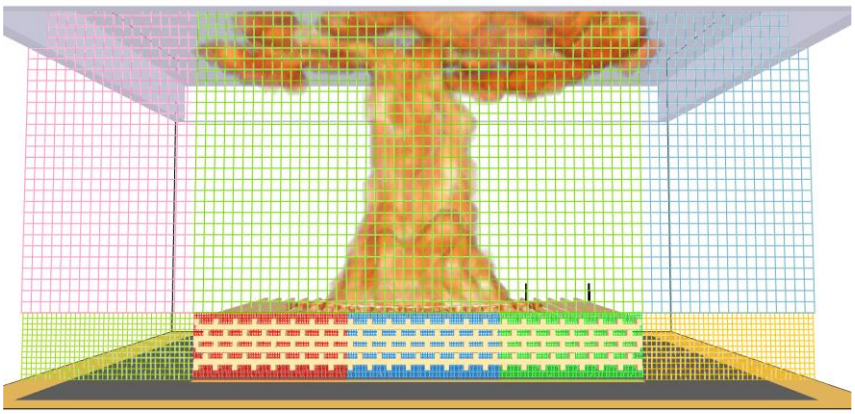

Figure 47: FDS mesh and grid cells for LB7 test

Results of the simulations follow in Figure 48 and Figure 49, which show that a generally excellent agreement has been achieved in terms of the key parameters, with the burn out apparently also well represented (though there are uncertainties derived from the residual

energy content in the char once flaming has ceased). A grid sensitivity study confirmed that it is feasible to relax the grid resolution within the gas phase, which we believe is an important practical advance and the first demonstration of this issue.

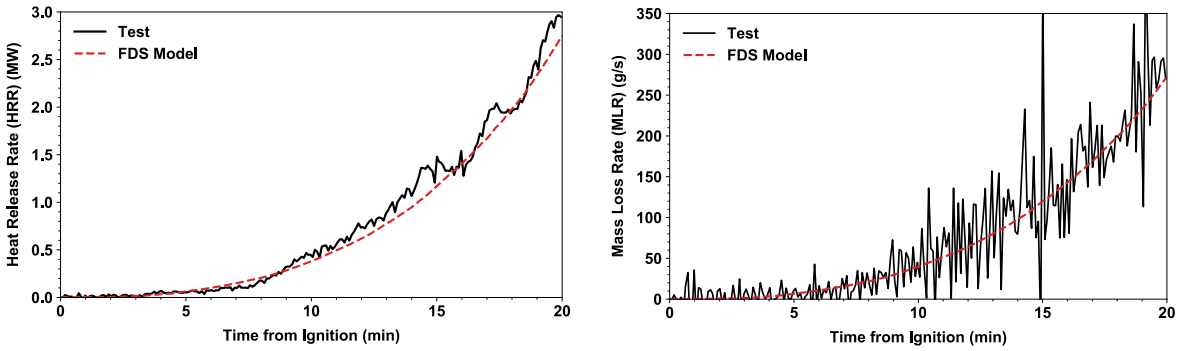

Figure 48: (a) Heat Release Rates comparison ; (b) Mass Loss Rate comparison, for WP2 LB7 test

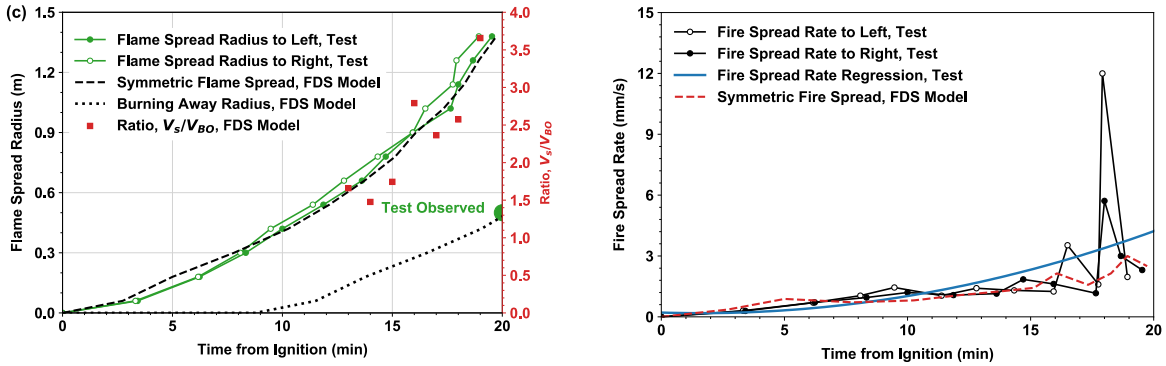

Figure 49: (a) Fire spread radius and burn-out comparison ; (b) Fire spread rate comparison, for WP2 LB7 test

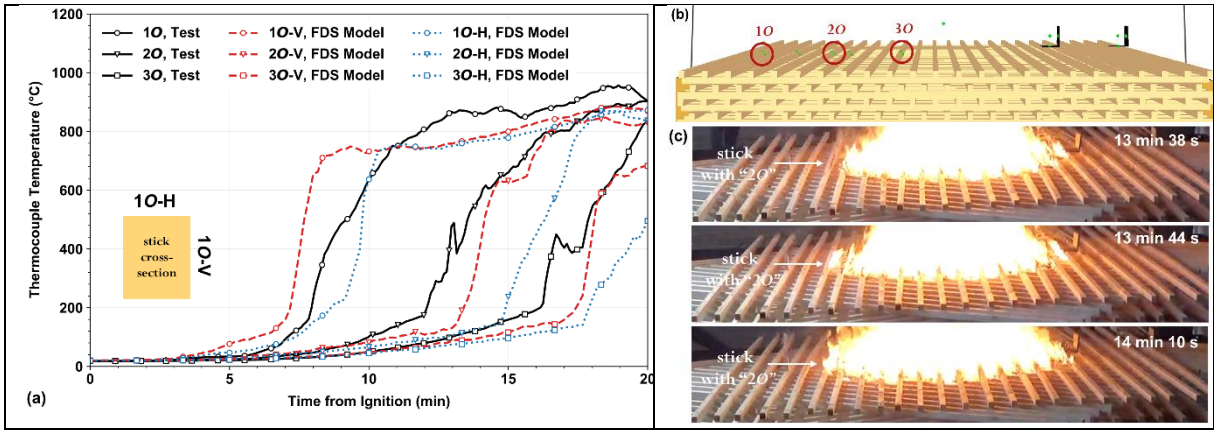

Figure 50: (a) Comparison of thermocouple temperatures on wood stick top layer between model and test, (b) Thermocouple instrumentation locations ; (b) Fire spread development on stick with thermocouple "2O".

Considering the potential fire impacts on structure it is also vital that predicted gas phase temperatures match the experiment within reasonable bounds._Thermocouples were 'stapled' on the horizontal surfaces of certain wood sticks referred as "1*O*", "2*O*" and "3*O*" (see Figure 46 and Figure 50 (b)). Figure 50 (a) shows comparison, where "-H" is at the same location as per the test and "-V" is on the adjacent vertical surface of the stick facing towards the fire spread direction. There is good broad agreement and the

vertical temperatures rise earliest corresponding to the observed prior ignition on vertical surfaces in the test as can be seen in Figure 50 (c).

It is also of interest to understand the sensitivities of the fire spread development to a range of physical and numerical parameters, spanning HRRPUA, soot yield, heat of combustion, ignition temperature, wood thermal inertia and wood emissivity. As per Figure 51 in each case the expected trend for fire spread radius is demonstrated, with relatively high sensitivities to heat of combustion and ignition temperature changes.

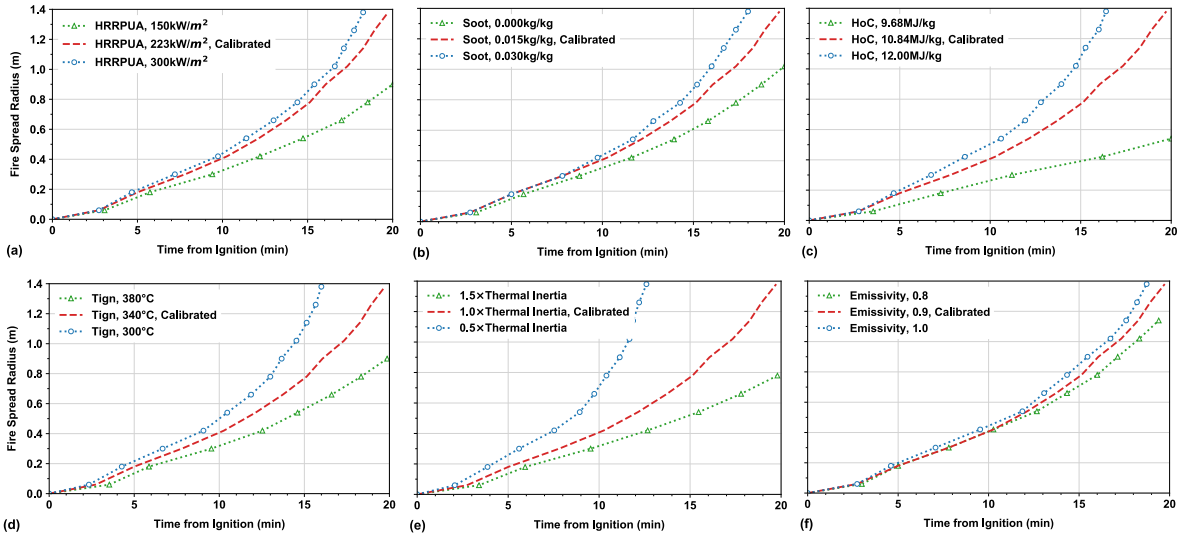

Figure 51. Physical parameter sensitivity on fire spread radius.

Ultimately these trends impact on the potential for development of different modes of fire spread, from "travelling" (V_S/V_{BO}~1), through "growing" (V_S/V_{BO}>1), to "fully developed" ($V_S/V_{BO}\rightarrow\infty$), since the burning rate, hence burn-out time, is relatively insensitive to fire conditions (cf. Gupta et al., 2020b) – see Figure 52.

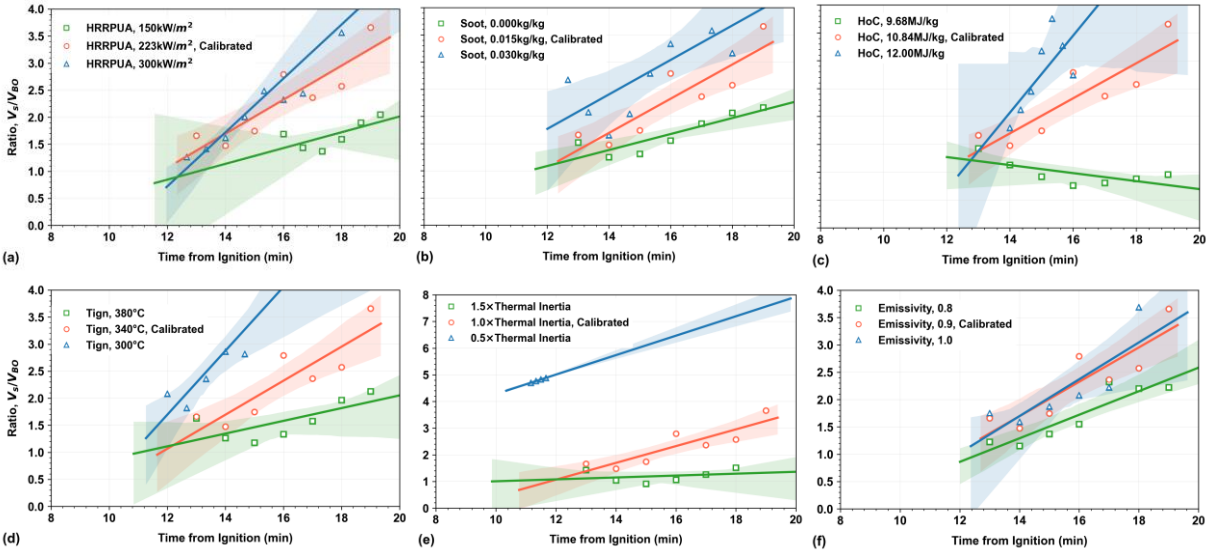

Figure 52. Physical parameter sensitivity on HRR.

RISE small-scale test (WP2 Task 2)

FDS simulations were performed of prescribed travelling fires in a simplified and elongated compartment matching that of the experimental series. The heat release rates in for the diesel fuel pools are prescribed and the effect of the downstands is studied for different placements of the six pools. In Figure 53 the flows along the structure are displayed by the centre column, i.e. 9 m from the back wall. Although there are differences in the precise values they are often of the same order; however there are significantly larger fluctuations in the measured velocity which may come from wind, uncertainties in the temperature measurements or estimation of the Reynolds number.

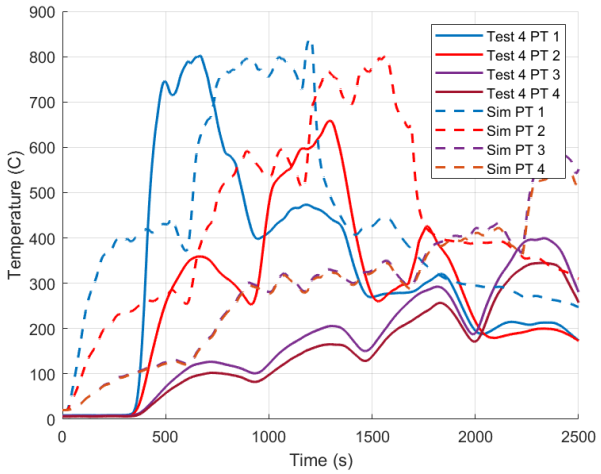

Figure 53: A comparison of the simulated and measured temperatures at plate thermometers (PTs) in WP2 Task 2 test 4

Ulster large-scale compartment tests (WP3)

A wood block model, based on 0.32m cubes, was developed as the main basis for exploring predictive capabilities for this more ambitious full scale test. The material used for the wooden fuel bed was entirely defined based on density of the wood measured while the conductivity & the specific heat were taken from previous EFTF modelling work (Yang, 2016). The heat of combustion, estimated from a bomb calorimeter test conducted at the University of Edinburgh, was corrected from a gross value of 18.0 MJ/kg to a net value of 16.84 MJ/kg.

The models used about 170,000 cells and required only around 40 hours to complete, using six meshes, despite being at compartment scale. Figure 54 to Figure 56 present the gas temperatures measured during test n°1 and the ones resulting from FDS (FDS "thermocouple" outputs). It can be observed that the global fire spread is well captured, as well as main tendency in terms of temperatures. The temperatures generated by FDS for lower levels tend to be over-predicted (presumably due to the simplified representation of the crib) but also much closer at middle and upper levels. Also the former display sharp growth/decay phases, while the latter are overlaid with a much more progressive growth/decay, which is expected according to the accumulation of hot gases. The model fails to reproduce some details, e.g. the lower values at TRL8 (thermocouple

tree highlighted on Figure 73, placed at 12.5 m from the back wall and at mid-width) where the plume is leaning further back into the compartment, and also the modest acceleration suggested by the slight compression of the test curves, possibly because the burning rate is enforced while in the test the rate will increase to some extent due to increasing radiative feedback. A difference is also observed in the descending branch of the fire curve, which could be explained by the CFD model's inability to properly capture glowing embers (which will have a markedly higher heat of combustion than the wood volatiles) as well as the heat accumulated within the compartment. But the methodology is not aimed at reproducing all of the details of the fire itself, rather for evaluating the overall heating of the structural elements of the compartment to, in the end, determine the mechanical behavior of the structure subjected to travelling (or spreading) fire. Steel temperatures measured on a central column were compared with the steel temperatures resulting from the CFD model (evaluated using two methods: one based on the incremental formula from EN1993-1-2 and other one linking CFD (FDS software) and FEM (SAFIR® software)). The results obtained through these two methods are quite similar and the steel temperature profiles globally showed a very good correspondence with the ones of the test: details regarding this work are provided in (Charlier et al., 2020b) and (Charlier et al., 2021).

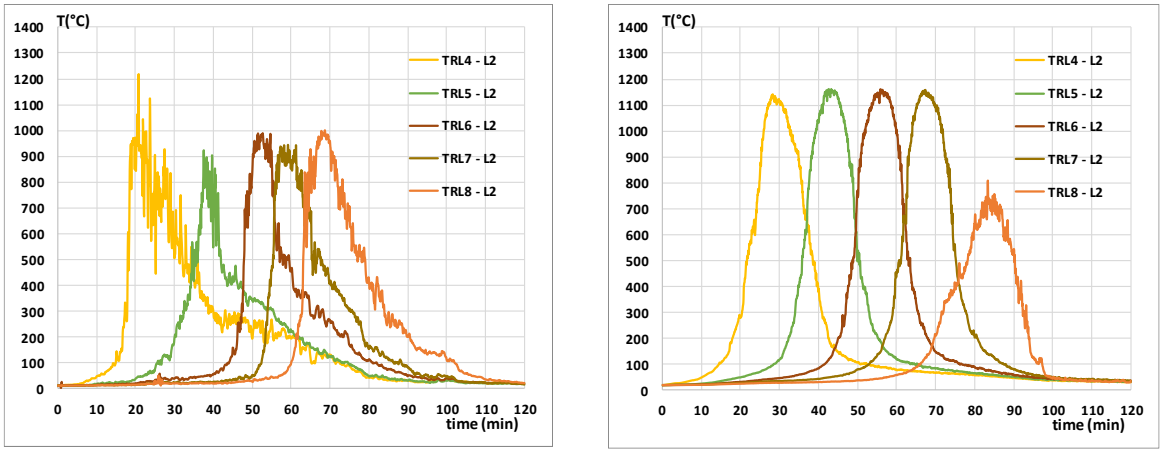

Figure 54: Comparison of gas temperatures for test n°1 at Level 2, 1.0m, (a) test measurements; (b) FDS results

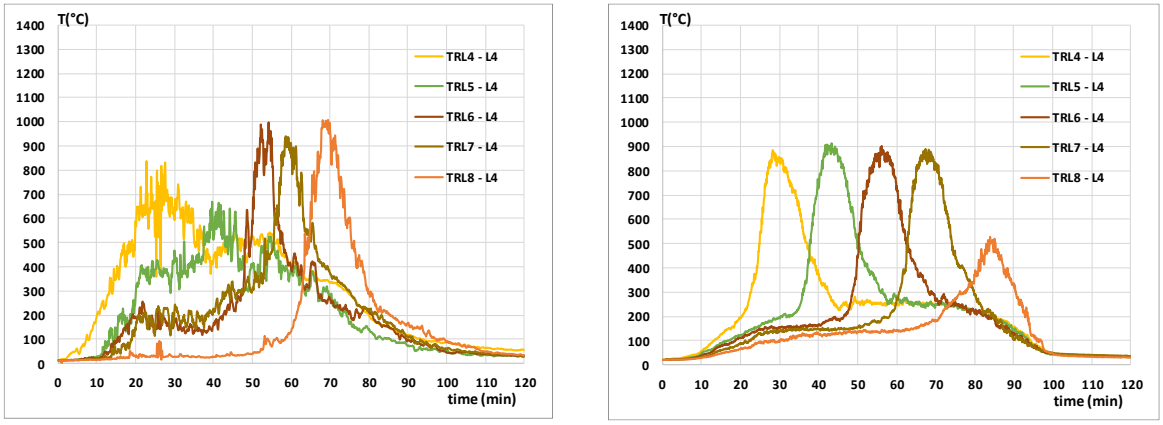

Figure 55: Comparison of gas temperatures for test n°1 at Level 4, 2.0m, (a) test measurements; (b) FDS results

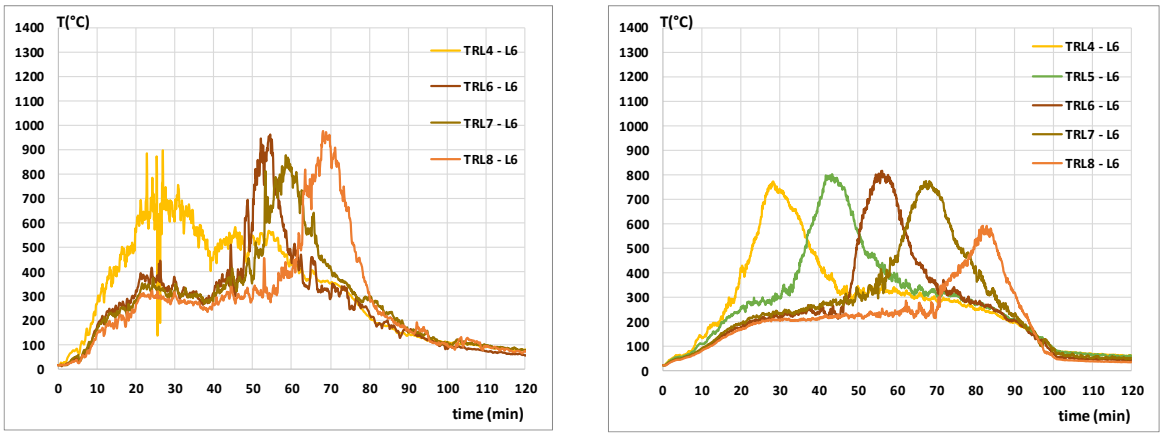

Figure 56: Comparison of gas temperatures for test n°1 at Level 6, 2.7m, (a) test measurements; (b) FDS results

The work done is innovative in several respects – previous crib fire models in CFD have been forced to compromise on resolving the detailed geometry, and have not demonstrated reproduction of a consistent set of fire parameters, i.e. it may be possible via modelling "tuning" to reproduce a fire spread rate, or heat release rate, but to capture spread, temperatures and burn-out simultaneously is very demanding. The grid scheme for these detailed models is innovative, somewhat mitigating their computational demands, and for the first time simulations of a full-scale compartment have been performed with a detailed model. The "wood block" model is also an innovation, is far more practical than the detailed models and following careful calibration has successfully reproduced the global fire parameters to an acceptable accuracy.

4.1.3. Conclusions

This study has explored the ability of CFD models, specifically FDS, to reproduce the results of various full-scale tests involving fire spread over timber cribs and/or continuous fuel-beds, and spanning a range of different modelling approaches, model validation/calibration exercises and relevant sensitivity studies.

Detailed models

It is shown that a "stick-by-stick" model with simple pyrolysis and an ignition temperature setup can reproduce the results of the Liège LB7 crib fire test (WP2 Task 1), spanning the full range of relevant fire parameters (fire spread rate, heat release rate and burn-out rate), all being comparable to the test data. This suggests the credibility of the model for representing travelling fires and providing insights into the mechanisms underpinning the fire spread. Indeed, initial results for application of the same model to the large compartment tests under WP3 suggests that it may also be capable of reproducing conditions at a more realistic scale, albeit with even greater computational demands and on the condition that the fire load is defined in an identical manner, as was done in TRAFIR. However, for different fuel geometries, i.e. different arrangements of sticks in the crib, the model would need to be recalibrated for each specification, as the required variation of the fitted parameters, i.e. ignition temperature, seems to be rather sensitive to fairly small changes in the crib geometry. Further work would be required to explore these aspects in more detail.

Pool fire models

For the WP2 Task 2 series of compartment fire tests conducted by RISE, both *a-priori* and *a-posteriori* simulations provided useful insights for a travelling fire represented by a prescribed successive ignition of pool fires. Spread rates for both models were pre-defined to match the target spread rates of the WP2 Task 2 (manual spread was utilised in these tests). The *a-posteriori* simulations for Test 4 demonstrated similarities in the maximum temperatures obtained and the quantitative flow speeds found. This supports the view that these types of simulations can be further utilized in order to understand the dynamics in travelling fire situations at full scale.

Wood block models

The more challenging case of representing and predicting fire spread over cellulosic fuels, constituted by wood cribs arranged as continuous fuel beds, in full-scale compartments, is explored in detail. The results obtained with simple crib representations using sets of wood blocks, which are rather bigger than the sticks, show a capability to adequately capture global aspects of the fire development behaviour, although not all of the details. Also the steel temperature profiles showed a generally good correspondence with those of the WP3 Tests 1 and 2 (for a given test and a given column; different profiles were obtained for different heights of the column). This is achieved with a model which is much less computationally demanding than a detailed stick-by-stick model, thereby with greatly improved potential for use in parametric studies, as reported below. Nevertheless, an important proviso is that the essence of the crib representation derived from an assumed freely burning model (c/o Degler et al., 2016) which if placed in heavily underventilated conditions may eventually begin to break down.

Also, a common conclusion for the detailed and simplified models is the challenge in representing the descending branch of the fire curve, thought to result partly from the fact that the heat of combustion value of the char is much higher than that of the wood volatiles (a factor not currently represented in the model) as well as the heat transfer effects associated with the glowing embers. Together with glazing failure representation, such aspects could be addressed and improved in future research.

4.2. Parametric studies (WP4)

4.2.1. Introduction

The next stage of establishing a simulation-based complement to experimental tests is to perform numerical experiments to investigate travelling fire behaviour. The parametrical variations seek to effectively extend the experimental dataset, thereby revealing the sensitivities of fire exposures to parameters of potential interest to designers.

4.2.2. Description of the activities

Experimental tests, due to their limited number, are not enough to cover all possible configurations encountered in practice, and are also practically constrained in terms of

physical dimensions. However, this weakness can potentially be overcome with help of advanced numerical tools. CFD numerical models, using FDS, were first calibrated to reproduce the experimental configurations of the fire tests. The developed model is then used to extend the investigation field by conducting a parametric study encompassing different fires and end-use situations, assessing the influence of several fundamental parameters and providing an overview of travelling fire potential against opening factor.

The broad range of scenarios studied encompasses different fires and end-use situations, i.e. spanning variations in the compartment geometry (including size and openings) and ventilation conditions, so as to generate an extended virtual experimental dataset spanning:

- Different fire loads (and therefore the occupation type): 511 MJ/m^2 (office); 250 MJ/m^2 (sparsely loaded office); 730 MJ/m^2 (commercial) (according to the Final Draft of EN 1991-1-2);
- Different opening surfaces: the height of the openings covers 25%/50%/75% of the compartment height;
- Different compartment dimensions: compartment plan dimensions of 30 m x 15 m/70 m x 25 m; ceiling 3 m (or 8m option).

The sensitivities of the developments in fire exposures to various input parameters have been assessed by a detailed analysis of the predictions, spanning:

- Global trend (summary text),
- Fire spread (graphical),
- Flame thickness (tabulated),
- Evolution of flaming zone (3D image),
- Burning rate (3D image),
- Gas temperature (2D slice files),
- Gas temperature - thermocouple trees (figures),
- Heat Release Rate (figure).

From the data generated via this analysis it is possible to extract some useful quantitative measures of fire behavior facilitating analysis of characteristic behaviours:

- fire spread,
- flame thickness,
- progression of the combustion zone,
- burning rate,
- gas temperatures,
- occurrence of a ventilation controlled situation or not.

Figure 57 presents an example of the kinds of qualitative differences observed, in this case varying the “opening ratio”, i.e. height of opening as proportion of compartment height, with the left hand image (from sc1) corresponding to a more enclosed fire at 25%, while the right hand image (from sc3) being a more open fire at 75% (the plan geometry is 29.4 x 15.4 m in each case). The fire moves more quickly in the former

case, and relatively early in the process it jumps to the end of the compartment and immediately transitions to a fully developed fire (no travelling behaviour took place), while with the additional heat loss in the latter case the fire has essentially reached the end wall as a travelling fire.

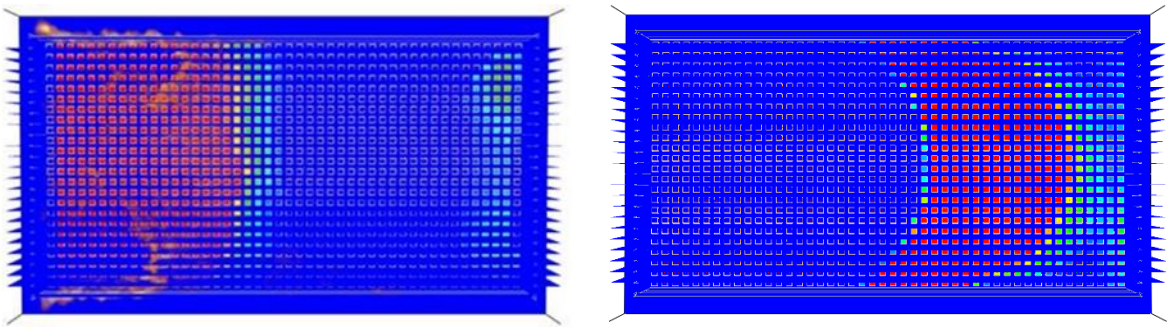

Figure 57: Crib burning rates (a) sc1, opening ratio 25%, 2000s; (b) sc3, opening ratio 75%, 8900s

Figure 58 shows a pair of images for the sc16 case, which is analogous to sc1 except in having a reduced fuel load, i.e. 250 MJ/m^2 rather than 511 MJ/m^2. Here, the fire has initially developed into a travelling fire, with burn-out at the rear progressing more rapidly, but the fire still transitioning to flashover before it has reached half the length of the compartment

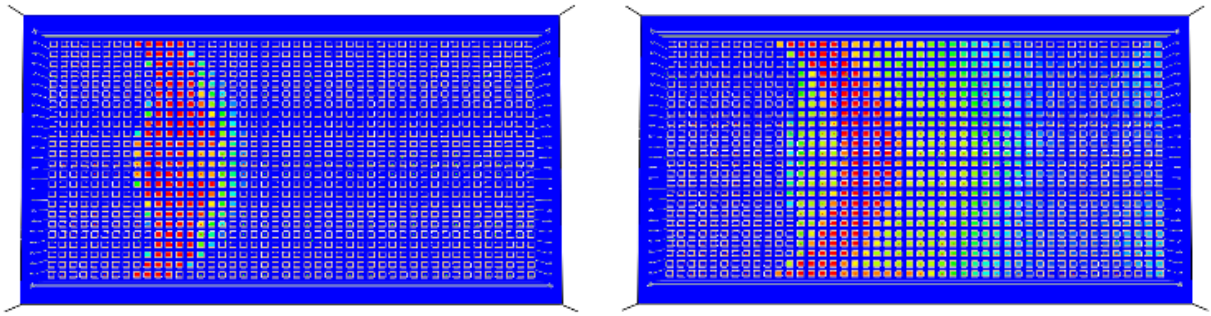

Figure 58: Crib burning rates for sc16 (a) 3500s; (b) 3960s

Thus, even within the scenarios where only opening height and fire load are changed a large variety of results were generated, arising from the complex interrelations of external heat loss, ventilation effects and the impacts on the fire size from varying the burn-out time. Further complexities arise when the overall scale of the compartment is increased; case sc24 has plan dimension increased by a factor of 5/3 but is otherwise identical to sc3 as per Figure 57 (b) above. Here, with a much greater "depth" into the centre of the compartment, some complex fire spread oscillations arise, presumably due to the lack of access to air further from the openings. A pause in burning in the centre is seen early on, but cribs towards the sides are later bypassed via an asymmetric fire progression (the fire eventually reversed and burned back down the sides), see Figure 59.

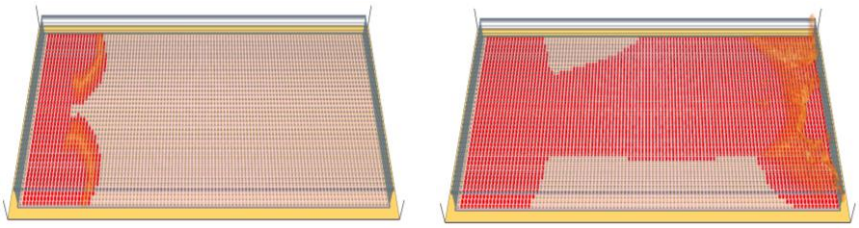

Figure 59: Heat release and ignited crib locations for sc24 (a) 7600s; (b) 17800s

Ceiling height was investigated by an increase from 3 to 8 m, in cases sc28-30, which are otherwise analogous to sc1-3 but also have an increased fire load (730 MJ/m^2). Figure 60 shows the progression of the fire in these cases, this being much slower overall with the much reduced impact of the hot ceiling to preheating of the fuel bed. Hence travelling behaviours arise with quite narrow "flame thickness" during much of the burning, despite the higher fire load. It has to be noted that in the sc28, the traveling fire reached 50% of the compartment length before the fast growth occurred which caused to the fire to cover the remaining 50%, placing this scenario as a borderline travelling case. They also show a much reduced sensitivity of the opening factor on the fire spread rates, these being mainly fuel-controlled fires which are dependent on local conditions (Gupta et al., 2020b).

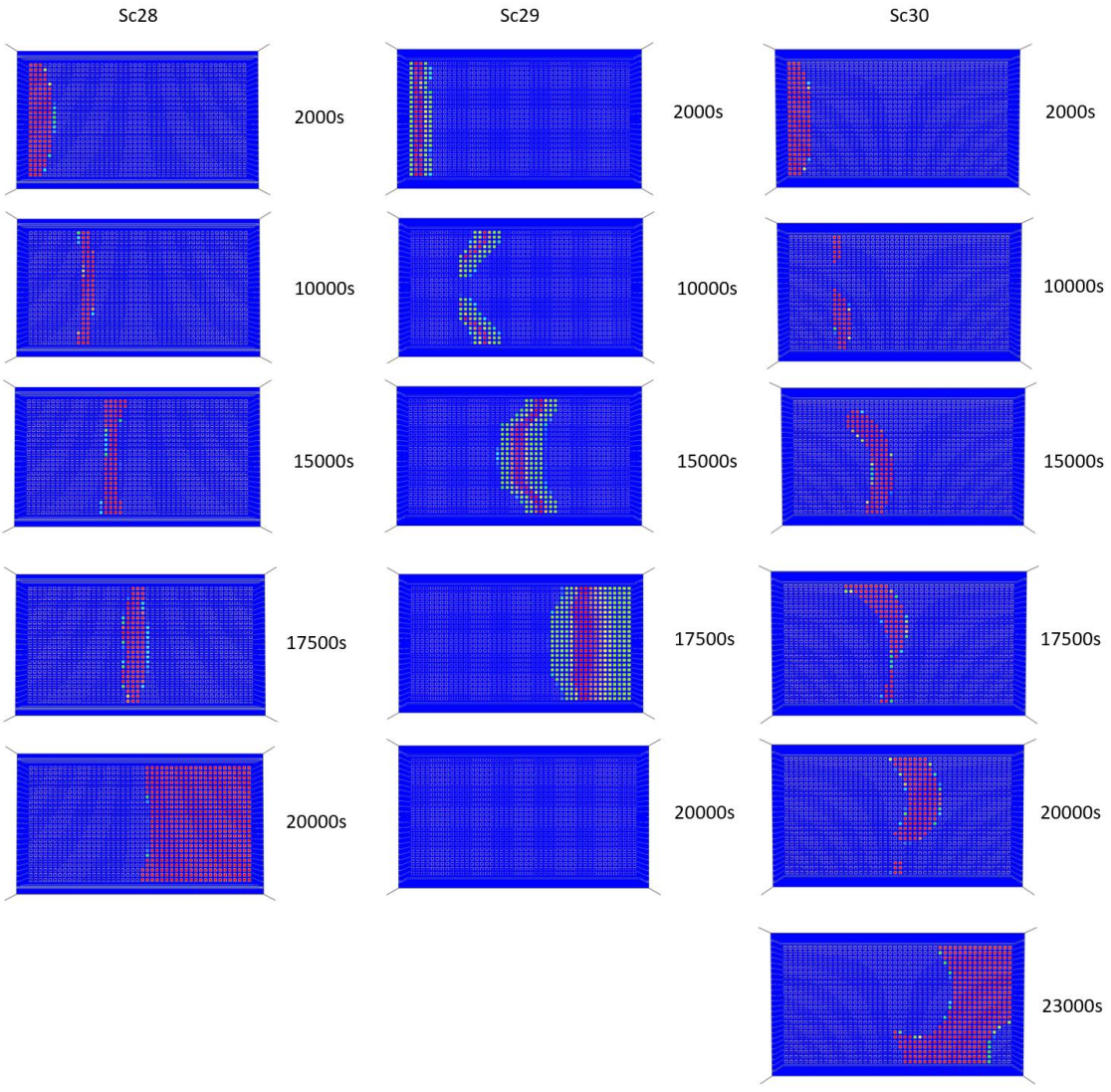

Figure 60: Burning rate of sc28, sc29 and sc30 in function of time

Detailed analysis is done for a total of 16 scenarios, at a geometrical scale bigger than has previously been reported for crib fire modelling, and it was again possible to interpret all of the observed trends in terms of fundamental principles of fire dynamics.

While it must be recognised that there are many embedded assumptions and simplifications, this extensive modelling study has progressed the WP1 analysis pioneered earlier (Charlier et al., 2020) and permits an assessment of the conditions required for fire spread, while also giving an indication of some of the influential parameters and likely sensitivities. In particular, as seen in the examples above, it is observed that the compartment dimensions, the total opening area and the fire load showed a significant combined influence on the fire behaviour. The compartment dimensions and the total opening area can be both accounted for through the use of one parameter: the opening factor, $O = \left(A_v\sqrt{h_{eq}}\right)/A_t$ ($m^{1/2}$) with A_v being the total area of vertical openings on all walls (m^2), h_{eq} being the weighted average of window heights on all walls (m) and A_t the total area of enclosure (walls, ceiling and floor, including openings) (m^2). Modifying the opening factor (consistently with experimental observations in TRAFIR WP3 tests & Gupta et al., 2020a), and the fire load, shows a significant influence on the fire behaviour as reported below.

A "Binary classification" (0 or 1) is used in the analysis, with a value of "1" corresponding to a travelling fire, i.e. where a region of fire moves while the value "0" is for situations with only growing compartment fires, all of eventually supported flashover, i.e. rapidly accelerating fire spread – compare the examples presented in Figure 57 above, where sc1 jumps to a fully developed fire before burn-out has started at the rear, hence is deemed not "travelling" (0), while for sc3 the fuel adjacent to the back wall only ignites when the fire has almost reached it, hence labelled "travelling" (1). In fact some scenarios were classified as "1" (travelling fire scenario) even though they also supported a brief flashover, because the latter occurred at the very end of the compartment due to interaction with the backwall (only if flashover occurred after the fire front passed 75% of the length), while for intermediate scenarios sc28 and sc40, the 0.5 value is given).

Global results analysis is performed with respect to the opening factor, with each scenario represented by a point. One given color is used for a series of scenarios having similar compartment dimensions and fire load (given in the legend) but different opening surfaces, resulting in different opening factors. The points of a given series are connected through dotted lines, only for sake of clarity. Figure 61 provides an overview for all the scenarios considered. The legend provides first the compartment dimensions (length x width x height, in meters) and then the fire load (in MJ/m^2). The total number of scenarios launched is not enough to define a unique and general criterion distinguishing travelling fire scenarios from other fire scenarios. Nevertheless, it is possible to identify trends which can be interpreted in terms of fundamental principles of fire dynamics. For a given opening factor, the potential for a travelling fire scenario is increased by low fire load, and a low distance between openings on opposite sides, i.e. compartment width. For a given fire load (and therefore a given occupancy type), a higher opening factor increases the risk of having a travelling fire scenario.

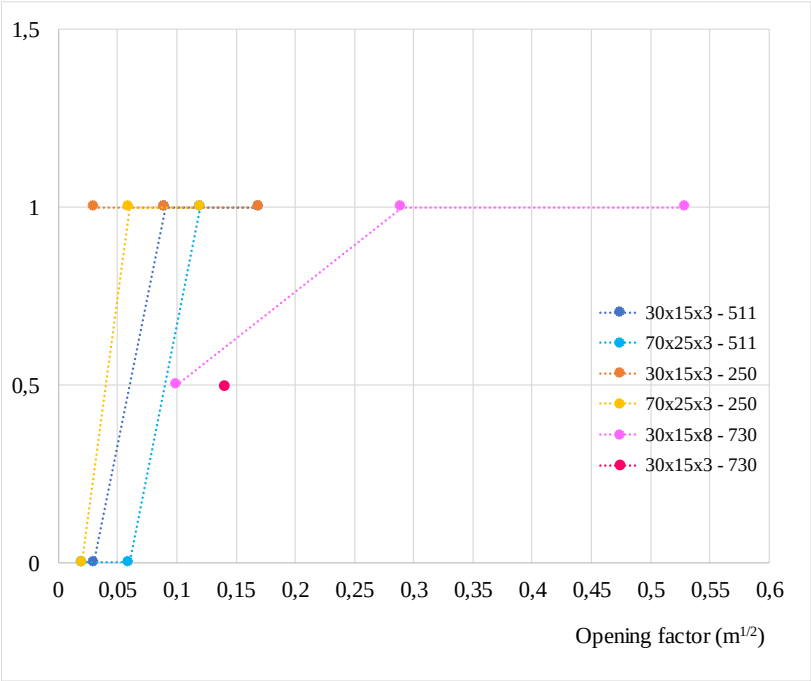

Figure 61: Binary values (1 for travelling fire, 0 for without) for different opening factors, all scenarios

The simulations done are innovative in attempting to represent travelling fires in CFD simulations at much larger geometrical scales than has previously been reported, and far beyond that which it is possible to study experimentally.

4.2.3. Conclusions

The comparative analysis supports valid comments on sensitivities, particularly in terms of burning modes, i.e. growing, travelling, runaway and flashover. Systematic analysis of these behaviours with respect to opening factor has permitted the identification of trends of fire development for different parameters, at a much larger scale than has been examined experimentally (and considering different fire loads than the one tested). It was shown that some conditions did not lead to a travelling behaviour.

In qualitative terms, for cases with greater opening factors the fire is less likely to become intense and spill out of the enclosure boundaries – and thus more likely to support a travelling fire. By contrast, in cases with greater compartment widths, the lack of oxygen to the centre tends to mitigate against the development of a travelling fire and support an eventual flashover transition – though sometimes this is preceded by oscillations of fire spread rate.

The quantitative analysis also shows that in general, larger opening factors tend to support travelling fires, while more constrained cases tend to go to flashover. Travelling fires are more likely to be supported with lower fuel loads (such as those corresponding to sparsely loaded offices), while the “limit opening factor” for transition between modes tends to increase with both fuel load and the distance between the openings across the compartment width (which limits access to oxygen). Finally, even with high ceilings, high fire load cases (such as those corresponding to commercial areas) may only support travelling fire at significant opening factors.

In practice, a range of other variables will affect spread behaviours, including the types and distribution of fuel loads within the compartment (only a uniformly distributed fuel load was considered), the thermal properties of the boundaries, progressive glazing failure and the effects of external winds, but further work would be required in order to attempt to quantify these.

5. Analytical procedure

5.1. Inspection of some existing travelling fire models (WP5)

5.1.1. Introduction

The first part of this Work Package was an exploration of the general capabilities of existing "analytical procedures" in order to establish any specific limitations and aspects that need further development, thereby informing the subsequent work on a new analytical model. The scope extended to characterisation of a travelling fire and its thermal effects. Two different methodologies (iTFM, ETFM) are applied to study of different experiments, supporting conclusions on their merits and remaining deficiencies. In particular, the utility of Hasemi's localised fire model was carefully examined, as well as fuel load effects and the role of the hot layer in the far field. Due to the large demands of undertaking these aspects exclusively 1D representations were studied, according to the test definitions. It is recognised that the role of a t^2 phase could be considered in further work.

5.1.2. Description of the activities

The general capabilities of existing "analytical procedures" were explored, examining:

- The Improved Travelling Fire Methodology (**iTFM**) (Rackauskaite et al., 2015) which is the latest development of models established by group led by Rein et al. (Imperial College London, formerly University of Edinburgh (Rein et al., 2007))
- The Extended Travelling Fire Methodology (**ETFM**) framework (Dai et al., 2020) which is the state-of-the-art implementation of the models established by Dai et al. (University of Edinburgh), i.e. the current project team members.

Model capabilities were examined in relation to the full-scale tests conducted within the scope of the TRAFIR project, i.e. wood crib travelling fire test (WP2, "Influence of near field & far field") and the series of full-scale compartment travelling fire tests (WP3, "large-scale fire tests"). There are some differences in the assumed conditions reflecting different purposes and interests of simulations of this nature.

Improved Travelling Fire Methodology **(iTFM)**

Analysis was performed with the iTFM model for each of the WP3 "large-scale" fires, and initially adopting *design* values of rate of heat release and fire load density extracted from the guidance in Eurocode 1 (EN1991-1-2) for an assumed office building scenario. In recognition of the fact that this burning rate was judged to be lower than the estimated values deduced from interpretation of the results of the tests, a further series of simulations was run where estimates of rate of heat release were back-calculated from the characteristic mass loss rate obtained in the tests. In addition, a further parametric analysis is undertaken to explore the significance of a number of the uncertain inputs to the model:

- the flame thickness (influencing the "fire size"): 3m or 5m (given the observations made during the WP3 "large-scale" tests);

- the flapping angle: 4° (minimum value), 6.5°C (mean value) or 15° (maximum value).

This permits identification of the most appropriate assumed input values, and the best match to the observed fire spread rates, for this particular scenario.

Extended Travelling Fire Methodology (**ETFM**) framework

Analysis with the ETFM framework was first undertaken with respect to the timber crib travelling fire test performed by RISE within the scope of WP2. Steel beam temperatures were available at regular intervals along the compartment centreline permitting a systematic analysis of trends during fire spread, i.e. to examine the role of preheating from the hot smoke layer.

Thereafter, the same WP3 "large-scale" tests are examined as for iTFM, but in all cases experimentally extracted parameters are adopted, so as to best inform the further validation of the model (validation has previously been reported with respect to the Veselí travelling fire test (Dai et al., 2020)), but that test has a different arrangement with a window opening only on the front wall). Parameters used as model inputs were extracted following careful analysis of the measured mass loss rates, in conjunction with bench scale tests for reaction-to-fire properties of the spruce sticks.

Analysis and discussion

The comparison of results provided by iTFM with WP3 "large-sale" tests allows the highlight of potential limitations. Initially considering the design RHR_f value, and for high opening factors (referring to test n°1), i.e. when a travelling fire scenario is expected to occur, temperatures are clearly overestimated in iTFM except for thermocouples lying within the fuel load. The time during which the temperatures are high is as well too long. This leads to too high steel temperatures and therefore to overly conservative results. For low opening factors (referring to test n°3) to such extent that a compartment fire and/or a flashover is expected, the methodology also presents drawbacks (too high peak temperatures and too short period where temperatures are above 500°C).

Considering the back-calculated RHR_f test value, initially for test n°1, there is a better correspondence in terms of fire spread, however, the steel temperature obtained via iTFM remains too high and the time period during which the steel temperature is above 500°C is longer except for level 4 and 5. This can be explained due to the smoke layer leading to longer high temperature for upper levels. Moreover, as peaks of high temperature in the test had a short duration, steel did not have enough time to rise in temperature, leading to a bigger difference between iTFM and the test for steel temperature than for gas temperature. Rather improved correspondence is obtained for test n°2. For low opening factors (referring to test n°3) to such extent that a compartment fire and/or a flashover is expected, the methodology seems to again present some drawbacks (too high peak temperatures and too short period where temperatures are above 500°C). Moreover the

parametrical analyses examining flame thickness, flapping angle and RHR_f showed a variation of over 200°C.

The comparison of results provided by the ETFM framework with WP2 "Influence of near field & far field" and WP3 "large-scale" tests showed that in the near-field, when the flame impinges the ceiling, as occurred in WP3 tests, the ETFM framework prediction is comparable to the experimental measurement: spanning 600°C to 1000°C in the near field, while the tests span 500°C to 900°C; but when the flame does not impinge the ceiling, as per WP2 test, using "Hasemi" for near-field may become invalid, hence temperatures are over-predicted; it is suggested to use an alternative correlation for calculating the near-field heat flux in these cases, e.g. Heskestad model. It is also suggested to consider another model to evaluate the thermal impact on columns which are not embedded into the flames.

In the far-field, once the travelling fire cases are at 'clear' fuel-load controlled situation, i.e., WP2 "Influence of near field & far field" test, WP3 "large-scale" test n°1, the ETFM framework tends to over-predict the far-field temperature, when the actual measured temperatures at far-field are below 400°C. This is due to the current limitation of FIRM zone model being utilised in the ETFM framework where only one opening is considered, hence more heat is confined within the compartment. This limitation could be overcome when using more advanced zone models, e.g., CFAST, or OZone. Once the measured temperatures at the far-field are above 400°C, the ETFM framework prediction provides a better match, though there are large error bars.

In terms of error bars, for the near-field, those of the test and the ETFM framework both tend to increase with decreasing opening size; for the far-field, the error bar for the tests is below 100°C, however the ETFM framework could reach as high as 450°C, derived from uncertainties on heat loss, which is a limitation of the embedded zone models.

For situations where the fire spread rate is affected by the ventilation location more significantly, i.e., WP3 "large-scale" test n°3, the assumed constant value is a current model deficiency. Proper interpretation of the extent of the observed over-prediction is rather obfuscated by discrepancies in the timing of the fire development and movement – this being generally underpredicted by the iTFM methodology while in the ETFM framework this parameter is adopted as an input but in the current version of the code only a constant value can be used.

5.1.3. Conclusions

The results of the existing models clearly show the role of near field and far field thermal impacts on the structural response. However, for both models examined (iTFM & ETFM framework) it is apparent that representations of fire temperatures, and hence steel member temperatures, are generally on the conservative side, sometimes markedly so, and this is a particular problem for near field fire impacts (which seems to depend on flame length with respect to the ceiling, i.e. whether impingement can be expected), but also extends to the far field via both approaches. Although safety is of course sought for, overly conservative results are not favourable in terms of structure optimization and

sustainability (through avoidance of material waste) and excessive margins should be avoided.

For the iTFM, as the opening factor is not directly considered, the performance of the model inevitably varies, with acceptable results in certain scenarios but too severe in others. This along with the fact that the model does not consider any variation of temperature along the height of the compartment seem to be the major aspects to improve.

For the ETFM framework, in cases when the flame does not impinge the ceiling, as per WP2 test, using "Hasemi" equations for near-field may become invalid, hence temperatures are over-predicted; it is suggested to use an alternative correlation for calculating the near-field heat flux in these cases, e.g. Heskestad model. It is also suggested to consider another model to evaluate the thermal impact on columns which are not embedded into the flames.

The study also highlights the potential importance of considering variable fire spread rates which may be adopted to generalise model capabilities. Furthermore, it is recommended that guidelines should be provided to assess when such models (representing "clear" travelling fires) should be considered, acknowledging that the ventilation conditions do play a non-negligible role in this matter.

5.2. Development of a new analytical model (WP5)

5.2.1. Introduction

The final objective of this Work Package is the development of an improved analytical model for the characterization of a travelling fire and its thermal effect, whose results to be compared with experimental and numerical results, and to implement it in a simple calculation tool.

An improved analytical model was developed: the proposed model provides temperatures which vary along the height of the compartment and which depend on the ventilation conditions, two limitations which were highlighted from analyzing existing models. This model should only be applied when a travelling fire scenario is identified as relevant scenario (guidance provided in WP4 "Parametric studies"). The proposed model is based on sufficient simplification to allow its implementation in a simple tool (the fire spread is kept in 1D, as existing models): an Excel file (with VBA macro) presenting a user-friendly interface to allow users applying the model in an easy way. The first simple tool allowing to obtain the steel temperature of a member subjected to a travelling fire was developed: it computes the radiative and convective heat fluxes components which depend on the location of the target in the compartment.

The results obtained while applying this model were compared with results from the experimental campaigns (the WP3 "large-scale" tests presenting a travelling nature: tests n°1 and n°2, and the WP2 test "Influence of near field & far field" involving wood cribs) and from some of the numerical simulations highlighting a cleat travelling behaviour

(scenarios 3, 9 and 18) performed in the frame of TRAFIR project, showing globally a good correspondence.

5.2.2. Description of the activities

An analytical method to characterize the thermal effect generated by travelling fires, and to evaluate the resulting temperature of a steel structural member is detailed in this section. The method consists in three successive steps:

1. Evaluation of the fire geometry and its position in the compartment;
2. Evaluation of the flame temperature in the compartment;
3. Evaluation of the steel temperature of a structural member placed in the compartment.

The following assumptions are considered:

- The compartment is modelled as a parallelepipedal rectangle (see Figure 62);
- The plan view is divided into bands of equal width;
- The fire load is uniformly distributed and covering the whole floor surface;
- The fire starts in the band close to one façade and spreads from band to band;
- The effect of the ventilation is considered through a possible diminution of the of heat release in the burning bands (if and when the fire gets ventilation controlled);
- The spread rate is given as an input and remains constant during the fire;
- The fire load can be defined at another level than the floor level;
- The openings defined in the method are considered as fully open.

The complete description of the method, as well as the explanations indicating how to use the simple tool, can be found in a separate document “Design Guidance” (the Deliverable 7.1).

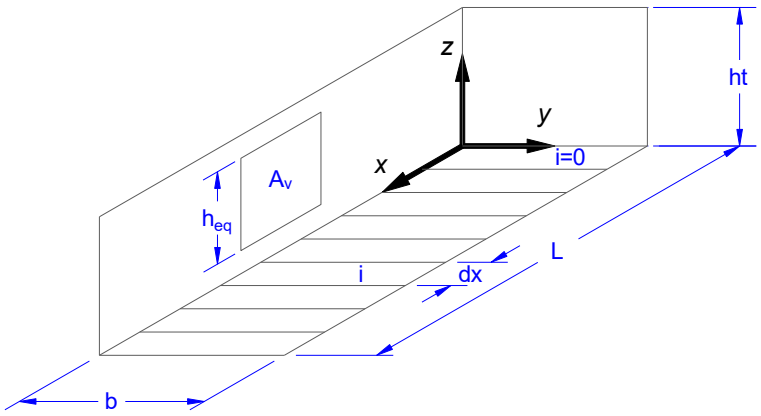

Figure 62: Simplified representation of the compartment to apply the analytical procedure

Step 1 – Location of the fire : inputs

The following symbols are used (referring to Figure 62): *dx* = width of each band, n_{dx} = quantity of bands and the index *i* is used to denote the band number. *Band(1)* extends from *x=0* to *x=dx*, *band(i)* extends from *x=(i-1).dx* to *x=i.dx*, etc. At time t=0, fire starts in *band(1)* only and will thus spread towards increasing values of *i*, i.e. to *band(2)*, and then *band(3)*, etc. Inputs describing the width of the bands *dx*, the geometry of the compartment, the openings dimensions, the fire load (and related parameters such as the

rate of heat release density, etc.), the fire spread rate v and the time step have to be defined.

Step 1 – Location of the fire : outputs

Number of burning bands

The state of each band during the fire is either *burning* or *not burning* depending whether combustion is taking place or not at this moment in this band. This is characterised by a binary variable *burning* that has the value of *1* or *0*. The initial values are:

$$burning(1) = 1$$
$$burning(i) = 0 \qquad i=2,\ldots,n_{dx}$$

The propagation is driven by the fire spread rate. When a band i has an adjacent band i-1 or i+1 that has been burning for a duration $t_{prop} = \frac{dx}{v}$, the value of burning(i) is set to 1. When the fire load density in a band drops down to 0, burning in this cell becomes 0.

Power features

The analytical procedure takes into account the effect of the ventilation through parameters A_v (total area of vertical openings) and h_{eq} (equivalent height of the openings). The burning rate R (kW/m^2) in the compartment may be modified during the course of the fire. It is (momentarily) decreased when the fire is air controlled, as explained below. The initial value of R is RHR_f. The following procedure is followed.

1. The total power Q released by the fire in the compartment is evaluated through the following, A_{band} being the area of one band:

$$Q = \sum_{i=1}^{n} R \times A_{band} \times burning(i)$$

2. The limit value Q_{lim} given by the following equation (Kawagoe's equation, see EN 1991-1-2 equation (E.6)) is computed:

$$Q_{lim} = 0.1\ m\ H\ A_v\ h_{eq}^{0.5}$$

If $Q \leq Q_{lim}$ then $R = RHR_f$.
If $Q > Q_{lim}$ then R is adapted to have $Q = Q_{lim}$, namely:

$$R = \frac{Q_{lim}}{\sum_{i=1}^{n} A_{band} \times burning(i)}$$

Fire load density

The fire load density q in a band depends on the band i and on time. The initial value is $q_{f,d}$ in all bands and this value can decrease during the course of the fire, eventually down to *0*.

$$q(i) = f(t) \qquad i=1,\ldots,n_{dx}$$

In each band i, the variation of the fire load density as a function of time depends on the value of the logical *burning* and on the value of the actual burning rate R:

$$\frac{dq(i)}{dt} = 0 \quad if\ burning(i) = 0$$
$$\frac{dq(i)}{dt} = -R \quad if\ burning(i) = 1$$

Flame length

The combustion area is delimited by the frontside and backside of the burning bands. To obtain the flame length, a diameter D of the fire basis needs to be defined. It is taken as the minimum of b (width of the compartment and therefore width of the combustion area) and the length of the combustion area F (see Figure 63). The flame length is then computed by (see EN 1991-1-2 equation (C.1)):

$$L_f = -1.02\ D + 0.0148\ Q_{loc}^{2/5} + h_{base}$$

where D is the diameter of the fictitious localised fire inscribed in the combustion area and Q_{loc} the power released by the fictitious localised fire inscribed in the circular combustion area, computed by the following equation: $Q_{loc} = R \times \pi\ D^2/4$.

Step 2 – Flame temperature : inputs

A vertical discretization is applied to evaluate the flame temperature. The floor-to-ceiling distance (along *z* coordinate) is divided into several layers of identical thickness. The thickness d_z of the layers has to be defined as input, and is rounded down (if needed) to generate layers that all have the same thickness. Knowing the flame length (i.e. height, along *z* coordinate), the flame is therefore also discretized, following dz. At Step 1 (Location of the fire), a time step *dt* was introduced by the user, for the only purpose of calculating the outputs related to Step 1. In the present Step 2, a new time step Δt is needed, for the purpose of calculating the outputs related to Steps 2 and 3.

Step 2 – Flame temperature : outputs

The flame temperature is computed by Heskestad's model (see EN1991-1-2 equations C.2 and C.3):

$T(z) = 900$ for $z < h_{base}$

$T(z) = 20 + 0.25\ Q_c^{2/3}\ (z-h_{base}-z_0)^{-5/3} \leq 900°C$ for $h_{base} \leq z$

where $Q_c = 0.8\ Q_{loc}$ by default (EN 1991-1-2 Annex C (4));

$z_0 = -1.02\ D + 0.00524\ Q_{loc}^{2/5}$ (elevation of the virtual origin of the flame (EN 1991-1-2 equation (C.3));

h_{base} is the height of the fire load basis [m].

Note: The fire is represented as a rectangular prismatic solid flame, and the temperature in the solid flame only depends on the considered height *z*. At a given height, it is assumed to be constant in the whole horizontal section of the solid flame.

Step 3 – Heat fluxes and temperatures of a steel element : inputs

The solid flame is divided, in the direction of the width of the compartment, into several strips. The following symbols are used (referring to Figure 63): *dy* = breadth of the strips (along *y* coordinate), *ndy* = quantity of strips (along *y* coordinate) and the index *j* is used to denote the strip number. *Strip(1)* extends from *y=0* to *y=dy*, *strip(j)* extends from *y=(j-1).dy* to *y=j.dy* and so on. A_x and A_y give the position (along x and y respectively) of the axis of the vertical steel member.

Inputs describing the breadth of the strips along y, information related to the steel structural element (its position in the compartment, the envelope of its cross section, its section factor, its height at which results are sought for) and information related to the convective and radiative heat transfer (convection coefficient, surface emissivity of the steel, fire emissivity) have to be defined. The considered structural element can also be seen on Figure 63.

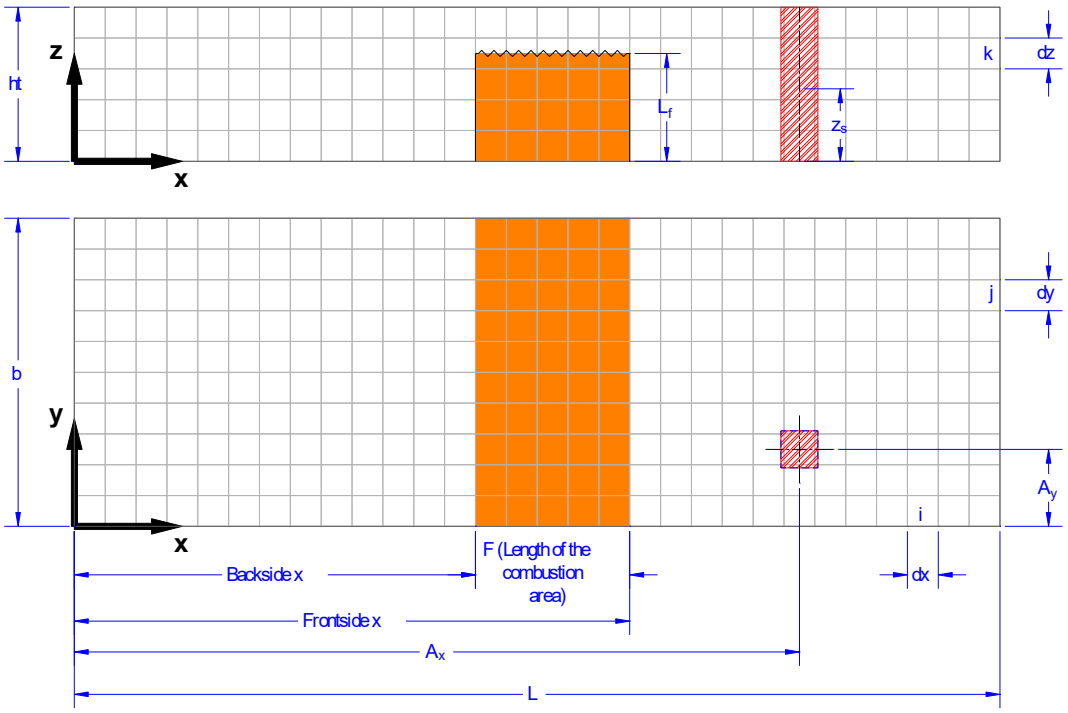

Figure 63: Full discretization of the compartment and of the rectangular prismatic solid flame, and location of the structural steel member (x,y,z)

Step 3 – Heat fluxes and temperatures of a steel element : outputs

Heat fluxes

Two situations can be encountered:

- Situation 1 – The flame doesn't impact the ceiling of the compartment, i.e. $L_f < ht$ (see Figure 64)
- Situation 2 – The flame impacts the ceiling of the compartment, i.e. $L_f \geq ht$ (see Figure 65).

Depending on the situation and depending on the location of the target (i.e. where the heat transfer computation needs to take place); different zones are defined (see Figure 64 and Figure 65). The Appendices detail two tables summarizing the heat flux components which are considered in the different zones, as well as the formulas to calculate these heat flux components (based on EN 1991-1-2 and on the previous RFCS project "LOCAFI" (Vassart et al., 2017)).

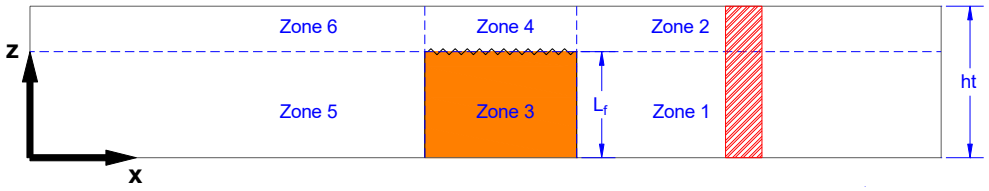

Figure 64: Zones for fire model if the flame does not impact the ceiling

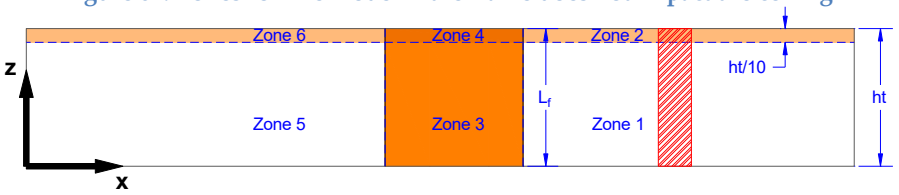

Figure 65: Zones for fire model if the flame impacts the ceiling

Steel temperatures

The steel temperature is computed according to EN1993-1-2 equation 4.25. A coupling with a zone model should be done to consider the effect of the hot gas layer. For this, the evolution of the fire are and localisation (output from Step 1) can be considered as input.

Comparison with experimental and numerical results

The results obtained while applying this model were compared with results from the experimental campaigns and from numerical simulations performed in the frame of TRAFIR project. Globally, a good correspondence is achieved, and some results are presented in the Appendices.

5.2.3. Conclusions

Two documents were produced: (1) a report detailing the simplified analytical model developed to describe the travelling fire, (2) a report presenting the results obtained while applying this model to the TRAFIR experimental campaigns and numerical simulations. For the Task 3, the model was implemented in an Excel file with VBA macro (presenting a user-friendly interface).

The model allows to evaluate (as a function of time): the fire geometry and its location, the rate of heat release, the fire load, the flame length, the gas temperatures in near field (flames), the radiative and convective heat fluxes components and the temperature in a steel member placed in the compartment (which is function of the target location in the compartment).

This model is based on recent developments made in the field of travelling and localised fires: it combines features from the ETFM framework and from the virtual solid flame

method developed in the frame of the previous RFCS project “LOCAFI”, providing results which vary along the height of the compartment and which depend on the ventilation conditions, aspects which were not tackled by existing travelling fire models. This model has to be applied when a travelling fire scenario is identified as relevant scenario and has to be coupled with a zone model (considering the fire area evolution established through the application of the TRAFIR analytical procedure).

The comparison of the steel temperatures measuring during the large scale fire tests presenting a clear travelling nature (WP3 “large-scale” tests n°1 and n°2) with the steel temperatures obtained from the analytical model exhibits a good correspondence with the following limitations: too high steel temperatures in the vicinity of the fuel (which is safe-sided) and an underestimated descending branch. This reveals, within the limits of the modelled compartments, that the proposed analytical model appears to be appropriate to evaluate the temperature of steel structural elements.

6. Application tools

6.1. Implementation of the new model in FEM software SAFIR (WP6)

6.1.1. Introduction

The model has been implemented in a completely new module (.exe file) called TRAFIR4SAFIR, also written in FORTRAN, that can be run independently and which: 1) computes the fire propagation and the travelling nature of the fire, according to the TRAFIR analytical model; 2) writes in a transfer file the information requested by SAFIR to compute the temperatures in the structure. The format of this file is the same as the one developed in the RFCS project FIRESTRUC and used so far when the thermal environment has been computed by CFD software such as FDS. The advantages of this procedure are:

- It does not lead to an excessively complex and intricate version of SAFIR.
- It leads to a lighter, easier to develop, to code and to debug software, with shorter run times.
- This code and the transfer file that it produces can be used for calculating the temperature in a structure, not only with SAFIR but with any other code/software that can read the format of this transfer file.
- This new software will of course be made available for free to anyone interested, whereas the SAFIR software is only available after buying a licence.
- This new software will also be easier to maintain, to adapt and perhaps to develop for anyone in the future whereas, if it had been embedded in SAFIR, this would require having access to the code of SAFIR and having deep understanding of the whole structure of this code.

6.1.2. Description of the activities

Several files are mentioned below to describe the new development, allowing to represent travelling fires in SAFIR software:

- TRAFIR4SAFIR.EXE is the executable file that computes the travelling fire evolution and creates the transfer file for SAFIR;
- TRAFIR.TXT is the input file for TRAFIR4SAFIR;
- TRAFIR.OUT is the result of TRAFIR4SAFIR that shows the travelling fire evolution;
- BOX01.TXT is the transfer file created by TRAFIR4SAFIR. It should be renamed as “CFD.TXT” to be subsequently used by SAFIR.

The first step consists in launching the executable “TRAFIR4SAFIR” which reads the input data related to the compartment and to the fire load and computes on this basis the evolution of the travelling fire as well as some basic characteristics of the solid flame in the burning zone, such as the flame height. The equations coded here are the same as those coded in the Excel file (i.e. the simple tool) developed under WP5, with the

difference that all variables are integrated in a discrete manner in the simple tool whereas they may have a continuous evolution as a function of time in the new FORTRAN code. The input file needed to launch TRAFIR4SAFIR is given in TRAFIR.TXT, a file which can be directly generated through the simple tool (using the button “Export to TXT”) or be generated manually, using the provided “example file” (see below Figure 66 which shows an example of the input file ”trafir.txt”).

```
Scenario A of the design guide of RFCS project TRAFIR

Width_of_the_compartment 10 m
Length_of_the_compartment 100 m
Floor_to_ceiling_distance 3 m
Width_of_the_bands 1 m
Design_fire_load_density 250 MJ/m²
Rate_of_Heat_Release_density 250 kW/m²
Fire_spread_rate 6.66 mm/s
Combustion_factor 0.8 -
Effective_heat_of_combustion 20.0 MJ/kg
Total_area_of_vertical_opening 277.2 m²
Equivalent_height_of_the_openings 2.520 m
Time_step 151 s
Height_of_the_fire_load_basis 0.3 m
```

Figure 66: Input file for TRAFIR4SAFIR: example

Figure 67 shows how this information is reproduced at the head of the output file TRAFIR.OUT generated by TRAFIR4SAFIR, with some basic parameters already calculated such as the time that it takes for the fire to propagate through each band, the time it takes for a band to be consumed if there is no air control, the total amount of fire load in the compartment and the maximum power of the fire before it enters in an air controlled regime. Figure 68 shows how the results of the travelling fire are presented for every time step, namely the fuel load that remains in the compartment, the power of the fire, the vertical position of the top of the flame and, by several “x”, the bands which are burning. If the fire has entered in an air controlled regime, the “x” will be replaced by “9”, “8”, “7”, depending on the ratio between the power in the air controlled regime and the power that the fire would have without air control.

```
CHARACTERISTICS of the TRAFIR compartment and fire.
--------------------------------------------------

   Width of the compartment       :    10.000 m
   Length of the compartment      :   100.000 m
   Floor to ceiling distance      :     3.000 m
   Width of the bands             :     1.000 m
   Design fire load density       :   250.000 MJ/m²
   Rate of Heat Release density   :   250.000 kW/m²
   Fire spread rate               :     6.660 mm/s
   Combustion factor              :     0.800 -
   Effective heat of combustion   :    20.000 MJ/kg
   Total area of vertical openings:   277.200 m²
   Equiv. heigth of vert. openings:     2.520 m
   Time step of the TRAFIR calc.  :   151.000 s
   Height of the fire load basis  :     0.300 m

   The length of the compartment is devided into 100 bands of equal width.
   The width of the bands is : 1.000 m.

   It will take 150.150 s for the fire to travel the width of each band.
   It will take 1000.000 s for a band to be consumed if there is no air control.

   The total amount of combustible material in the compartment is 250.000 GJ.

   The maximum power of the fire before it enters into air control mode is 704.066 MW
```

Figure 67: Beginning of the output file TRAFIR.OUT: example

```
 time      Fuel    Power  Top of flame  Burning
  151    249.25     5.00         1.635  XX----------------------------
  302    248.11     7.50         1.908  XXX---------------------------
  453    246.60    10.00         2.097  XXXX--------------------------
  604    244.72    12.50         2.225  XXXXX-------------------------
  755    242.45    15.00         2.308  XXXXXX------------------------
  906    239.81    17.50         2.355  XXXXXXX-----------------------
 1057    237.07    20.00         2.308  XXXXXXXX----------------------
 1208    234.57    17.50         2.308  --XXXXXXX---------------------
 1359    232.07    17.50         2.308  ---XXXXXXX--------------------
 1510    229.57    17.50         2.308  ----XXXXXXX-------------------
 1661    227.07    17.50         2.308  -----XXXXXXX------------------
 1812    224.57    17.50         2.308  ------XXXXXXX-----------------
 1963    222.07    17.50         2.308  -------XXXXXXX----------------
 2114    219.57    17.50         2.308  --------XXXXXXX---------------
 2265    217.07    17.50         2.308  ---------XXXXXXX--------------
 2416    214.57    17.50         2.308  ----------XXXXXXX-------------
 2567    212.07    17.50         2.308  -----------XXXXXXX------------
 2718    209.57    17.50         2.308  ------------XXXXXXX-----------
 2869    207.07    17.50         2.308  -------------XXXXXXX----------
```

Figure 68: Presentation of the results in TRAFIR.OUT: example

TRAFIR4SAFIR also creates the transfer file (i.e. the file which allows to transfer information to SAFIR for the subsequent thermal analysis of the structural members) BOX01.TXT. This file has the same format than the one used when the thermal environment has been obtained from a CFD analysis (using FDS for example). This format was defined in the RFCS research FIRESTRUC. It has been used in real projects by many users of SAFIR. The basic information that is written in the transfer file consists, at different time steps and for a structured grid of so called control points in several sub-volumes of the compartment, of:

- The gas temperature at the control point;
- A value of zero (could be used for the coefficient of convection, but is not used by SAFIR)
- The radiant intensities coming from different directions to the control point.

Figure 69 shows how this information is organised, for a given time step. Each line corresponds to one location in the compartment and each column, starting at the third, is for one direction; the user can choose between 46 and 130 directions at each point.

```
TIME
    7399.0

INTENSITIES
    1173.2  0.  34186.  34186.  34186.  34186.  34186.  34186.  34186.  34186.  34186.
     293.1  0.    133.    133.    133.    133.    133.    133.  18274.  26194.  18274.
    1173.2  0.  34186.  34186.  34186.  34186.  34186.  34186.  34186.  34186.  34186.
     293.1  0.    133.    133.    133.    133.    133.    133.  18274.  26194.  18274.
    1173.2  0.  34186.  34186.  34186.  34186.  34186.  34186.  34186.  34186.  34186.
     293.1  0.    133.    133.    133.    133.    133.    133.  10978.  14863.  10978.
    1173.2  0.  34186.  34186.  34186.  34186.  34186.  34186.  34186.  34186.  34186.
     293.1  0.    133.    133.    133.    133.    133.    133.  10978.  14863.  10978.
    1099.8  0.  26401.  26401.  26401.  26401.  26401.  26401.  26401.  26401.  26401.
     293.1  0.    133.    133.    133.    133.    133.    133.    133.   9217.    133.
    1099.8  0.  26401.  26401.  26401.  26401.  26401.  26401.  26401.  26401.  26401.
```

Figure 69: Partial view of the transfer file: example

As for the analytical procedure (WP5), the computation of the gas temperature and radiant intensities depends on the zones in the fire compartment and whether the flame touches the ceiling or not, see Figure 70.

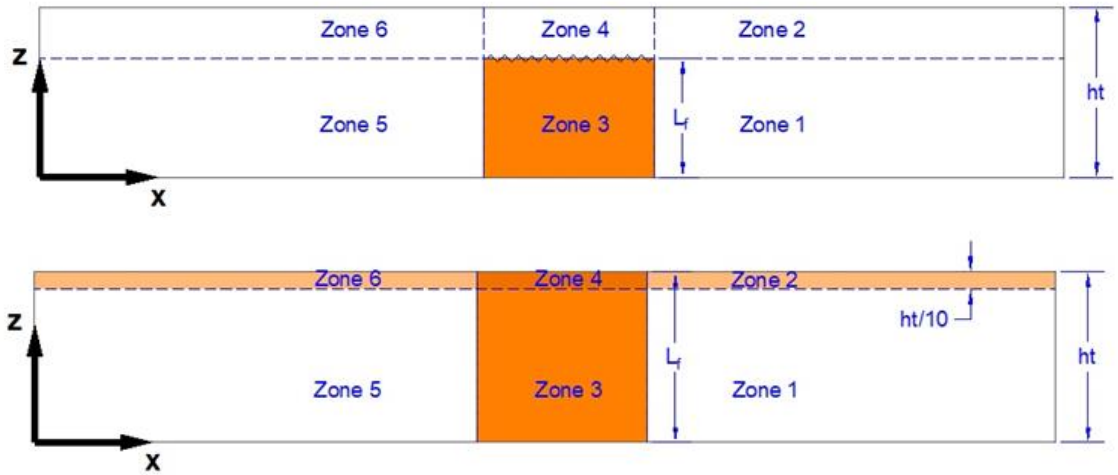

Figure 70: different zones in the fire compartment when the flame does not touch the ceiling (above) or when it touches the ceiling (below)

In zone 3, the gas temperature T_{gas} is computed according to the model of Heskestad and the isotropic radiant intensities I are computed according to Eq. 1.

$$I = \frac{1}{\pi} \cdot \sigma \cdot T_{gas}^4 \qquad (1)$$

where σ is the constant of Stefan-Boltzmann, equal to 5.67 x 10-8.

- In zones 2 and 6 when the flame touches the ceiling, the model of Hasemi is used to compute the radiant intensities and, because the flux of Hasemi comprises the convective as well as the radiative flux, the ambient temperature is written as the gas temperature.
- In zone 4,
  - If the flame is touching the ceiling, the model of Heskestad or the model of Hasemi is used, whichever is decided by the highest flux generated by both (after transformation of the flux of Hasemi into an equivalent temperature to make the comparison possible).
  - If the flame is not touching the ceiling, the gas temperature is from the Heskestad model, whereas the radiation intensities are computed separately for each of the 46 or 130 directions, depending on the temperature of the boundary that is met by a ray shot in the relevant direction, either the temperature of the top of the solid flame if the ray encounters the top of the solid flame, or the ambient in all other cases. The approach is based on the developments described in (Vassart et al., 2017) (Tondini et al., 2019) and is in accordance with EN 1991-1-2 Annex G.
- In zones 1 and 5, plus 2 and 6 if the flame does not touch the ceiling, the gas temperature is set at the ambient, whereas the radiation intensities are computed separately for each of the 46 or 130 directions, depending on the temperature of the boundary that is met by a ray shot in the relevant direction, either the temperature of Heskestad if the ray encounters the solid flame (on the side or on the top), or the ambient in all other cases. The approach is based on the developments described in (Vassart et al., 2017) (Tondini et al., 2019) and is in accordance with EN 1991-1-2 Annex G.

6.1.3. Conclusions

An independent standalone code, TRAFIR4SAFIR, has been written that can be run on 64 bits Windows operating systems, without any need of a licence for any other code. It computes the evolution of the travelling fire of which it gives the main results in the output file (amount of fuel remaining in the compartment, power released by the fire, length of the flame, location of the fire…) and produces a transfer file that can be used by SAFIR to compute the temperatures in a structure of any shape (any orientation of the elements, any shape of the sections, protected or not…).

6.2. Implementation of the new model in FEM software OpenSees (WP6)

6.2.1. Introduction

The analytical travelling fire model developed in the project (WP5) was implemented into the pre-existing SIFBuilder model, which is an OpenSees-based open-source software framework (Dai 2018; Dai et al., 2020). Guidance on running the software is summarised and more details are available separately.

6.2.2. Description of the activities

The analytical travelling fire model developed in the project (under WP5) was implemented into the pre-existing SIFBuilder model, which is an OpenSees-based open-source software framework (Dai 2018; Dai et al., 2020). The realisation of the new model follows the same workflow as the current available localized fire model in OpenSees, thereby integrating the travelling fire representation and associated heat transfer analysis, which in turn is coupled to the thermo-mechanical analysis for modelling 3D structural response.

After inputting basic information for generating the structural model, including the geometrical details of the compartment, the user defines the structural loading and thereafter the fire loading information (i.e. fuel load characteristics), which are maintained throughout the entire analysis. Then, when running the code, the travelling fire module interacts with the heat transfer module via their interfaces at each time step in order to determine the transient fire imposed boundary conditions at the structural surfaces. Both the spatial and temporal non-uniform heat fluxes for different structural elements, produced from the analytical model, are updated at each time step according to the travelling fire location in the compartment.

Subsequently, the heat transfer analysis module is launched and the nodal temperature histories are automatically mapped to the fibres of the structural mesh for each structural member. Following the heat transfer analysis, all of the structural members are analysed together and the final thermo-mechanical analysis is performed on the whole structure. Hence, the output generated is the result of a thermo-mechanical analysis in response to the travelling fire for the global structural analysis.

Some details of the implementations and procedures follow (full guidance for running the software is provided separately while the dedicated OpenSees source for fire development can be found on GitHub: http://openseesforfire.github.io).To start, follow the instructions at OpenSees official website:

https://opensees.berkeley.edu/OpenSees/user/download.php

Then replace the openSees.exe with the version provided in TRAFIR (WP6.2) UEDIN, and run this example TRAFIR_Example.tcl

```
1  ##########################################################################################
2  #####                                                                                #####
3  #####                              TRAFIR Model Example Script                       #####
4  #####                                                                                #####
5  ##########################################################################################
6
7  # This Tcl model works in SVN commit version 87
8
9  # For testing TRAFIR model with heat transfer module under SIFBuilder
10 # Written by: Xu Dai (x.dai@ed.ac.uk; xudai1987@gmail.com), Dec. 2020, University of
   Edinburgh
11 # SI unit i.e. meter, newton, second
12
13 wipe;
14 set dataDir TRAFIR_Example;
15 file mkdir $dataDir;
16
17 # Define STRUCTURAL MODEL
18 SIFBuilder -type Frame -ndm 3;
19 SIFXBay 8.0 7.0 7.0 8.0;
20 SIFZBay 2.0 3.0 3.0 2.0;
21 SIFStorey 3.0;
```

i.e. enter at the prompt: >source TRAFIR_Example.tcl

Here, each bay length is defined in metres (m):

X Bay: 8.0m, 7.0m, 7.0m, 8.0m; 4 bays in total in x direction

Z Bay: 2.0m, 3.0m, 3.0m, 2.0m; 4 bays in total in z direction

Y is vertical

The steel material definition follows EN 1993; examples of assigned cross-section dimension (units in m) to the relevant beam/column series, i.e. UB 406x178x54 and HE400B:

```
22
23 # ASSIGN SECTION
24 AddMaterial steel 1 -type EC3 2.35e8  2.1e11;
25 AddSection ISection 1 1 0.4026 0.1777 0.0077 0.0109;    # $d $bf $tw $tf, UB 406x178x54
26 AddSection ISection 2 1 0.4000 0.3000 0.0135 0.02405;   # $d $bf $tw $tf, HE400B
27 AssignSection XBeams 1;
28 AssignSection ZBeams 1;
29 AssignSection columns 2;
```

All column bases are fixed, a uniformly distributed load is applied for all beams (unit: N/m):

```
30
31 # Set BOUNDARY CONDITION
32 SetBC fixedJoint -Locy 0;
33
34 # Define LOADING
35 #AddLoad -SIFJoint 2_2_2 -load 0 600000 0;
36 AddLoad -SIFMember allBeams -load 0 -15856 0;
37
```

The TRAFIR model is triggered here via keyword TRAFIR, defining the fire at floor number 0, ignition line source and fire travel direction prescribed; opening size is also defined with total opening width, sill height, and soffit height (units in m):

```
38 # FIRE DEFINITION
39 AddFire -floor 0 -type TRAFIR -IgnitionLine point1 0 0 0 point2 0 0 10.0
   -fireTravelDirection AntiClockWise;
40
41 # MORE FIRE INFO
42 AddFirePars -floor 0 -type TRAFIR -ventWidth 25 -sillHeight 0.5 -soffitHeight 2.5;
```

A uniform fuel load is assigned with examples of fuel base height 0.3 m, fire spread rate 2 mm/s, fuel load density 511 MJ/m^2, and HRRPUA 250 kW/ m^2:

```
44   # FUEL LOAD DISTRIBUTION DEFINITION
45   AddFuel -RMFD 1 -floor 0 -fuelBaseHeight 0.3 -SpreadRate 2.0 -FuelLoadDensity 511
     -HRRperArea 250;
```

The structural FEM model mesh control is setup here. 6 elements per beam/column. Linear geometry transformation is considered via geomTransf keyword (P-Delta effect could also be used via changing this to “P-Delta”):

```
46
47   # BUILD MODEL
48   BuildModel -MeshCtrl 6 6 6 -geomTransf Linear;
```

Display windows are then setup along with required structural response monitoring.

```
55
56   # Define OUTPUT RESULTS
57   SIFRecorder SIFJoint -file $dataDir/SIFJoint_1_1_1_Disp.out -time -joint 1_1_1 disp;
58   #SIFRecorder SIFJoint -file $dataDir/SIFJoint_10_1_1_Disp.out -time -joint 10_1_1 disp;
     #to debug
59   #SIFRecorder SIFMember -file $dataDir/SIFXBeam_5_1_1_Mid_Deflect.out -time -xBeam 5_1_1
     mid-deflect;
60   #SIFRecorder SIFMember -file $dataDir/SIFZBeam_3_1_1_Mid_Deflect.out -time -zBeam 3_1_1
     mid-deflect;
61   #SIFRecorder SIFMember -file $dataDir/SIFColumn_5_2_1_Mid_Deflect.out -time -column
     5_2_1 mid-disp;
62   #SIFRecorder SIFMember -file $dataDir/SIFSlab_1_1_1.out -time -slab 1_1_1 mid-deflect;
```

In this case only fire load is analysed (examples of combined loads are shown in comments below (following #), 9 data points for data transfer from 1D for a slab, or 15 data points for 2D for beams/columns heat transfer to structural model):

```
63
64   # Apply LOADS & Define ANALYSIS & Define HT OUTPUT
65   SIFAnalyze Fire -dt 10 -output $dataDir -datapoints 9;
66   #SIFAnalyze selfWeight -dt 0.2 Fire -dt 20 -output $dataDir -datapoints 9;
67   #SIFAnalyze selfWeight -dt 0.2 Load -dt 0.1 Fire -dt 20 -output $dataDir -datapoints 9;
68   #SIFAnalyze Load -dt 0.1 Fire -dt 30 -duration 960 -output $dataDir;
69   #SIFAnalyze Load -dt 0.1;
70
71   # Print KEY INFO
72   print $dataDir/domain.out
73
74   wipe;
75   #wipeSIFBuilder;
```

During the fire analysis, the fire modelling status is rendered to the screen using OpenGL:

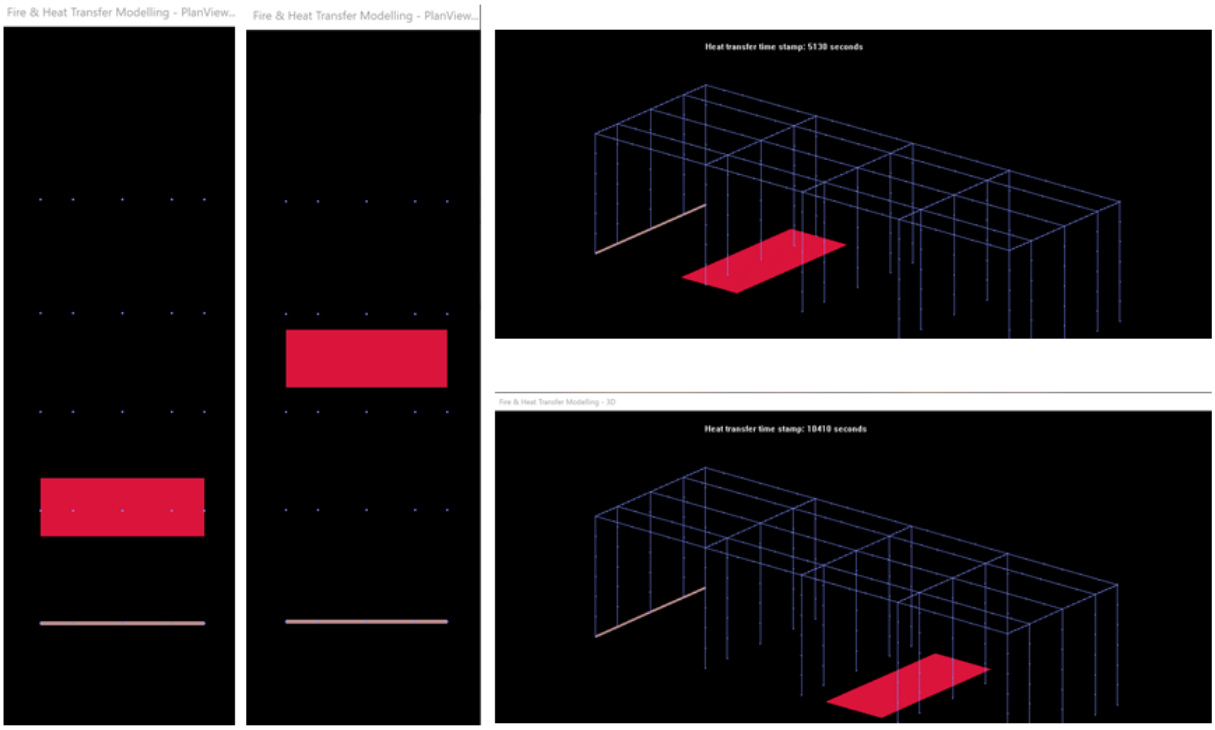

Innovation in this work is that it provides practitioners and researchers a platform to review and improve the model (and coding) in future.

6.2.3. Conclusions

A new version of OpenSees expands on the previous capabilities in providing an alternative access to the newly developed analytical model, and integrating it with an advanced and efficient structural analysis; the resulting software framework therefore provides a flexible approach for examining the impact of fire on structural behaviour under realistic design fire scenarios, at greatly reduced cost in time and effort.

6.3. Design guidance (WP7)

6.3.1. Introduction

A Design Guide, presented in a single document, was prepared. It contains a simplified version of the project, the description of the analytical method to characterize the thermal impact caused by a travelling fire as well as realistic case studies (how to apply the method through worked examples).

6.3.2. Description of the activities

The first part of the design guide provides simplified version of the project scientific content. Then, the design guide provides some major key learnings from the numerical analyses launched with FDS as well as a clear description of the analytical procedure (it is detailed how to use the tool to ease the use of the method).

Finally, the design guide describes several realistic worked examples, based on real buildings and on the EN1991-1-2, following the analytical procedure described at the beginning of the guide. The application of the procedure is described step-by-step, to help the user clearly understand how to handle and use the method and the simple tool in which it was implemented. It is important to highlight that the provided information does not represent validated designs nor unique analysis results; they are presented here as examples to help the user understand how to use the methodology and to assess the differences which may be observed while varying relevant parameters.

Several buildings with modern architecture were chosen to apply the TRAFIR methodology. In this document, the occupation types “office” and “sparsely loaded office” (open space office with limited combustibility furniture, paperless office without archives, according to EN 1991-1-2 Final Draft 2020) are considered. Indeed, the CFD parametric analyses conducted in the frame of this project (WP4) showed that a travelling fire scenario is more likely to take place for these occupancies (or for other occupancies with similar fire loads). The fire loads and rate of heat release densities of these occupancies were considered. Several fire front spread rates were considered: from back-calculation based on EN 1991-1-2 and from (Grimwood, 2018). The analytical procedure considers “openings” and not “windows”, it is therefore required to make an assumption regarding the breakage of the windows during the fire. For most of the scenarios, 90% of the windows are considered as broken (i.e. as openings): it covers the intended breakage of the glazing by the rescue teams. For one scenario, a different situation is chosen: 30% of the windows are considered as broken (it has to be noted that it is not possible to define openings which vary as a function of time in the tool). For each case study, the following aspects are described and analysed: how the tool is used, the number of burning bands, the burning rate, the flame height, the total power in the compartment and finally the steel temperature of a column (see for example in Figure 71 the temperature evolution in a column HE 200 A supposed to be placed in the centre of a sparsely loaded office whose dimensions are 18m x 42m x 3m). For this building, the glazing is placed on 100% of the compartment perimeter, with a height of 1.5m, and it is assumed that 90% of the glazing is broken.

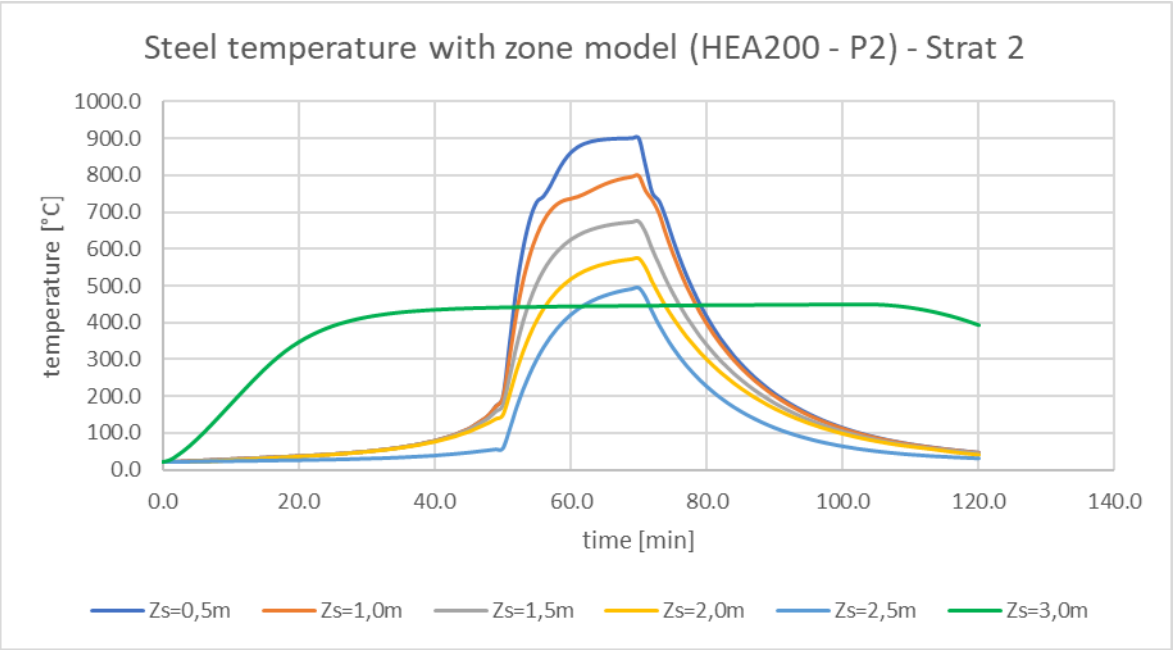

Figure 71: Design guide example: the temperature evolution in a column HE 200 A for case study B

6.3.3. Conclusions

The design guide summarizes the main development of the TRAFIR project, provides some major key learnings from the CFD numerical analyses launched with FDS as well as a clear description of the analytical procedure and of how to use the simple tool to ease the use of the method). In addition, seven realistic worked examples, based on real buildings and on the EN 1991-1-2, following the TRAFIR analytical procedure. The application of the procedure is described step-by-step, to help the user clearly understand how to handle and use the method and the simple tool in which it was implemented.

7. General conclusions and perspectives

7.1. Actual applications

TRAFIR developments were shared throughout the project with practitioners (design offices, consultancy offices, members of technical committees for the revision of Eurocodes) who have shown a high interest in these developments.

The analytical procedure developed in the frame of TRAFIR led to a travelling fire model for structural design which is relevant for large spaces in modern constructions which are in accordance with expectations of today's society. It was implemented in a simple tool (Excel file) with user-friendly interface. The comparison of the steel temperatures measured during the large scale fire tests (presenting a clear travelling nature) with the steel temperatures obtained from the analytical model globally exhibits a good correspondence. This reveals that the proposed analytical model appears to be appropriate to evaluate the temperature of steel structural elements and may be used by design offices for practical applications. The procedure was detailed and applied step-by-step in a design guide. These developments provide all the required material to the engineers, architects, fire service personnel and local authorities to characterize a travelling fire and evaluate the steel temperature of a structural member subjected to such scenario.

In addition, the procedure was implemented in two widely recognized FEM software: SAFIR® and OpenSees, ensuring the application of the model not only in analytical analyses but also in complex numerical models, involving complex geometries.

7.2. Technical and economic potential

The several experimental campaigns which were launched in the frame of TRAFIR brought important technical advancements which are of interest for future testing:

- The work performed in WP2 "Characterization of fuel loads" led to devise a well-established methodology, from the ignition system up to the fire load arrangement, to perform natural fire tests leading to a desired fire growth rate coefficient. This methodology could be used in the future as a standard method for natural fire tests in order to allow a comparison of different conditions (ventilations, geometry, nature of the boundaries) (Gamba et al., 2020).
- The work performed in WP2 "Influence of near & far field" and WP3 "Large-scale natural fire tests" provided experimental data for both controlled and uncontrolled travelling fires in large compartment. This unique data will support a better understanding of fire dynamics and the improvement of thermal models (Anderson et al., 2020) (Nadjai et al., 2020).

Furthermore, the numerical analyses (using CFD) also brought significant technical improvements which will support subsequent CFD simulations and the understanding of the conditions leading (or not) to a travelling fire scenario:

- New guidance on approaches to representation of fire spread in detailed "stick-by-stick" models, facilitating use of such approaches for generalising the results of tests to consider variations of design parameters and variable or uncertain input parameters.
- Establishment of a "wood block" model which is a practical vehicle for exploring travelling fire behaviours are the scale of large compartments, thereby considering the role of compartment geometry (including openings and ceiling height) and fuel load density, at much reduced cost compared to experimental approaches.
- The results of the parametric analyses can be used to pursue and refine the investigation of the influence of the compartment and fire parameters on the fire scenario.

The state of the art performed at the start of the project highlighted that existing models were considering overly simplified assumptions (for example: uniform temperature along the height of the compartment in the near field and no consideration of the ventilation conditions). Finally, the analytical procedure which was implemented in a simple tool, in two FEM software and described in a design guide, represent "deployment kit" for structural safety, optimization and enhanced sustainability (through avoidance of material waste), resulting in economic and environmental benefits.

7.3. Future work to be undertaken

Further research would be needed to improve the following points:

- to assess the glazing breakage evolution; influencing the fire dynamics (both for numerical and analytical models);
- to better understand what influences the fire front speed – and therefore to be able to provide guidance regarding this parameter;
- exploration of the impact of alternative fuels on dynamics of compartment fires, i.e. plastics and mixed fuels, as there are known limitations in extrapolating from observations derived from timber cribs to "real" fuels (cf. Gupta et al., 2021);
- to assess the impact of fuel islands on the fire spread over a large space;
- to develop and improved CFD representation of the cooling phase of the fire to include the role of the char and glowing embers.

Publications

Journal Papers

- Anderson, J., Sjöström, J., Temple, A., Charlier, M., Dai, X., Welch, S., Rush, D. (2020) "FDS simulations and modelling efforts of travelling fires in a large elongated compartment", Fire and Materials, doi:10.1002/fam.2933
- Charlier, M., Gamba, A., Dai, X., Welch, S., Vassart, O., Franssen, J.-M. (2020) "Modelling the influence of steel structure compartment geometry on travelling fires", Proceedings of the Institution of Civil Engineers – Structures and Buildings, doi:10.1680/jstbu.20.00073
- Charlier, M., Glorieux, A., Dai, X., Alam, N., Welch, S., Anderson, J., Vassart, O., Nadjai, A. (2021) "Travelling fire experiments in steel-framed structure:numerical investigations with CFD and FEM", Journal of Structural Fire Engineering, Vol. [ahead-of-print] No. [ahead-of-print]. doi:10.1108/JSFE-11-2020-0034
- Dai, X., Welch, S., Vassart, O., Cábová, K., Jiang, L., Maclean, J., Clifton, G.C. & Usmani, A. (2020) "An Extended Travelling Fire Method Framework for performance-based structural design", Fire & Materials (Special Issue Paper) 44(3):437-457 doi:10.1002/fam.2810
- Dai, X., Welch, S. & Usmani, A. (2017) "A critical review of "travelling fire" scenarios for performance-based structural engineering", Fire Safety Journal 91C: 568-578, doi:10.1016/j.firesaf.2017.04.001
- Gamba, A., Charlier, M., Franssen, J.-M. (2020) "Propagation tests with uniformly distributed cellulosic fire load", Fire Safety Journal 117, 103213, doi: 10.1016/j.firesaf.2020.103213

Conference Papers (Delivered with oral presentations)

- Charlier, M., Gamba, A., Dai, X., Welch, S., Vassart, O. & Franssen, J-M. (2018) "CFD analyses used to evaluate the influence of compartment geometry on the possibility of development of a travelling fire", Proceedings of the 10th International Conference on Structures in Fire, Belfast, UK, pp. 341-348
- Charlier, M., Vassart, O., Dai, X., Welch, S., Sjöström, J., Anderson, J., Nadjai, A. (2020) "A simplified representation of travelling fire development in large compartment using CFD analyses", Proceedings of the 11th International Conference on Structures in Fire, Brisbane, Australia, doi:10.14264/5af38e2
- Dai, X. & Welch, S. (2019) "Characterising Natural Fires in Large Compartments for Structural Design – Revisiting An Early Travelling Fire Test (BST/FRS 1993) with CFD", Proc. 3rd Int. Conf. Structural Safety under Fire & Blast (CONFAB), 2-4 September 2019
- Dai, X., Welch, S., Rush, D., Charlier, M. & Anderson, J. (2019) "Characterising natural fires in large compartments – revisiting an early travelling fire test (BST/FRS 1993) with CFD", Proc. 15th Int. Conf. & Exhibition on Fire Science & Engineering (Interflam 2019), Royal Holloway College, Nr Windsor, UK, 1-3 July 2019

- Dai, X., Welch, S. & Usmani, A. (2018) “An Extended Travelling Fire Method Framework for Performance-Based Structural Design”, Proc. ASTM E05 Workshop on Advancements in Evaluating the Fire Resistance of Structures, Washington DC, 6-7 December 2018
- Dai, X., Welch, S. & Usmani, A. (2017) “A critical review of travelling fire scenarios for performance-based structural engineering”, Proc. 11th Int. Symp. Fire Safety Science, Lund, Sweden, June 2017, pp. 568-578
- Franssen, J.-M., Gamba, A., Charlier, M. (2019) “Towards a standardized uniformly distributed cellulosic fire load”, 3rd International Fire Safety Symposium IFireSS, Ottawa, Canada
- Nadjai, A., Alam, N., Charlier, M., Vassart, O., Dai, X., Franssen, J.-M., Sjöström, J. (2020) “Travelling fire in full scale experimental building subjected to open ventilation conditions”, Proceedings of the 11th International Conference on Structures in Fire, Brisbane, Australia, doi:10.14264/987a305
- Nadjai, A., Alam, N., Charlier, M., McGillighan, J., Vassart, O. (2021) “Experimental and Numerical Investigations on Steel Columns Compartment Subjected to Travelling Fires”, accepted for the 9th European Conference on Steel and Composite Structures (Eurosteel), Sheffield, UK

Acknowledgment

The TRAFIR consortium would like to thank the following companies/entities for their support.

- The European Commission, for sponsoring the whole project.
- Severfield Ltd, local partner to FireSERT, for erecting the structural steel frame of the WP3 test compartment (large scale tests).
- Sean Timoney & Sons Ltd, local partner to FireSERT, for providing the testing space for the WP3 test compartment (large scale tests).
- FP McCann Ltd, local partner to FireSERT, for sponsoring the hollow core precast concrete slabs, back wall and the concrete blocks for the WP3 test compartment (large scale tests).
- CROSSFIRE Ltd, for sponsoring the fire protection facilities for the structural columns of the WP3 test compartment (large scale tests).
- Severfield (NI) Limited for sponsoring the steel platform used for recording the mass loss for the WP3 test compartment (large scale tests).
- The consortium is grateful to Sylvain Desanghere and Christophe Thauvoye for their advices regarding CFD.
- This work has made use of the resources provided by the Edinburgh Compute and Data Facility (ECDF) (http://www.ecdf.ed.ac.uk/).
- The consortium is grateful to EPSRC (grant number: EP/R029369/1) and ARCHER for financial and computational support as a part of their funding to the UK Consortium on Turbulent Reacting Flows (www.ukctrf.com).
- South Älvsborgs Rescue Service Association (SÄRF) for the provision of the WP2 Task 2 testing site and safety support for the duration of the WP2 Task 2 experiments.

References

Brandon, D. (2020) “Brief Summary Report Fire Safe implementation of visible mass timber in tall buildings – compartment fire testing”, RISE report 2020:94, ISBN 978-91-89167-79-7

Cadorin, J.F. (2003) “Compartment Fire Models for Structural Engineering”, PhD thesis (Liège University).

CEN (European Committee for Standardization) (2002), EN 1991-1-2: Eurocode 1: Actions on structures – Part 1-2: General actions – Actions on structures exposed to fire, CEN, Brussels, Belgium

Charlier, M., Gamba, A., Dai, X., Welch, S., Vassart, O. & Franssen, J-M. (2018) “CFD analyses used to evaluate the influence of compartment geometry on the possibility of development of a travelling fire”, Proceedings of the 10th International Conference on Structures in Fire, Belfast, UK, pp. 341-348

Charlier, M., Gamba, A., Dai, X., Welch, S., Vassart, O. & Franssen, J.-M. (2020) “Modelling the influence of steel structure compartment geometry on travelling fires”, Proceedings of the Institution of Civil Engineers – Structures and Buildings, doi:10.1680/jstbu.20.00073

Charlier, M., Vassart, O., Dai, X., Welch, S., Sjöström, J., Anderson, J. & Nadjai, A. (2020b) “A simplified representation of travelling fire development in large compartment using CFD analyses”, Proceedings of the 11th International Conference on Structures in Fire, Brisbane, Australia, doi:10.14264/5af38e2

Charlier, M., Glorieux, A., Dai, X., Alam, N., Welch, S., Anderson, J., Vassart, O. & Nadjai, A. (2021) “Travelling fire experiments in steel-framed structure:numerical investigations with CFD and FEM”, received for production (February 2021) by the Journal of Structural Fire Engineering.

Dai, X. (2018) “Extended Travelling Fire Method Framework with an OpenSees-based Integrated Tool SIFBuilder”, PhD thesis, School of Engineering, University of Edinburgh, UK https://era.ed.ac.uk/handle/1842/33088

Dai, X., Welch, S. & Usmani, A. (2017) “A critical review of “travelling fire” scenarios for performance-based structural engineering”, Fire Safety Journal 91C: 568-578, doi: 10.1016/j.firesaf.2017.04.001Dai, X., Welch, S., Rush, D., Charlier, M. & Anderson, J. (2019) “Characterising natural fires in large compartments – revisiting an early travelling fire test (BST/FRS 1993) with CFD”, Proc. 15th Int. Conf. & Exhibition on Fire Science & Engineering (Interflam 2019), Royal Holloway College, Nr Windsor, UK, 1-3 July 2019

Dai, X., Welch, S., Vassart, O., Cábová, K., Jiang, L., Maclean, J., Clifton, G.C. & Usmani, A. (2020) "An Extended Travelling Fire Method Framework for performance-based structural design", Fire & Materials (Special Issue Paper) 44(3):437-457 doi:10.1002/ fam.2810Degler, J., Eliasson, A., Anderson, J., Lange, D. & Rush, D. (2015) “A-priori modelling of the Tisova Fire Test as input to the experimental work”. In: The First International Conference on Structural Safety under Fire & Blast. Glasgow, Scotland, UK; 2015:429-438.

Drysdale, D. (2011) “An Introduction to Fire Dynamics”, 3rd ed., John Wiley & Sons

Edinburgh Compute and Data Facility (ECDF), [online] U of Edinburgh [Viewed 31 December 2020]. Available from: http://www.ecdf.ed.ac.uk

Gamba, A., Charlier, M. & Franssen, J.-M. (2020) “Propagation tests with uniformly distributed cellulosic fire load”, Fire Safety Journal 117, 103213, doi:10.1016/j.firesaf.2020.103213

Grimwood, P. (2018) “Structural fire engineering: realistic ‘travelling fires’ in large office compartments”, International Fire Professional, Issue No 25

Gupta, V., Hidalgo, J.P., Cowlard, A., Abecassis-Empis, C., Majdalani, A.H., Maluk, C. & Torero, J.L. (2020a) “Ventilation effects on the thermal characteristics of fire spread modes in open-plan compartment fires”, Fire Saf. J. 103072, doi:10.1016/j.firesaf.2020.103072

Gupta, V., Osorio, A.F., Torero, J.L. & Hidalgo, J.P. (2020b) “Mechanisms of flame spread and burnout in large enclosure fires”, Proc. Comb. Inst. 38, Brisbane, Australia, 24-29 January 2021 doi:10.1016/j.proci.2020.07.074

Gupta, V., Torero, J.L. & Hidalgo, J.P. (2021) “Burning dynamics and in-depth flame spread of wood cribs in large compartment fires”, Comb. Flame 228:42-56 doi:10.1016/j.combustflame.2021.01.031

Horovà, K. (2015) “Modeling of Fire Spread in Structural Fire Engineering”. PhD thesis, Czech Technical University, Prague, Czech Republic

Kawagoe, K. (1958) “Fire behavior in rooms”, Report 27, Building Research Institute, Ministry of Construction, Tokyo, Japan

Kirby, B.R., Wainman, D.E. & Tomlinson, T.L. (1999) “Natural Fires in Large Scale Compartments”, Int. J. Eng. Performance-Based Fire Codes 1(2):43-58

Kumar, S., Miles, S. Welch, S., Vassart, O., Zhao, B., Lemaire, A.D., Noordijk, L.M., Fellinger, J.H.H. & Franssen, J.-M. (2007) FIRESTRUC - Integrating advanced three-dimensional modelling methodologies for predicting thermo-mechanical behaviour of steel and composite structures subjected to natural fires, RFS-PR-02110, Publishable Report, European Commission

McGrattan, K., Hostikka, S., Floyd, J., McDermott, H. & Vanella, M. (2021) Fire Dynamics Simulator (Version 6) User’s Guide, National Institute of Standards and Technology NIST Special Publication 1019, 6th edition, doi:10.6028/NIST.SP.1019

Rackauskaite, E., Hamel, C., Law, A. & Rein, G. (2015) “Improved formulation of travelling fires and application to concrete and steel structures”, Structures 3:250–260 doi:10.1016/j.istruc.2015.06.001

Rein, G., Zhang, X., Williams, P., Hume, B., Heise, A., Jowsey, A., Lane, B. & Torero, J.L. (2007) “Multi-storey fire analysis for high-rise buildings”, Proc. 11th Int. Interflam Conf., London, UK, pp. 605–616

Sjöström, J. & Lange, D. (2014) “An investigation of the lumped capacitance assumption for unprotected steel members”, Proceedings of the 8th international conference on Structures in Fire, China.

Thomas, I.R. & Bennetts, I.D. (2005) “Fires in enclosures with single ventilation openings - Comparison of long and wide enclosures”, Fire Safety Science 6: 941–952

Tondini, N., Thauvoye, C., Hanus, F., Vassart, O. (2019) “Development of an analytical model to predict the radiative heat flux to a vertical element due to a localised fire”, Fire Safety Journal 105: 227-243, doi:10.1016/j.firesaf.2019.03.001

Torero, J.L., Majdalani, A.H., Abecassis-Empis, C. & Cowlard, A. (2014) “Revisiting the compartment fire”, Fire Safety Science 11: 28-45 doi:10.3801/IAFSS.FSS.11-28

UK National Supercomputing Service (ARCHER), [online] [Viewed 31 December 2020]. Available from: http://www.archer.ac.uk

Vassart, O., Hanus, F., Obiala, R., Brasseur, M., Franssen, J.M., Scifo, A., Zhao, B., Thauvoye, C., Nadjai, A., Sanghoo, H., Zaharia, R. & Pintea, D. (2017) “Temperature assessment of a vertical steel member subjected to localised fire (LOCAFI)”, EUR 28577 (EN), Grant Agreement n° RFSR-CT-2012-00023

Welch, S., Jowsey, A., Deeny, S., Morgan, R. & Torero, J.L. (2007) “BRE large compartment fire tests – characterising post-flashover fires for model validation”, Fire Safety Journal, 42 (8): 548-567 doi:10.1016/j.firesaf.2007.04.002

Yang, P.Y. (2016) “Computational modelling of fire spread in a full-scale compartment fire test”, IMFSE thesis, School of Engineering, University of Edinburgh, UK https://imfse.be/theses

List of figures and tables

Appendices

Large-scale tests (WP3): instrumentation and data logging system

Measurement of gas and steel temperatures

Temperatures in the test compartment were recorded at different locations and levels using thermocouples. All thermocouples used for monitoring of temperatures in the compartment and in the test structure were type K-310 with bead size measuring 1.5 mm. The length of all thermocouples was 3 m. Thermocouples were provided in the form of trees as well as individual sensors. The thermocouple trees were divided into two groups, the ones within the central zones along the fuel bed between gridlines B and C and the ones in the outer zones, outside the fuel bed. The central trees within the fuel bed were equipped with thermocouples provided at six different levels. The first thermocouple was provided at 0.5 m from the floor finish level while the last one was provided at 2.7 m as shown in Figure 72. In case of trees provided outside the fuel bed, only three thermocouples were provided at selected levels. The first thermocouple was provided at 1 m from the floor finish level while the second and the third were provided at 2 m and 2.5 m respectively. The positioning of the thermocouples adopted for thermocouple trees outside the fuel bed is shown in Figure 72.

The thermocouple trees within the fuel bed were provided in the central part of the compartment along the longer dimension between the gridlines B and C. In total, eleven thermocouple trees were provided during the tests. Three thermocouples trees were provided each along gridlines B and C near the dummy columns while the remaining five were provided along the centreline of the compartment as shown in Figure 73 (label “TRL”).

In addition to the data recorded in the compartment, temperatures were also recorded in the steel frame during the tests. Temperatures in the steel frame were recorded in the dummy columns and the selected beams. It should be realised that no arrangements were made to record the temperatures in any of the protected structural columns. In addition to columns, temperatures in the interior beams of the test compartment were also monitored during the fire tests. In all cases, the instrumentation was assigned in the middle of the beams near the thermocouple trees. Each beam was instrumented with three thermocouples, two on the flanges and one on the steel web. The first thermocouple was provided in the bottom flange while the second thermocouple was provided in the middle of the steel web. The last thermocouple was provided in the top flange as shown in Figure 74 and Figure 75.

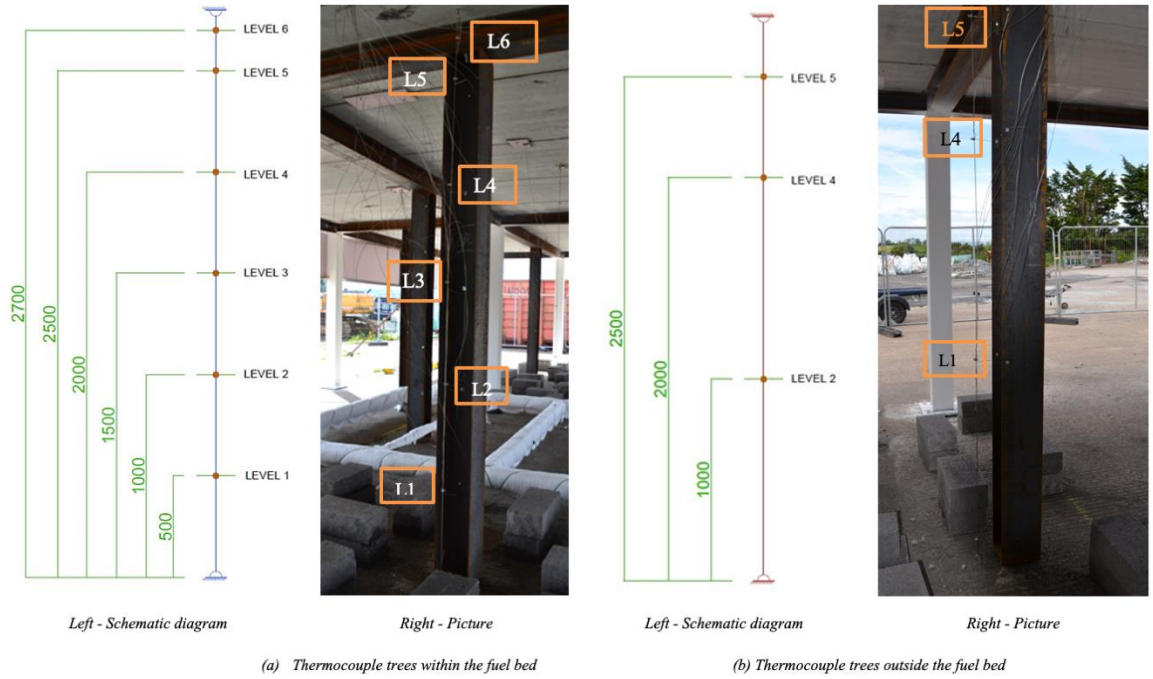

Figure 72: Details of the thermocouple trees within the fuel bed (left) and outside the fuel bed (right)

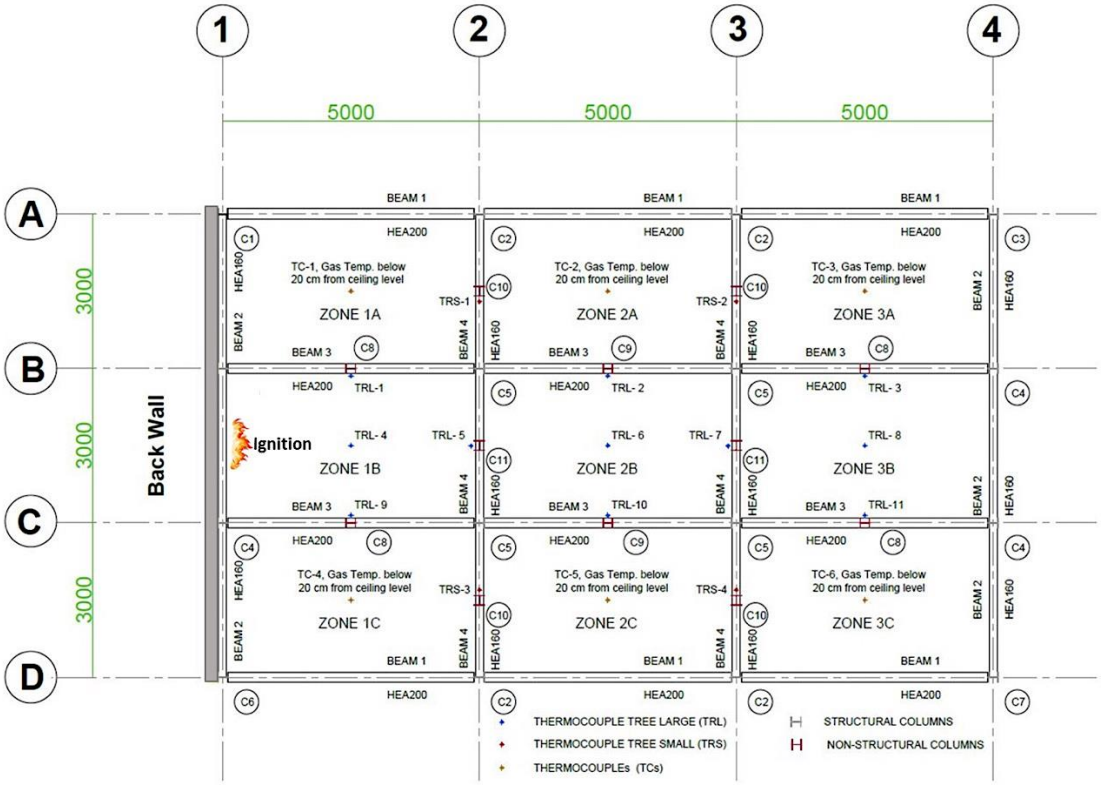

Figure 73: Location of thermocouple trees in the test compartment and positioning of thermocouples at ceiling

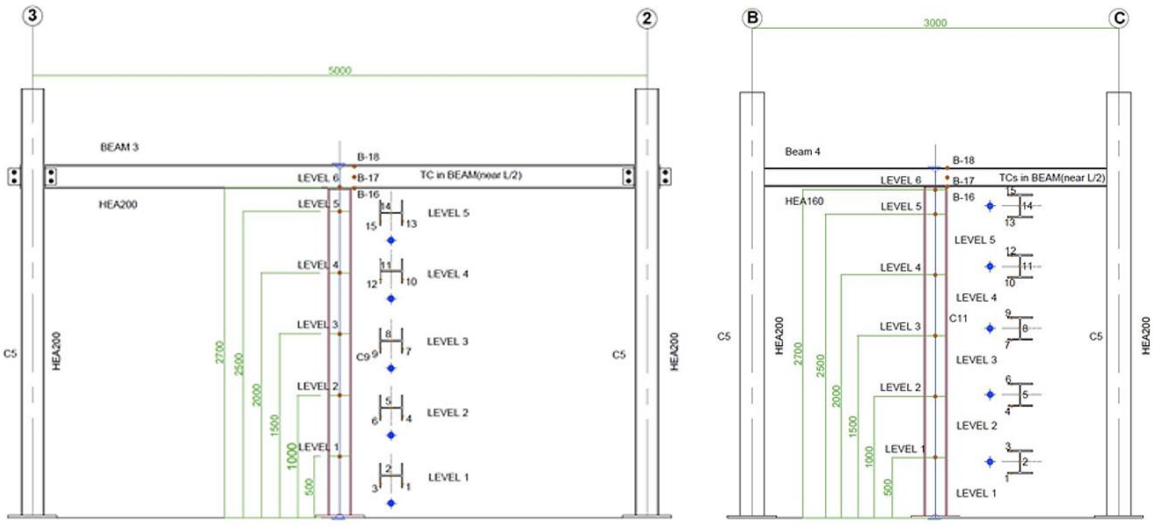

(a) Column C9 (b) Column C11

Figure 74: Thermocouple positioning in the central dummy columns C9 (left) and C11 (right) and beams

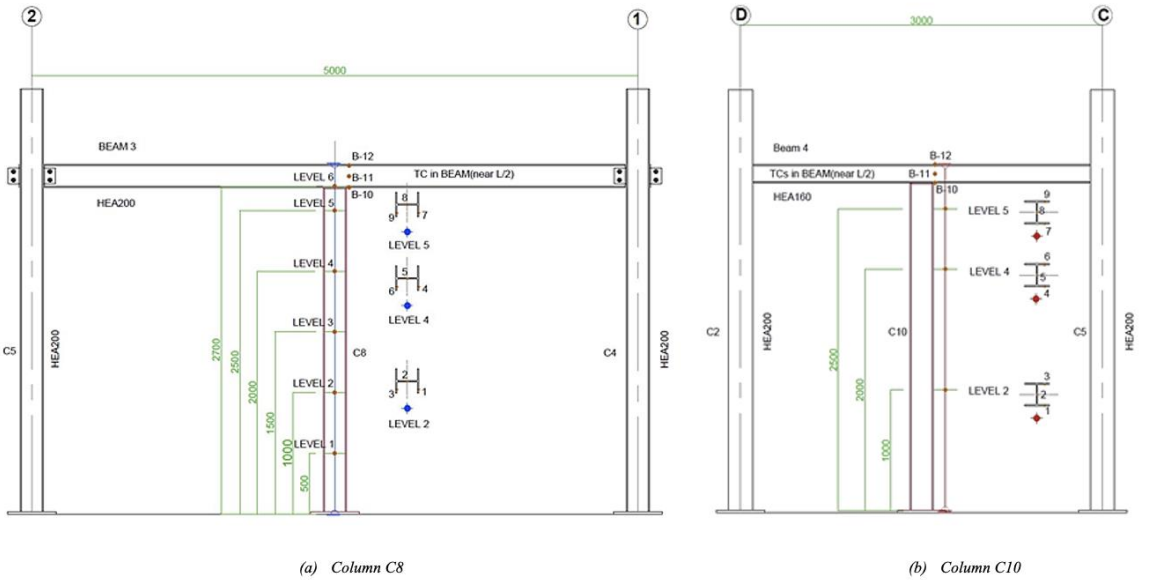

(a) Column C8 (b) Column C10

Figure 75: Thermocouple positioning in the non-central dummy columns C8 (left) and C10 (right) and beams

Measurement of heat fluxes

To record the heat fluxes, two Gardon Gauges (GGs) and Thin skin calorimeters (TSCs) were applied in the central part of the test compartment. These heat flux gauges were installed on a board which was positioned at 1.5 m from the edge of the fuel bed as shown in Figure 76. The first GG and TSC were provided at 1 m level from the floor finish level while the second GG and TSC were provided at 2 m from the floor finish level. At each level along with GGs and TSCs, a thermocouple was also assigned to monitor the temperatures. The positioning of the TSCs at ceiling level was kept similar during the three tests and were inspected after each test. As the TSCs provided within the fire bed were destroyed during Test 1, a fresh set of the TSCs was provided during Test 3 while no arrangements were made during Test 2.

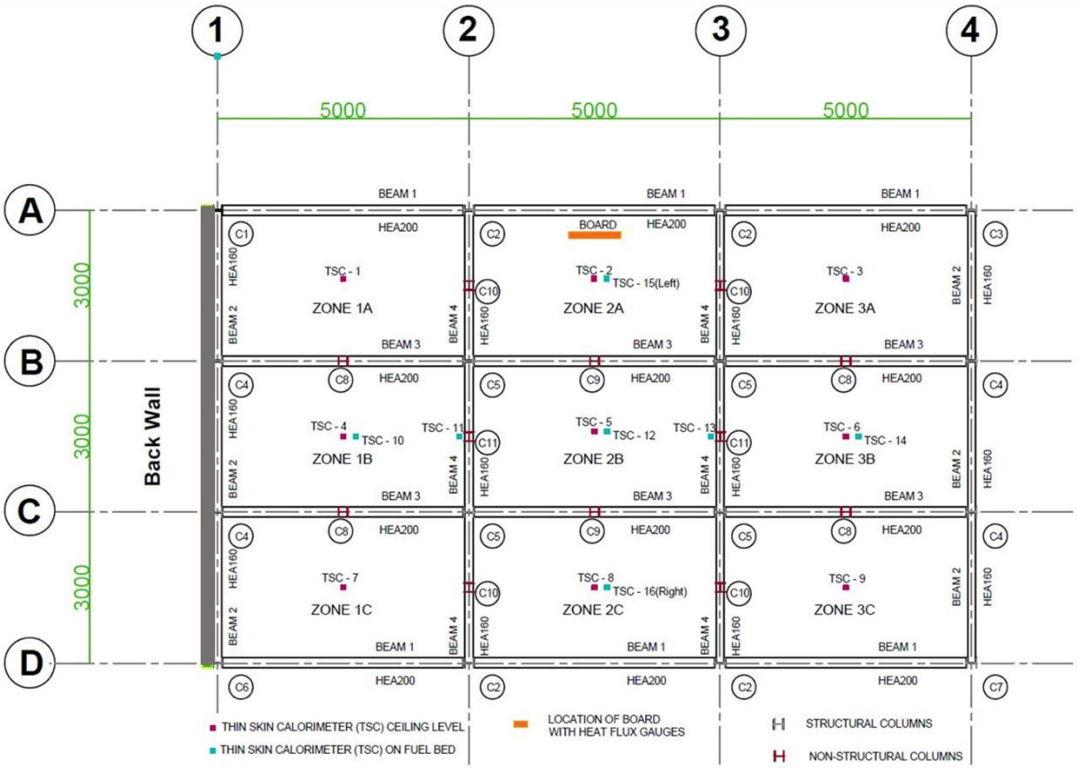

Figure 76: Location of board with heat flux gauges

Measurement of mass loss

One of the key aspects of the large-scale fire tests was monitoring the mass loss of the fire fuel. The mass loss was monitored in the middle of the test compartment between gridlines 2 and 3 using a steel platform as shown in Figure 78. The steel platform was 3 m long x 5 m wide and was supported using four load cells a shown in Figure 77. The load cells were calibrated at FireSERT, Ulster University, before being applied for the data monitoring purposes. To avoid any damage to the platform during the fire tests, fire blanked was wrapped around the steel elements. The load cells were also protected using the fire blanket to avoid any damage resulting from rise in temperatures.

Figure 77: Preparing the steel platform for the mass loss recording (4 load cells)

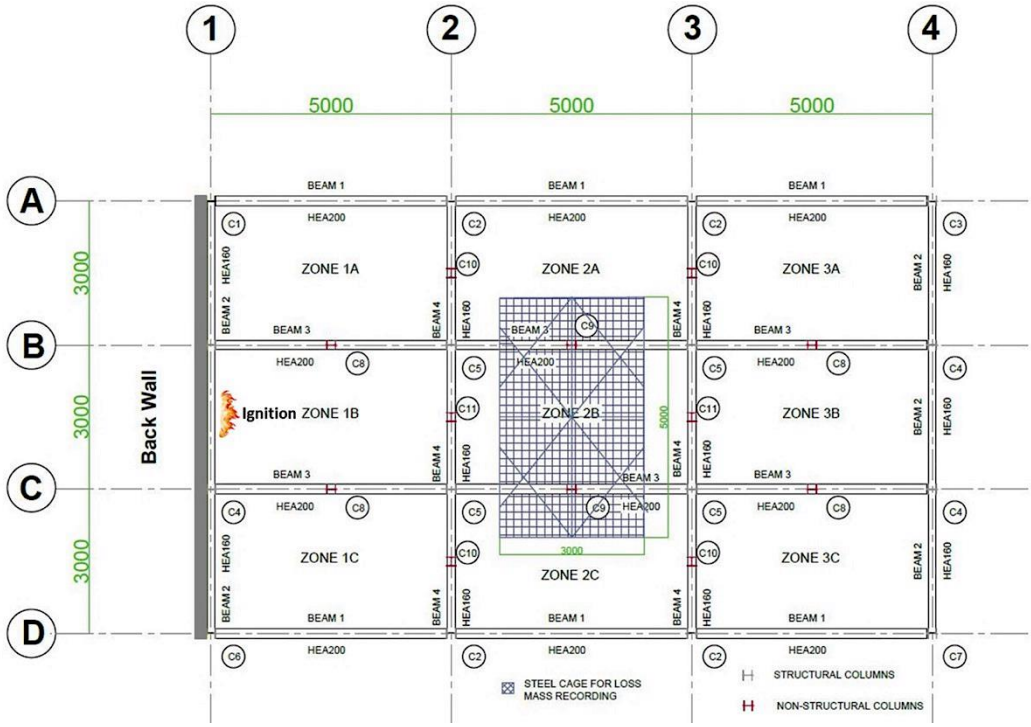

Figure 78: Positioning of platform in the compartment for mass loss recording

The data logging system

All the assigned sensors were connected to the data logging system through extension cables. The extension cables were stretched along the roof and were connected with the data loggers stationed in the site office as shown in Figure 79. A layer of fire blanked was laid under these cables to evade any damage from the heat during the tests.

(a) Panoramic view of the test compartment showing extension cables running across the roof

(b) The data loggers

Figure 79: The extension cables for data sensors and the data loggers

Analytical model: heat fluxes computation

Introduction

The following heat fluxes components will be used:

- $F_{r,f}$ refers to the radiative heat flux emitted by the fire surface and received by the steel member.
- $F_{r,b}$ refers to the radiative heat flux emitted by the surrounding background and received by the steel member.
- $F_{r,s}$ refers to the radiative heat flux emitted by the steel member.
- F_c refers to the convective heat flux received by the steel member from its surrounding environment.
- F_{tot} refers to the total resulting heat flux received by the steel member at a certain height.

All heat fluxes are expressed in W/m². Depending whether the flame impacts the ceiling and in which zone of the compartment the target lies (see Figure 64 and Figure 65), the following heat fluxes components will be added in the total heat flux balance. The two tables below summarize the heat flux components which are considered in the different zones, whereas the formulas to calculate these heat flux components are detailed in the next sub-sections.

Table IV: Heat flux components in Scenario 1

Scenario 1 – The flame doesn't impact the ceiling of the compartment						
Heat flux component	**Zone 1**	**Zone 2**	**Zone 3**	**Zone 4**	**Zone 5**	**Zone 6**
$F_{r,f}$	+	+			+	+
$F_{r,b,ambient}$	+	+			+	+
$F_{r,b,Heskestad}$			+	+		
$F_{r,b,Hasemi}$						
$F_{r,s}$	+	+	+	+	+	+
F_c	+	+	+	+	+	+

Table V: Heat flux components in Scenario 2

Scenario 2 – The flame impacts the ceiling of the compartment						
Heat flux component	**Zone 1**	**Zone 2**	**Zone 3**	**Zone 4**	**Zone 5**	**Zone 6**
$F_{r,f}$	+				+	
$F_{r,b,ambient}$	+				+	
$F_{r,b,Heskestad}$			+	+*		
$F_{r,b,Hasemi}$		+		+*		+
$F_{r,s}$	+	+	+	+	+	+
F_c	+	+	+	+	+	+

* Both Heskestad's and Hasemi's components are computed but only the maximum value is kept, following EN 1991-1-2.

$F_{r,f}$ - radiative heat flux emitted by the fire surface & received by the steel member

The fire is schematized as a virtual solid flame, and the following equations are based on EN1991-1-2 Annex G and the outcomes of the RFCS project LOCAFI (Grant Agreement n° RFSR-CT-2012-00023). Referring to the schematic plan view (x,y) depicted on Figure 81, on each *face l* – with *l = 1 to 4* – of the rectangular envelope around the steel member at height z_s, the radiative heat flux received from an infinitesimal area on the fire surface to an infinitesimal area on located at the height of interest on the steel member is computed by the following equation

$$dF_{r,f,A_1} = \frac{\cos\theta_1 \cos\theta_2}{\pi S_{1-2}^2} \sigma \varepsilon_f \varepsilon_m \left(T_{A_2} + 273{,}15\right)^4 dA_2$$

where

- $d\Phi_{A_1-A_2} = \frac{\cos\theta_1 \cos\theta_2}{\pi S_{1-2}^2} dA_2$ is the view factor between two infinitesimal areas A_1 and A_2 (see EN1991-1-2 equation G.1 and Figure 80);
- dA_1 refers to an infinitesimal area on the *face l* – located at the height of interest on the steel member – which receives the radiative heat flux;
- dA_2 refers to an infinitesimal area on the surface of the solid flame which emits the radiative heat flux.
- T_{A2} is the local temperature (cnfr Heskestad model) of the fire at height z_s [°C];
- σ = 5,67.10^{-8} is the Stefan–Boltzmann constant [Wm^{-2}K^{-4}];
- ε_m (generally = 0,7) is the surface emissivity of the member [-];
- ε_f (generally assumed to be = 1) is the surface emissivity of the fire [-].

The view factor $d\Phi_{A_1-A_2}$ measures the fraction of the total radiative heat leaving a given radiating surface that arrives at a given receiving surface. Its value depends on the size of the radiating surface A_2, on the distance from the radiating surface to the receiving surface S_{1-2} and on their relative orientation (through angles θ_1 and θ_2). The view factor for a member face from which the fire is not visible is taken equal to zero. In the TRAFIR simple tool, the view factor is calculated assuming that each *face l* is shifted to be located on the section axis.

The total radiative heat flux received by dA_1 from all the fire surfaces is obtained by

$$F_{r,f,A_1} = \int_{fire\ surface} \frac{\cos\theta_1 \cos\theta_2}{\pi S_{1-2}^2} \sigma \varepsilon_f \varepsilon_m \left(T_{A_2} + 273{,}15\right)^4 dA_2$$

As the present model assumes that the radiative heat flux F_{r,f,A_1} is homogeneous on a *face l* (at the height of interest), the total radiative heat flux received by *face l* (at the height of interest) is thus computed by

$$F_{r,f,l} = \sum_{fire\ surface} \frac{\cos\theta_1 \cos\theta_2}{\pi S_{1-2}^2} \sigma \varepsilon_f \varepsilon_m \left(T_{A_2} + 273{,}15\right)^4 dA_2$$

where $dA_2=dx.dy$ or $dy.dz$ depending on the location on the fire surface. The total resulting radiative heat flux $F_{r,f,tot}$ received from the fire by the steel member at height z_s is computed as the average of the $F_{r,f,l}$ weighted by the dimensions of the edges of the steel section envelope, namely

$$F_{r,f,tot} = \frac{C_x\left(F_{r,f,2} + F_{r,f,4}\right) + C_y\left(F_{r,f,1} + F_{r,f,3}\right)}{2\left(C_x + C_y\right)}$$

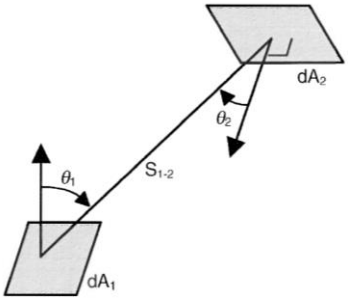

Figure 80: Geometrical parameters for the view factor between two infinitesimal areas

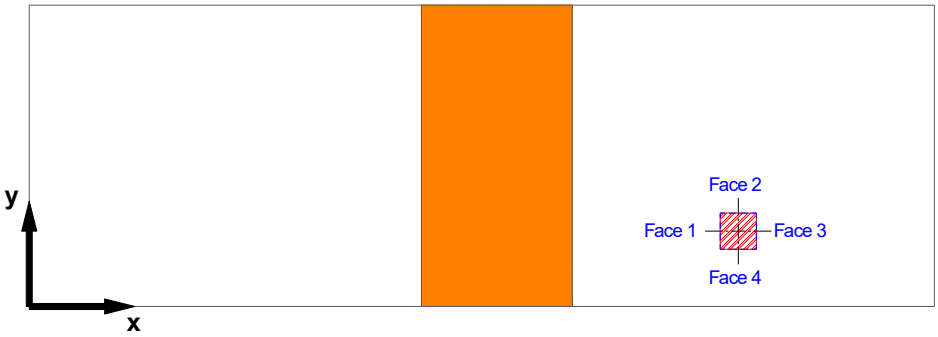

Figure 81: Plan view (x,y) of the compartment: faces of the steel element (rectangular envelope)

$F_{r,b}$ - radiative heat flux emitted by the surrounding background & received by the steel member

The radiative heat flux received from the surrounding background by the steel member at height z_s is computed in a different manner depending on the zone where it lies.

(a) If the point of interest is situated in ambient air (assuming the ambient background to be at 20°C).

$$F_{r,b,ambient} = \sigma\varepsilon_f\varepsilon_m(20 + 273{,}15)^4$$

It corresponds to zones 1, 2, 5, 6 when the flame does not impact the ceiling, and to zone 1,5 when the flame impacts the ceiling.

(b) if the point of interest is in the solid flame (i.e. zones 3 and 4):

$$F_{r,b,Heskestad} = \sigma\varepsilon_f\varepsilon_m\left(T_{A_2} + 273{,}15\right)^4$$

where T_{A2} is the local temperature (cnfr Heskestad model) of the fire at height z_s in °C.

(c) if the point of interest is in the horizontal layer underneath the ceiling when flame impacts the ceiling, i.e. in zone 2,4,6 in Figure 65 (cnfr Hasemi model, EN1991-1-2 equations C.4 to C.8):

$$F_{r,b,Hasemi} = \begin{cases} 100000 & if\ y \leq 0{,}30 \\ 136300 - 121000\,y & if\ 0{,}30 < y < 1{,}0 \\ 15000\,y^{-3{,}7} & if\ y \geq 1{,}0 \end{cases}$$

where

- $F_{r,b,Hasemi}$ is in W/m²
- y is a dimensionless parameter given by $y = \frac{r+(ht-h_{base})+z\prime}{L_h+(ht-h_{base})+z\prime}$
- r is the x-component of the horizontal distance (in m) between the *equivalent* vertical axis of the fire (see Note 1 below) and the steel member axis, given by the following formula (cnfr Figure 63):

$$r = \begin{cases} \left(Backside_x + \frac{D}{2}\right) - A_x & if\ A_x < Backside_x + \frac{D}{2} \\ 0 & if\ Backside_x + \frac{D}{2} \leq A_x \leq Frontside_x - \frac{D}{2} \\ A_x - \left(Frontside_x - \frac{D}{2}\right) & if\ Frontside_x - \frac{D}{2} < A_x \end{cases}$$

- $ht - h_{base}$ is the distance, in m, between the fire source basis and the ceiling
- z' is the vertical position of the virtual heat source, in m, given by

$$z' = \begin{cases} 2{,}4D\left(Q_D^{*2/5} - Q_D^{*2/3}\right) & if\ Q_D^* < 1{,}0 \\ 2{,}4D\left(1{,}0 - Q_D^{*2/5}\right) & if\ Q_D^* \geq 1{,}0 \end{cases}$$

  where $Q_D^* = Q_{loc}/(1{,}11.10^6.D^{2{,}5})$

- L_h is the horizontal flame length, in m, given by

$$L_h = 2{,}9(ht - h_{base})(Q_H^*)^{0{,}33} - (ht - h_{base})$$

  where $Q_H^* = Q_{loc}/(1{,}11.10^6.(ht - h_{base})^{2{,}5})$

Note 1:
Hasemi's model is a localised fire model whose thermal action is computed while considering a circular based fire. Any distance from such fire source is then computed from the axis of the circle. In the present project, the fire source is assumed to be represented by a rectangular prismatic solid flame, implying a rectangular (or square) based fire. The lack of a heat flux model for such situation has motivated the authors to generalize Hasemi model as presented above, i.e. by stretching the axis of the fire source onto a whole rectangle which may – in cases where F < b – reduce to a single line parallel to the width of the compartment.

(d) if the point of interest is in the solid flame in the top layer near the ceiling (i.e. when flame impacts the ceiling, in zone 4):

$$F_{r,b,max} = Max\left(F_{r,b,Heskestad}; F_{r,b,Hasemi}\right)$$

Note 2:

The Figure 82 can help understanding how the different models are considered. With b and F being respectively the width and the length of the burning area, three cases can be encountered: F>b, F=b, F<b.

If F>b;

- To evaluate the flame length, a diameter with *D*=b is considered;
- To apply Heskestad model (i.e. zones 3 and 4), the diameter *D* and equivalent power Q_{loc} are considered. The flame temperature obtained while applying Heskestad model is function of z, and for a given height is valid wherever the point of interest is (within the whole rectangular burning area of size b*F).
- To apply Hasemi model (i.e. zones 2,4,6 if the flame impacts the ceiling), a diameter *D* and equivalent power Q_{loc} are considered. Then, it is considered that only the extreme parts of the burning area (at b/2 distance from the back of the fire and from the fire front) present a variation along x coordinate (i.e. $r \neq 0$). Within the remaining central part, there is no variation of the result (i.e. $r = 0$). Furthermore, there is no variation along *y* coordinate, within the whole fire area.
- To compute the radiative heat flux received from the external surface of the virtual solid flame (i.e. to zones 1, 2, 5, 6 when the flame does not impact the ceiling, and to zone 1,5 when the flame impacts the ceiling), the whole burning area is supposed to be a rectangular prismatic solid flame

If F=b;

- To evaluate the flame length, a diameter with *D*=B=F is considered;
- To apply Heskestad model (i.e. zones 3 and 4), a diameter *D* and equivalent power Q_{loc} are considered. The flame temperature obtained while applying Heskestad model is function of z, and for a given height is valid wherever the point of interest is (within the whole rectangular burning area of size b*F).
- To apply Hasemi model (i.e. zones 2,4,6 if the flame impacts the ceiling), a diameter *D* and equivalent power Q_{loc} are considered. The central part of the burning area corresponds to the axis of the fire (i.e. $r = 0$), and results vary along x coordinate elsewhere (there is no variation along *y* coordinate within the whole fire area).
- To compute the radiative heat flux received from the external surface of the virtual solid flame (i.e. to zones 1, 2, 5, 6 when the flame does not impact the ceiling, and to zone 1,5 when the flame impacts the ceiling), the whole burning area is supposed to be a rectangular prismatic solid flame

If F<b;

- To evaluate the flame length, a diameter with *D*=F is considered;
- To apply Heskestad model (i.e. zones 3 and 4), a diameter *D* and equivalent power Q_{loc} are considered. The flame temperature obtained while applying

Heskestad model is function of z, and for a given height is valid wherever the point of interest is (within the whole rectangular burning area of size b*F).

- To apply Hasemi model (i.e. zones 2,4,6 if the flame impacts the ceiling), a diameter D and equivalent power Q_{loc} are considered. The central part of the burning area corresponds to the axis of the fire (i.e. $r = 0$), and results vary along x coordinate elsewhere (there is no variation along y coordinate within the whole fire area).
- To compute the radiative heat flux received from the external surface of the virtual solid flame (i.e. to zones 1, 2, 5, 6 when the flame does not impact the ceiling, and to zone 1,5 when the flame impacts the ceiling), the whole burning area is supposed to be a rectangular prismatic solid flame.

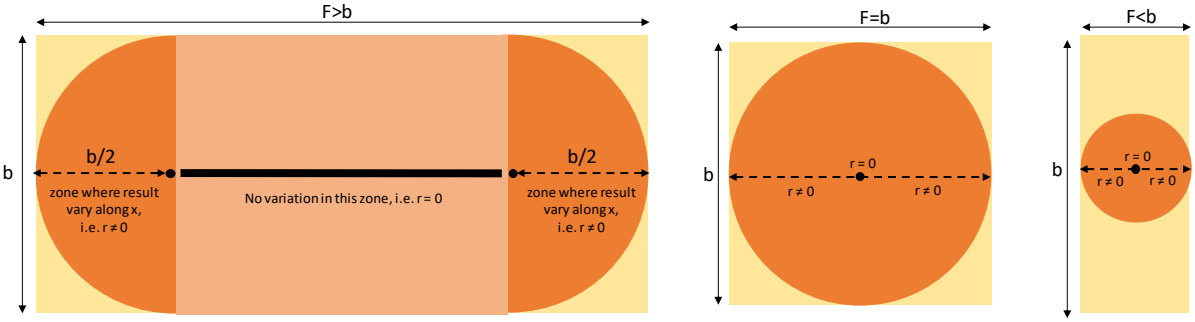

Figure 82: Virtual solid flame: 3 cases

Actually, when applying Hasemi model, the results are only a function of the horizontal distance x (i.e. parallel to the length of the compartment, since there is no variation along y coordinate) and the schemes from Figure 82 should be represented in 1 dimension, as depicted on Figure 83 (implying that this situation applies whatever the value of y (coordinate parallel to b).

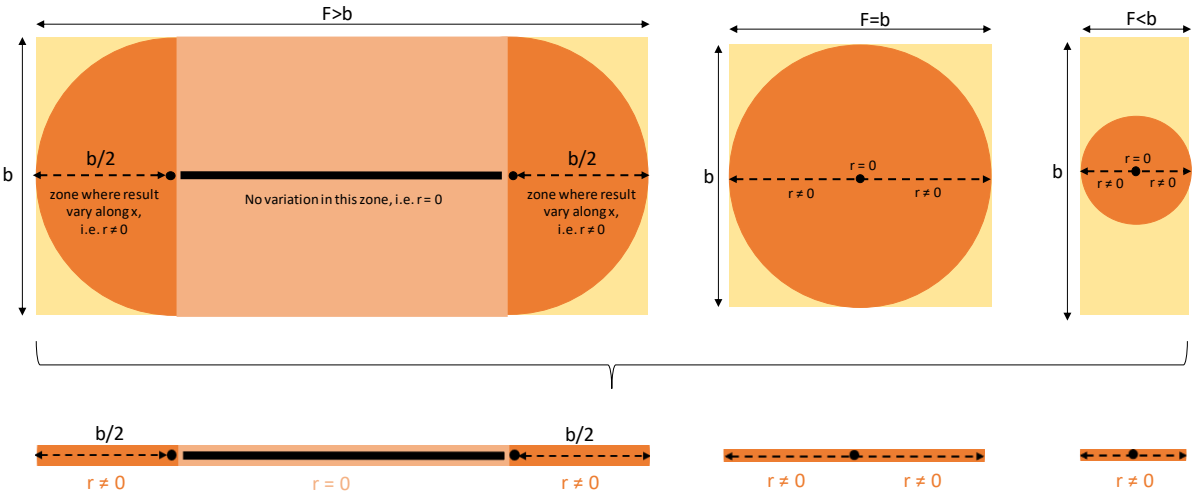

Figure 83: Virtual solid flame: 3 cases (linear scheme according to x coord.)

$F_{r,s}$ - radiative heat flux emitted by the steel member

The radiative heat flux emitted by the steel member is computed by

$$F_{r,s} = -\sigma\varepsilon_m(T_s + 273{,}15)^4$$

where T_s is the steel temperature at height z_s, in °C.

F_c - convective heat flux received by the steel member from its surrounding environment

The convective heat flux received by the steel member from its surrounding environment is computed by

$$F_c = \alpha_c(T_g - T_s)$$

Where

- α_c (considered equal to 35 when natural fire models are used, according to EN 1991-1-2) is the coefficient of heat transfer by convection, in [W/m²K];
- T_g is the gas temperature in the vicinity of the steel member at height z_s, in °C, namely:
  - in zones 1, 2, 5 and 6: the ambient background temperature (assumed to be at 20°C);
  - in zones 3 and 4: T_{A2} (the local temperature of the fire at height z_s computed by Heskestad model).

F_{tot} - total resulting heat flux received by the steel member at a certain height

The total resulting heat flux F_{tot} received by the steel member at height z_s is computed as

$$F_{tot} = F_{r,f,tot} + F_{r,b} + F_{r,s} + F_c$$

In the simple tool, the sheet "Steel" allows to observe the evolution of the heat fluxes $F_{r,f,l}$ (with l = *1 to 4*), $F_{r,f,tot}$, $F_{r,b}$, $F_{r,s}$, F_c and F_{tot} in the form of graphic and table of numbers (see example in Figure 84 and Figure 85).

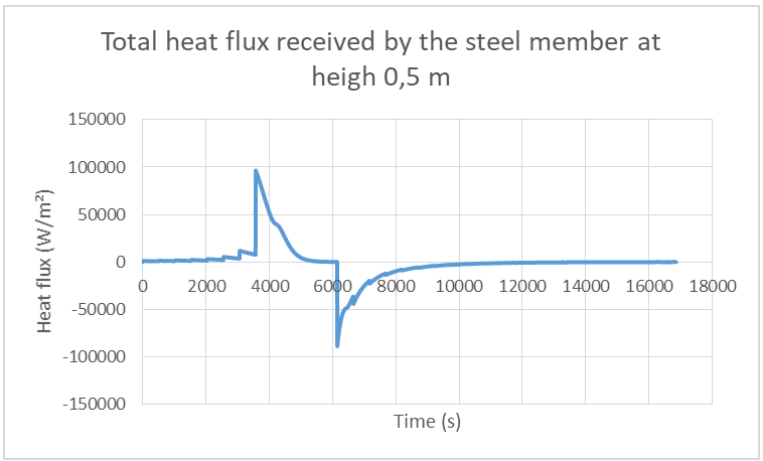

Figure 84: Heat fluxes – graphical information

		Radiative heat fluxes								Convective heat flux	Total heat flux
		From fire						From surrounding background	From steel member		
Sample	Time (s)	Fr,f,1 (W/m²)	Fr,f,2 (W/m²)	Fr,f,3 (W/m²)	Fr,f,4 (W/m²)	Fr,f,tot (W/m²)	Zone	Fr,b (W/m²)	Fr,s (W/m²)	Fc (W/m²)	Ftot (W/m²)
713	3560	40427,4945	15818,8169	0	12780,7217	16834,3313	Zone 1	293,116788	-2367,94432	-7037,54082	7721,96293
714	3565	40427,4945	15818,8169	0	12780,7217	16834,3313	Zone 1	293,116788	-2380,38638	-7060,21845	7686,84325
715	3570	0	0	0	0	0	Zone 3	75178,7809	-2392,81521	23717,2166	96503,1823
716	3575	0	0	0	0	0	Zone 3	75178,7809	-2552,95921	23434,0482	96059,8698

Figure 85: Heat fluxes – numerical information

Analytical procedure: comparison with experimental results

The results obtained while applying the TRAFIR analytical procedure were compared with results from the experimental campaigns and numerical simulations and some results are presented here below.

The Figure 86 to Figure 90 present the comparison of steel column temperature measured from the TRAFIR WP3 Test 2 (labelled "TEST") with the steel column temperature obtained while applying the TRAFIR analytical procedure (labelled "Tool"). The considered central column is a HE 200 A hot rolled profile, placed next to TRL7 (see Figure 73) and for which temperatures were measured at five levels (see Figure 74). In Figure 90, the combination with zone model was done while using OZone software (Cadorin, 2003) (for Level 5, the maximum steel temperature resulting from both calculation methods (hot zone and TRAFIR) is plotted). The Figure 91 provides the evolution of the flame thickness (i.e. distance between fire front and burnout) observed during test n°2 versus the one obtained through the TRAFIR model (the flame thickness plotted for the analytical procedure corresponds only to the "travelling phase", not the growing and decaying phases). The following observations can be made:

- The global heating profiles are well captured by the model, and are safe-sided.
- For levels 1 and 2 (closer to the ground level) the difference is around 90°C (the steel temperature is 900°C for the model versus 810°C for the test n°2). For levels 3 and 4 the difference is a bit higher, about respectively 150°C and 190°C (the steel temperature is 900°C for the model versus respectively 750°C and 710°C for the test n°2). For level 5 (closer to the ceiling level), the steel peak temperature is similar, about 710°C.
- The time during which the steel temperatures are high (i. e. above 500°C – threshold chosen because the steel effective yield strength is 78% of its ambient value at 500°C) is slightly longer for the model than for test n°2 for levels 1, 2 and 3. However, for levels 4 and 5 a very good match is observed with 30 minutes for both the test °2 and the model.
- However, for steel temperatures above 700°C (threshold chosen because the steel effective yield strength is 23% of its ambient value at 700°C) the difference is more important: the model overestimates slightly the time during which temperatures are above this temperature. Applying the model, steel temperatures are above 700°C during 25 minutes for levels 1, 2, 3 and 4 and during 15 minutes for level 5, while for test n°2 they exceed 700°C during approximately 10 minutes for levels 1 and 3, during 12 minutes for level 2 and during 5 minutes for levels 4 and 5.
- The model does not capture the varying flame thickness (indeed, the fire front spread and the fire back spread are equal and constant, resulting in a constant flame thickness), but proposes an acceptable average representation.

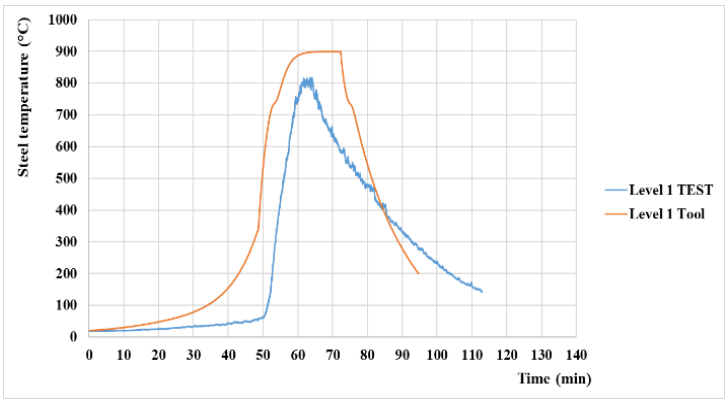

Figure 86: Steel temperature Test n°2 VS Model Level 1 (z=0.5m)

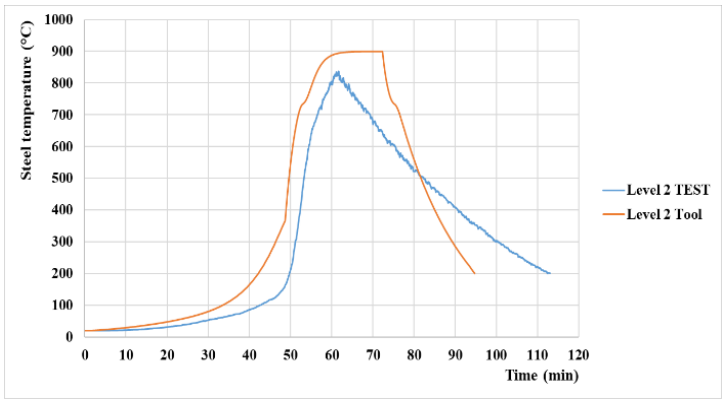

Figure 87: Steel temperature Test n°2 VS Model Level 2 (z=1m)

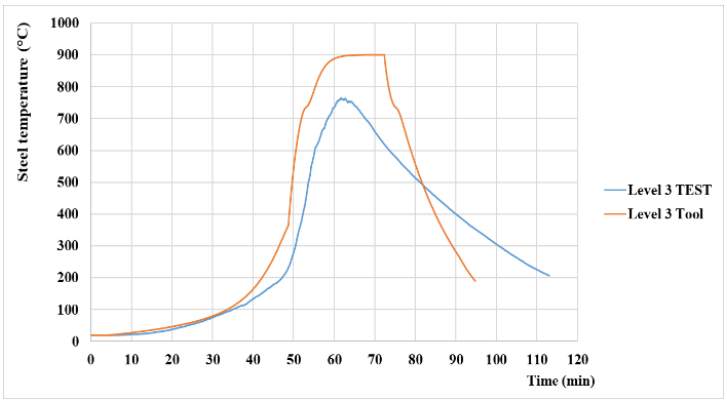

Figure 88: Steel temperature Test n°2 VS Model Level 3 (z=1.5m)

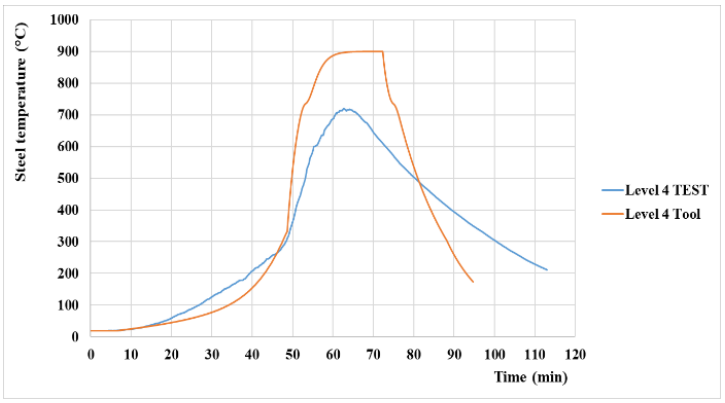

Figure 89: Steel temperature Test n°2 VS Model Level 4 (z=2m)

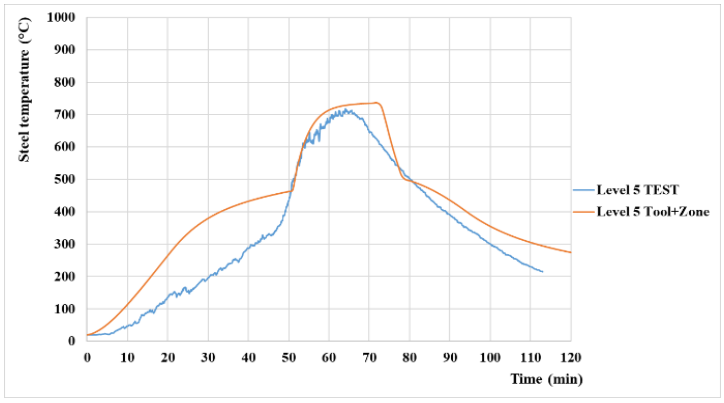

Figure 90: Steel temperature Test n°2 VS Model Level 5 (z=2.5m)

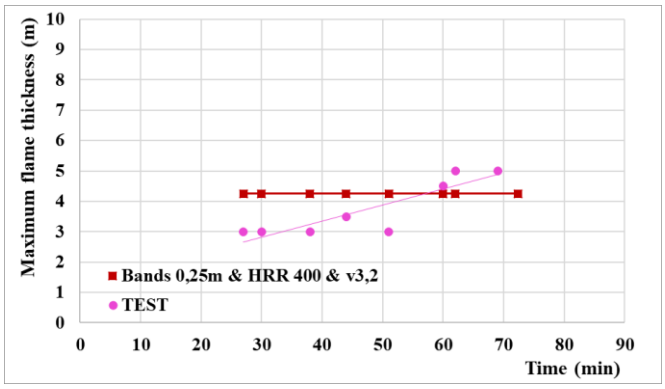

Figure 91: Flame thickness of test n°2 versus TRAFIR model as a function of time

The analytical procedure also allows to globally capture the heating profiles of the WP2 Task 2 timber test for which a lower rate of heat release density was evaluated. Nevertheless, the results do not match the spike in temperatures at higher levels as the fire passes.

When comparing the results for CFD simulations presenting a clear and fairly steady travelling fire, a good correspondence is met. But as soon as a simulation highlights more complex fire behaviours (for example: strong acceleration – or runaway – leading to a small and local flashover towards the end of the compartment, local underventilation, etc): the correspondence is not always achieved. Indeed, inherently to its analytical and simplified nature, the developed procedure does not allow to take into account such phenomena.